UNIVERSIDAD PONTIFICIA COMILLAS

ESCUELA TÉCNICA SUPERIOR DE INGENIERÍA (ICAI)

OFFICIAL MASTER'S DEGREE IN THE ELECTRIC POWER INDUSTRY

Master’s Thesis

Assessing power system reliability under temperature-dependent variables

A case study of the Brazilian Power System

Author: Matheus Gonçalves Costa

Supervisor: Pablo Rodilla

Co-Supervisor: Gabriel Cunha

Madrid, August 2025

Master’s Thesis Presentation Authorization

THE STUDENT:

MATHEUS GONÇALVES COSTA

Matheus Gonçalves Costa

Digitally signed by Matheus Gonçalves Costa
DN: cn=Matheus Gonçalves Costa, o, ou, email=math.goncacosta@gmail.com, c=BR
Date: 2025.08.26 23:11:19 +02'00'

THE SUPERVISOR

PABLO RODILLA

Signed: …………………… Date: 27/08/2025

THE CO-SUPERVISOR

GABRIEL CUNHA

Signed: Gabriel Rocha de Almeida Cunha

Digitally signed by Gabriel Rocha de Almeida Cunha
DN: cn=Gabriel Rocha de Almeida Cunha, o=PSR, ou=PSR, email=gabriel@psr-inc.com, c=BR
Date: 2025.08.26 17:59:34 -03'00'

Date: 27/08/2025

Authorization of the Master’s Thesis Coordinator

Dr. Luis Olmos Camacho

Signed: …………………… Date: 27/08/2025

UNIVERSIDAD PONTIFICIA COMILLAS

ESCUELA TÉCNICA SUPERIOR DE INGENIERÍA (ICAI)

OFFICIAL MASTER'S DEGREE IN THE ELECTRIC POWER INDUSTRY

Master’s Thesis

Assessing power system reliability under temperature-dependent variables

A case study of the Brazilian Power System

Author: Matheus Gonçalves Costa

Supervisor: Pablo Rodilla

Co-Supervisor: Gabriel Cunha

Madrid, August 2025

SUMMARY

This work focuses on explicitly representing key variables of the power sector under temperature-dependent conditions, with particular emphasis on electricity demand and generator availability. By jointly modeling these two critical dimensions, the thesis seeks to evaluate the reliability of the Brazilian National Interconnected System (SIN) under stress conditions, particularly in the context of growing exposure to climatic extremes.

The SIN, coordinated by the Independent System Operator (ONS), supplies nearly the entire country, except for the state of Roraima, which is still electrically isolated but expected to be interconnected by the end of 2025. The system is divided into four major subsystems (SE/CO, S, NE, N), each with distinct socioeconomic, climatic, and load characteristics. The relevance of demand forecasting and generator availability analysis lies not only in their role for short-term operations, but also in medium- and long-term planning, capacity expansion, and market mechanisms. Currently, the country is discussing the implementation of capacity auctions, which will seek to contract firm capacity, mostly from thermal plants, to meet demand at critical times. Incorporating temperature into these variables is particularly critical in Brazil, where heat waves and seasonal variability significantly affect both consumption patterns and thermal unit performance.

To address this challenge, a comprehensive and historically consistent database was compiled. For demand, semi-hourly records from the ONS API were compiled and complemented by the identification of critical daily peaks. For climate, hourly records of temperature from the National Institute of Meteorology (INMET) were collected, consolidated, and treated with statistical methods, seeking to solve the missing data set and apply a clustering process to select representative weather stations for each subsystem, ensuring both spatial and climatic diversity.

On the demand modeling side, two families of methods were applied. Econometric regression (OLS) and time-series models (ARIMAX and SARIMAX) were used to forecast monthly demand and critical daily profiles, incorporating economic indicators, temperature-based variables such as Heating and Cooling Degree Days, and seasonal harmonics. Variable selection was performed using backward elimination and LASSO regularization to enhance interpretability and robustness. Finally, Monthly dummies variables and an alternative with Dynamic Harmonic Regression was applied to represent the seasonality. A stochastic scenario generation procedure was implemented through a double bootstrap of historical climate data, preserving temporal

correlations across stations and allowing for the inclusion of linear warming trends, in order to provide future temperature scenarios and in this sense analyze the probabilistic distribution of the forecasted demand.

The results demonstrate that explicitly incorporating temperature improves predictive accuracy of demand by reducing RMSE by over 38% on average in the monthly forecast demand process. Also, superior results are obtained when ARIMA models are applied, compared with traditional OLS and with the SARIMA models. In the hourly forecast assessment, the impacts by considering the temperature are clear, with some months presenting differences above 10% for the same hour under different temperature conditions.

Finally, the reliability of the system is assessed under the generated forecast demand for 2028, considering a temperature-dependent outage probability for the thermal generators. For this purpose, taking as a starting point the database made available from the official forecasts from the Brazilian System Operator, the capacity requirement for the thermal fleet is estimated, and subsequently stress tested considering the temperature scenarios. The methodology applies a cut-based approach to the Brazilian interconnected system, accounting for hydroelectric reservoirs with explicit regulation constraints, stochastic renewable generation scenarios built from ERA5 reanalysis data through the TSL platform, and a gamma distribution to represent the aggregated expected forced outage of thermal capacity per subsystem. In total, one hundred inflow and renewable scenarios are combined with one hundred peak demand scenarios, focusing on the critical hours of supply between 5 p.m. and 2 a.m., generating a broad set of stress conditions.

The results confirm that the most critical deficits occur at sunset (5–7 p.m.), when solar falls while demand remains high. Deficits exceed 10 GW and surpass 13 GW in extreme scenarios, while even median cases reveal structural deficits above 5 GW. When thermal failures are modeled as temperature dependent, the capacity requirement rises by about 500 MW, highlighting the systemic risks of ignoring climate dependency. Economically, this additional capacity equates to R$ 412 million per year under current firm capacity benchmarks, rising to nearly R$ 2 billion if contracted under emergency auctions, as occurred in 2021. These findings stress the need to explicitly integrate climate dependencies in planning and underscore the importance of adding flexible capacity capable of supporting the system during sunset peaks.

FOREWORD

I am deeply grateful to my family, whose support and encouragement have guided me through the challenges of my academic and professional path.

I also extend my thanks to the Centro de Estudos Econômicos do Setor Energético and PSR Energy Consulting for their financial and institutional support in making this Master’s program possible.

As a reflection of this journey, I recall the words: “When I left you, I was but the learner. Now I am the master.”

TABLE OF CONTENTS

LIST OF EQUATIONS

LIST OF FIGURES

LIST OF TABLES

1 INTRODUCTION

In recent years, South America has faced unprecedented climatic events, notably severe temperature anomalies. The years 2023 and 2024, the most recent in history, were listed, “by far”, as the hottest on record.

Subregion/region	Temperature ranking	Anomaly (°C) relative to:	
		1991–2020	1961–1990
Mexico	Warmest or second warmest	+1.09 [1.01–1.19]	+1.79 [1.45–2.10]
Central America	Warmest	+0.96 [0.77–1.09]	+1.44 [1.26–1.63]
Caribbean	Warmest	+0.97 [0.80–1.09]	+1.46 [1.07–1.69]
South America	Warmest or second warmest	+0.87 [0.72–0.99]	+1.43 [1.21–1.60]
LAC	Warmest or second warmest	+0.90 [0.76–1.00]	+1.47 [1.27–1.63]

Figure 1. 2024 temperature ranking (1900–2024) and anomalies for Latin America and Caribe [WORL25]

These years were also marked by the occurrence of strong heat waves. In Argentina, the highest temperature ever in Buenos Aires was recorded in 2024, the city with the largest population in Argentina. In the same year, Buenos Aires also faced the longest heat wave in history, with 14 days above 32º C. In Brazil, after heat waves in March and April, September 2024 was characterized as the hottest, with anomalies of 7º C above the record [WORL25].

The surge in electricity demand, primarily driven by increased air conditioning usage, has raised concerns about the ability of these South America Power systems to meet peak loads. In Argentina, such heat waves led to record imports from Argentina, in addition to possible load shedding, due to extreme conditions in the local transmission grid and high thermal unavailability [BUEN24]. In Brazil, the National Electric System Operator (ONS) reported successive new peaks, leading to surpassing for the first time the symbolic mark of 100 GW of instantaneous demand, during a heat wave in November 2023 [OPER23].

In this context, according to the annual assessment carried out by ONS, the National Interconnected System (SIN) presents a significant deterioration in its reliability levels in the short and medium term, with both power supply criteria being violated from 2026 onwards [OPER24]. In response to these challenges, exacerbated by the dominance of intermittent renewable expansion in the current context, Brazil has initiated the implementation of a capacity market mechanism, known as the Reserve Capacity Auction (LRCAP), aimed at contracting mainly faster thermal power plants to ensure sufficient firm capacity to meet peak demand periods, especially during evening hours when solar generation declines. However, the LRCAP has faced regulatory hurdles, including its cancellation in 2025 due to court appeals.

Given these pressing issues, there is an urgent need to assess the Brazilian power system's reliability under temperature-dependent variables. This assessment is crucial for developing strategies to enhance the system's resilience against climatic extremes and ensuring a stable electricity supply for the nation's growing demand.

1.1 THESIS OBJECTIVES

This thesis aims to evaluate the reliability of the Brazilian power system under temperature-dependent conditions, focusing on the projected expansion of the system by 2028. The specific objectives are:

- Develop a temperature-sensitive medium-term hourly electricity demand projection for the Brazilian Power System, incorporating historical climate data and socioeconomic factors into advanced forecasting models.
- Assess the reliability of the Brazilian electricity system by analyzing temperature-dependent generator availability.
- Evaluate the expected expansion of the Brazilian Power System by 2028, considering projections and plans from key institutions such as the ONS (Operador Nacional do Sistema Elétrico), EPE (Empresa de Pesquisa Energética), and ongoing development and construction projects.
- Benchmark the system’s reliability against international standards and propose recommendations for capacity planning and policy adjustments to enhance system resilience.

1.2 THESIS STRUCTURE

This dissertation is organized into six chapters. This chapter presents the introduction and research objectives. The second chapter presents a literature review, covering both official methodologies adopted by international operators and academic approaches. The third chapter describes the proposed methodology, while the fourth brings together data analysis, calibration, and monthly and hourly demand projections. The fifth chapter applies these projections to reliability assessments of the Brazilian electricity system. Finally, the sixth chapter presents the conclusions and prospects for future work.

2 LITERATURE REVIEW

Electricity demand constitutes a fundamental element in the operation and planning of power systems, acquiring particularly significant relevance over medium- and long-term horizons. Understanding and forecasting demand with precision is essential not only to guarantee the stability and security of energy supply, but also to optimize economic and operational resources, thereby contributing directly to the efficiency and sustainability of modern power systems.

Historically, in South America electric system planning has been deeply shaped by the central role of large hydroelectric plants with storage reservoirs. These reservoirs have traditionally provided flexibility by regulating water inflows and storing energy, allowing generation to be modulated in response to fluctuations in demand. This capability created a structural dependence that defined the logic of energy planning for decades.

However, profound transformations in economic, environmental, and technological contexts have introduced mounting challenges. In Brazil, for instance, the reduction in viable areas for constructing large reservoirs, coupled with the increasing penetration of intermittent renewable sources such as wind and solar, has rendered the system less flexible and more vulnerable to risks associated with supply volatility. This evolving scenario has generated an urgent need for more detailed demand forecasts, particularly with hourly granularity, which is indispensable for maximizing the efficient integration of renewable resources and for ensuring the rational use of existing assets.

The physical importance of precise demand projections is directly linked to system reliability. Accurate forecasting is decisive for preventive and scheduled maintenance of generation and transmission assets. Reliable demand estimates allow operators to plan interventions, replacements, and expansions of the transmission grid, thereby enabling more efficient use of infrastructure and reducing the frequency of costly emergency investments, which are typically less effective and more burdensome.

Forecast accuracy is also fundamental for optimizing the so-called “economic value of water,” an indicator of the opportunity cost associated with the storage of water in hydroelectric reservoirs. This metric captures the trade-off between immediate use of stored water and its preservation for potentially more critical future periods. In hydrothermal systems such as Brazil’s, misaligned operational decisions based on inaccurate forecasts may result in the premature depletion of reservoirs, triggering the unnecessary activation of thermal generation at high operational costs [CAMP17].

Beyond its operational and physical dimensions, electricity demand forecasting exerts a profound commercial impact. In organized electricity markets, as in Brazil, Chile, and Peru, expectations about future demand trajectories directly shape contracting decisions and investment strategies in new projects [MBBR13, MBBR16]. Significant forecasting errors may lead either to over-contracting, unduly burdening final consumers, or to under-contracting, exposing the system to financial and systemic risks. Such imbalances are often mitigated through emergency measures, as historically observed in Brazil and elsewhere in South America, which are generally associated with higher costs and less efficient long-term outcomes.

In practice, South American countries have historically relied on econometric models to forecast demand, often adopting top-down approaches based on macroeconomic projections. These methods are frequently complemented by bottom-up assessments, which incorporate detailed information from large industrial consumers, especially energy-intensive sectors such as mining and heavy industry. In Chile, for example, projections combine econometric modeling with direct surveys of major industrial and commercial clients, thereby providing a more granular understanding of future consumption patterns.

Nevertheless, purely econometric models, even when complemented by bottom-up data, have shown growing limitations in contexts marked by accelerated electrification and increasingly evident climate change. Recent heatwaves and the rising use of cooling systems in large urban centers underscore the critical importance of integrating climate variables, especially temperature, into demand models. The literature consistently highlights the strong correlation between higher average temperatures and peaks in electricity demand, a phenomenon exacerbated by climate change and by the increasing electrification of households, industries, and transportation. Studies on cooling, heat and electricity demand forecasting further reinforce that, in the absence of climate-sensitive modeling, operators risk underestimating both the frequency and the intensity of peak loads [DIAM18, FEAC15, NIMC19, STPJ23].

The incorporation of additional explanatory variables such as temperature, alongside traditional economic and industrial indicators, can represent a crucial methodological advance. This multidimensional approach may enable a more accurate capture of the actual dynamics of electricity demand, enhancing the robustness and precision of medium- and long-term forecasts if correctly addressed. Such forecasts are indispensable for effective and sustainable power system planning, especially in the face of structural transformations and growing uncertainty.

In conclusion, methodological enhancement in electricity demand forecasting is not merely desirable but indispensable to safeguard operational stability, economic efficiency, and environmental sustainability in South American power systems over the coming decades. This subject therefore constitutes a strategic theme of academic, industrial, and governmental relevance, at the intersection of energy policy, climate resilience, and system reliability.

2.1 OFFICIAL METHODOLOGIES APPLIED BY IN THE POWER SYSTEMS

The following section presents the principal methodologies employed for electricity demand forecasting by system operators and planning agencies in different countries. These methodologies play a central role in both the expansion and operation of power systems, since they guide strategic decisions related to system reliability, capacity sizing, the integration of renewable resources, and the formulation of public policies. Although they share common statistical and econometric foundations, their approaches differ significantly depending on the institutional, climatic, and structural characteristics of each country or region. Such differences are particularly evident when comparing hydro-dominated systems with those based on thermal or mixed portfolios, as well as when contrasting mature electricity markets with vertically integrated or regulated contexts.

This comparative analysis is intended not only to describe the current state of demand forecasting practices across power systems of varying sizes and regional profiles, but also to identify trends and challenges that shape the evolution of forecasting techniques. Issues such as the growing influence of climate change, the increased penetration of variable renewable energy sources, the demand from electrification of transport and industry, and the availability of increasingly granular data are driving methodological advances and diversification across different jurisdictions. In this sense, the present chapter introduces, in sequence, the methodologies adopted in Brazil, Peru, and Chile, followed by those used in the PJM Interconnection and in ISO New England, highlighting their distinctive features as well as critical remarks that emerge from academic and professional evaluations.

2.1.1 Brazilian methodology

The methodology for projecting monthly electricity demand in Brazil, developed by the Energy Research Office (EPE) in collaboration with the National System Operator (ONS), is fundamentally based on econometric models disaggregated by both consumer class and geographic subsystem, namely Southeast/Central-West, South, Northeast, and North. These projections are an integral part of the Annual Energy Operation Plan (PEN) cycle and are used to estimate the evolution of load in the National Interconnected System (SIN) over medium- and long-term horizons. The results of this modeling process have direct implications for the expansion of the country’s electrical infrastructure as well as for the formulation of national energy policies.

The modeling of monthly demand relies primarily on multiple linear regressions, using economic, sociodemographic, and sectoral variables as the main determinants of consumption. This modeling structure, consolidated under the Electricity Demand Projection Model (MDE), is calibrated by both consumer class and subsystem, which allows for a detailed representation of the Brazilian electricity demand. In the case of the residential class, for instance, demand is estimated as a function of demographic growth, household purchasing power, and tariff levels. This formulation seeks to capture the simultaneous effects of demographic expansion, variations in household real income, and the price elasticity associated with residential tariffs.

For the industrial sector, demand projections are constructed using indices of industrial physical production and specific consumption by subsector. Key segments such as steel, pulp and paper, cement, and food processing exhibit differentiated elasticities. In addition, qualitative information is collected directly from large industrial consumers in order to refine the projections. Finally, the commercial demand is modeled through variables that reflect the dynamism of the tertiary sector, particularly the Gross Domestic Product (GDP) of services and the number of registered commercial consumer units.

For the rural class, demand is estimated as a function of the gross value added of agriculture, the number of rural consumer units, and regional agricultural output. Public sector demand and public lighting are modeled using proxies for urbanization and demographic indicators, including urban growth, the extent of illuminated public areas, and the number of institutional consumer units.

From a geographic perspective, the econometric models are calibrated separately for each subsystem in order to account for the economic and climatic specificities of each region. This disaggregation ensures that the heterogeneity of the Brazilian power system is adequately represented, capturing the distinct consumption trajectories that characterize different parts of the country.

The projection of the hourly load curve represents a fundamental methodological advance in Brazil's energy planning, particularly in the context of the energy transition, the growing penetration of intermittent sources such as wind and solar, and the increasing importance of detailed temporal analyses for assessing reliability and determining the need for firm capacity. The methodology adopted by the Energy Research Office (EPE), formalized in Technical Note EPE-DEA-NT-005/2020, consists of eight systematic and integrated stages that focus on converting the projected monthly demand into hourly series consistent with the operational characteristics of the National Interconnected System (SIN).

The first stage involves the identification of typical load profiles for distribution companies. EPE begins the process by characterizing hourly load patterns based on historical supervision data. These profiles are grouped by similarity in intraday behavior and classified into four categories of days: weekdays, Saturdays, Sundays, and holidays. Each profile represents the percentage distribution of consumption over the 24 hours of the day.

The second stage refers to the evaluation of load parameters of interest. At this stage, EPE carries out a statistical analysis of historical load data from the distribution companies, including indicators such as peak demand, average load, load factors, and amplitude. These parameters are essential for calibrating and validating the hourly profiles and for assessing their applicability in future projections. The third stage is the selection of a weighting month. EPE chooses an "ideal" month to serve as the reference for weighting, giving priority to the one in which the adherence of the typical distribution company profiles to the real hourly curve of the SIN is maximized. This procedure ensures that the future extrapolation remains consistent with operational patterns observed in practice.

The fourth stage concerns the establishment of monthly equivalence for the identified profiles. Equivalence is calculated on the basis of the distribution of weekdays and non-weekdays, with the identified profiles being weighted to replicate the structure of days in the reference month. The purpose is to obtain a weighted hourly load vector that is representative of the monthly behavior.

The fifth stage is the construction of hourly consumption for the base year. With the weighted profiles, the series of hourly load for the base year, typically the most recent year with complete data, is built while preserving the daily, weekly, and monthly proportions observed historically. The sixth stage focuses on the calculation of the global hourly load. The hourly load of the distribution companies is aggregated, considering estimated electrical losses and adjustments between consumption and observed load. The global load is then reconciled with data provided by the National System Operator (ONS, in the Brazilian acronym) and the Electric Energy Trading Chamber (CCEE, in the Brazilian acronym).

The seventh stage addresses the calculation of losses and hourly differences. The methodology explicitly incorporates technical energy losses throughout the transmission and distribution networks and applies corrections to reconcile the differences between the idealized profiles and actual hourly measurement data. The eighth and final stage is the projection of the global hourly load. At this point, the projected monthly growth rate for each consumer class, as estimated by the econometric monthly load model, is applied to the base year's hourly curve, maintaining the intraday structure. This process produces the future hourly projections that serve as the basis for studies on system reliability, operating reserves, and generation expansion.

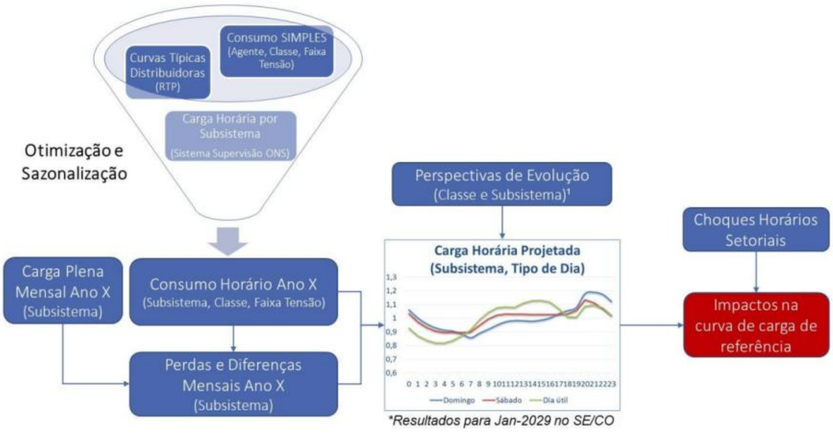

Figure 2. Schematic view of the EPE hourly forecast methodology. [EMPR20]

Unlike monthly demand, hourly demand is directly sensitive to climatic variables such as temperature and humidity. To address this, EPE start to study the introduction of climatological adjustments using indicators such as Heating Degree Days (HDD) and Cooling Degree Days (CDD), weighted by macro-region. Equivalent municipal temperatures are derived from meteorological station data provided by the Brazilian National Institute of Meteorology (INMET, in the Brazilian acronym) and are subsequently regionalized using population-weighted averages. These adjustments aim to capture the seasonality of thermal discomfort and its relationship with the use of air-conditioning and heating equipment, thereby adequately reflecting the impact of temperature on hourly electricity demand.

$$HDD = \sum_{n=1}^{N} (T_{ref} - T_n), \qquad for\ (T_{ref} > T_n)$$

$$CDD = \sum_{n=1}^{N} (T_n - T_{ref}), \qquad for\ (T_{ref} < T_n)$$

Equation 1 – CDD and HDD

2.1.2 Peruvian methodology

Electricity demand forecasting in Peru is conducted by the *Comité de Operación Económica del Sistema Interconectado Nacional* (COES-SINAC), which prepares monthly estimates for the medium-term horizon in support of the *Programa de Mediano Plazo de Operación* (PMPO) [COMI25], the medium-term planning. The methodology applied is based on statistical models of the ARIMA class (Auto-Regressive Integrated Moving Average), which are calibrated with economic restrictions to ensure macroeconomic consistency with the projections of the Central Reserve Bank of Peru (BCRP). The principal objective is to provide technical input for the programming of power system operation, thereby ensuring the balance between electricity supply and demand in the National Interconnected Electric System (SEIN).

The ARIMA model employed by COES is univariate and is applied to the historical series of what is referred to as the “vegetative demand” of the SEIN. This demand represents the system’s base load, excluding additional demand from large industrial consumers and large-scale projects scheduled for future connections. The purpose of modeling this isolated series is to ensure that the estimates reflect the organic behavior of electricity demand without distortions caused by large exogenous events.

The calibration of the model incorporates the country’s economic growth projections, particularly the annual Gross Domestic Product (GDP) forecasts prepared by the BCRP. Although ARIMA is traditionally a purely statistical model, in this case it is adapted by imposing restrictions on the confidence intervals of the projection, restrictions that are derived from the official economic growth targets estimated by econometric models. In this way, the trajectory of projected demand remains coherent with the official macroeconomic scenario, which enhances the credibility of the forecasts for energy planning purposes.

Following the modeling of vegetative demand, the next stage is the projection of what are termed “additional loads.” These loads are estimated using information supplied directly by electricity sector agents, through structured questionnaires and periodic data collection campaigns. Major developments such as the Talara Refinery, the Chancay Port Terminal, and Line 2 of the Lima Metro are modeled separately, using their respective commissioning schedules and the progressive load curves declared to COES. These projects exert a significant influence on the trajectory of national demand, which justifies their individual treatment in the modeling process.

The final aggregation of projected demand therefore incorporates three components: the ARIMA projection of vegetative demand, adjusted with economic restrictions; the specific projections of additional loads; and the inclusion of new energy projects or large-scale industrial expansions. The result is a robust forecast of national electricity load that is capable of reflecting both the steady growth of the installed base and the abrupt inflections caused by major industrial investments.

From a climatic perspective, the model acknowledges the existence of seasonal variations in demand, particularly those associated with heat waves. However, such fluctuations are not modeled explicitly through the inclusion of climate variables. Instead, they are treated statistically as irregular components or noise within the series.

2.1.3 Chilean methodology

Long-term electricity demand forecasting in Chile, carried out by the *Coordinador Eléctrico Nacional* (CEN), is developed through a methodological approach that integrates two complementary perspectives: a top-down projection based on econometric models and a bottom-up projection grounded in the direct collection of information from large consumers, in a very similar approach as applied by the Peruvian System Operator. The purpose of this integration is to produce monthly and hourly forecasts of electricity consumption in the National Electric System (SEN) for a horizon of up to twenty years, thereby providing critical inputs for system expansion and operational planning [COOR24].

The methodology begins with the classification of SEN consumers into three distinct groups. The first group consists of regulated and free customers in distribution zones, the second group encompasses free consumers in the copper mining sector, and the third group includes free customers in other industrial sectors such as pulp and paper, steel, cement, and ports, among others. Each of these groups exhibits specific consumption profiles and dynamics, which justifies differentiated approaches in data collection and modeling.

The bottom-up projection is based on the annual application of extensive surveys conducted with industrial and regional consumers. Companies provide their expectations for energy and power consumption, month by month, for each point of connection to the system. These reports indicate whether the values correspond to existing facilities or to projects planned for future operation. This database is carefully validated by CEN through historical data comparisons and, when necessary, through technical meetings to clarify inconsistencies. Distribution companies also report their expected load at the level of transformers, along with potential migrations of load between substations. These data are particularly important because they include emerging initiatives such as electromobility projects. The high level of granularity and precision is one of the strengths of this method, as it allows for the capture of local specificities and the anticipation of structural changes in consumption.

The top-down projection, in contrast, relies on aggregated econometric models that use macroeconomic variables as inputs, including GDP (through IMACEC), population growth, number of households, and sectoral production projections. This model provides estimates of monthly demand by bus within the SEN and serves two complementary purposes: it offers a way to approximate the demand of small free customers not covered by the surveys, and it acts as a validation instrument for the bottom-up projections. The parallel use of these two approaches ensures consistency between the information provided by companies and the broader structural economic trends.

The consolidated final projection is constructed by starting with the bottom-up base and calibrating it using the top-down results. This integration process involves reviewing the growth rates reported by companies and applying adjustments whenever significant discrepancies or evidence of overestimation are detected. Historically, large consumers have tended to inflate their forecasts and to anticipate the commissioning of their projects, which can result in systematic overestimation of future demand. For this reason, the top-down projection plays a crucial role as a quality control mechanism and as a means of smoothing these anomalies. The outcome of this process is a robust forecast, with coherent trend growth for buses without new projects and gradual increases in areas where effective industrial expansions are expected.

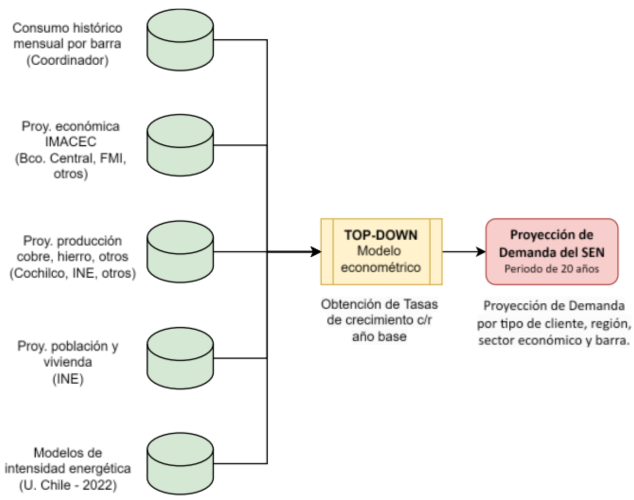

Figure 3. Schematic view of the Chilean demand forecast top-down approach. [COOR24]

The methodology also explicitly addresses new uses of electricity, such as electromobility and residential electrification. For transport, scenarios of replacement of combustion vehicles by electric ones are considered, incorporating penetration rates and average energy consumption per kilometer. These data are used to estimate the future load on the electricity system, disaggregated by region and feeder. For the residential sector, end-use modeling is applied to simulate the evolution of electricity demand for space heating, water heating, cooking, and other uses. Coefficients are adjusted according to dwelling type, energy access, and the fuels used.

$$E_{r,c,v,u,e,t} = N_{r,c,v,t} \cdot I_{r,v,u,e,t} \cdot A_{r,v,u,t} \cdot P_{r,v,u,e,t}$$

$E_{r,c,v,u,e,t}$ = Energy consumed in region *r*, commune *c*, housing type *v* (house or department), end use *u*, energetic *e* and year *t*.

$N_{r,c,v,t}$ = Number of homes by region *r*, commune *c*, type of housing *v* and year *t*.

$I_{r,v,u,e,t}$ = Energy intensity of each end use *u* (expressed in kWh/house) by region *r*, housing type *v*, energy *e*, and year *t*.

$A_{r,v,u,t}$ = Access to final use *u*, for each region *r*, housing type *v* and year *t*.

$P_{r,v,u,e,t}$ = Participation of each energy source *e*, in final use *u*, according to region *r*, housing type *v* and year *t*.

Equation 2 – End use energy consumption model applied by the Chilean Operator [COOR24]

Finally, hourly demand projections are derived from the aggregate energy forecast. Using the PLP and PLEXOS software packages, hourly profiles by bus are generated on the basis of typical daily curves. PLP applies four representative day types and distributes the monthly load into blocks using error minimization algorithms, while PLEXOS allows for independent adjustment of peak power in order to better model maximum demand. This modeling is essential for defining capacity requirements and ensuring system security.

A critical point of the Chilean methodology is its reliance on the good faith and accuracy of the information provided by large consumers. As mentioned, these actors tend to overestimate their projections, which directly impacts forecast accuracy. Another limiting factor is the absence of climate variables such as temperature, cooling degree days (CDD), and heating degree days (HDD) from the econometric models and final adjustments. This omission may complicate the anticipation of demand peaks during extreme weather events, which are highly relevant for operational planning and system robustness.

2.1.4 PJM methodology

The PJM Interconnection (PJM) is a regional transmission organization (RTO) that manages both the power system and the wholesale electricity market for thirteen states and the District of Columbia, including Pennsylvania, New Jersey, Maryland, Ohio, and Virginia, among others. PJM serves approximately sixty-five million people and operates one of the largest electricity markets in the world. Long-term demand forecasting in PJM constitutes a critical component of its resource adequacy processes, as it underpins the requirements of the capacity market through the Reliability Pricing Model (RPM), informs the Regional Transmission Expansion Planning (RTEP) process, and supports regulatory decisions under the Federal Energy Regulatory Commission (FERC).

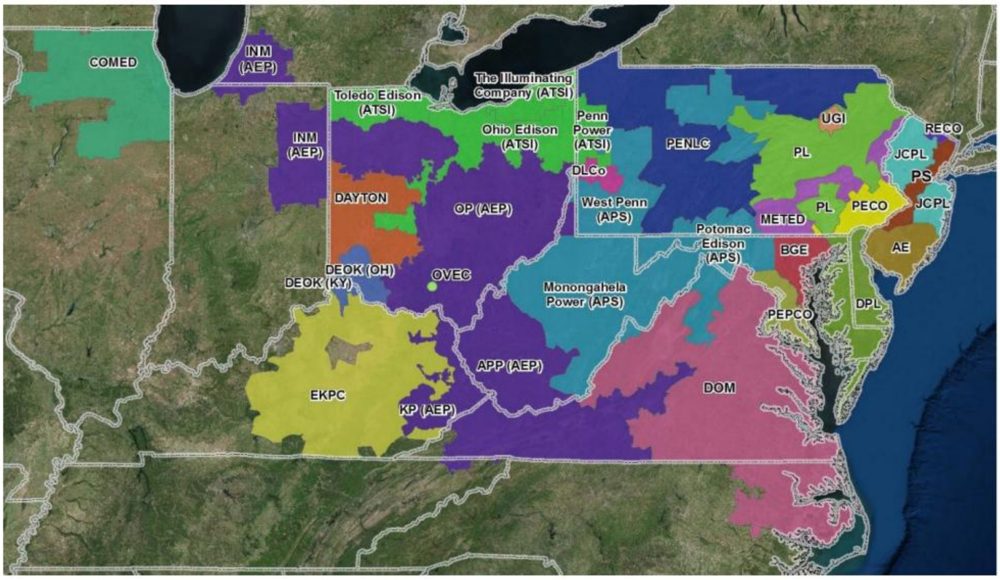

Figure 4. PJM map. [PJM25A]

The forecasting methodology employed by PJM is sectoral in structure and is designed to integrate both monthly and hourly models for the residential, commercial, and industrial segments. These models are parameterized according to end-use consumption through the Statistically Adjusted End-Use (SAE) framework. Inputs include socioeconomic data provided by Moody's Analytics, such as number of households, per capita income, and sectoral gross domestic product. In addition, saturation levels and energy efficiency parameters are sourced from the Energy Information Administration's Annual Energy Outlook (EIA/AEO), which provides annual estimates of end-use intensities. Hourly climatic records are also incorporated, including variables such as temperature, humidity, solar radiation, cloud cover, and wind speed, which are essential for capturing the impact of weather on short-term demand dynamics [PJM25A].

Since 2023, PJM has incorporated hourly weather data into its modeling framework, generating multiples traces per year and for each load zone, applying thirty-one weather years of historical data [PJM25B]. From these simulations, statistical percentiles are derived for demand, including P50 and P90. An hourly profile is generated by each zone, considering in the calibration process adjustments by weekday, weekend and major holidays. The load results are afterwards considered in system reliability studies, as reference scenario for the Forecast Pool Requirement (FPR) and the Effective Load Carrying Capability (ELCC), which sets the contracting guidelines for the reliability auctions.

The general structure of the model is based on a combination of monthly and hourly projections that originate from sectoral equations developed for the residential, commercial, and industrial classes. These equations are constructed within the SAE framework, where independent variables incorporate economic and technological indicators together with climatic data. Economic inputs are provided by Moody's Analytics and include projections of the number of households, real per capita income, active population, and sectoral gross domestic product. Data on saturation levels and equipment efficiency are obtained from the EIA's Annual Energy Outlook, processed and adapted for PJM by Itron. Climatic variables are sourced from hourly meteorological data series on temperature, relative humidity, solar radiation, cloud cover, and wind speed. These data are spatially weighted across the distribution companies (EDCs) in each zone to ensure representativeness of local weather conditions.

The sectoral equations are initially specified at the monthly level. In the residential sector, for example, the number of customers is projected on the basis of household data, while the average consumption per customer is estimated through linear regression models that incorporate heating, cooling, and other end uses as explanatory variables. The monthly results are then transformed into end-use indices representing heating, cooling, and other consumption. These indices are smoothed using a 365-day moving average and subsequently converted into daily indices, namely HeatIdx, CoolIdx, and BaseIdx. These daily indices are later employed as explanatory variables in zone-specific hourly models, which are calibrated using historical load data and hourly climatic observations.

With respect to distributed photovoltaic generation, its treatment in the PJM forecasting methodology is explicit and exogenous. Historical loads are reconstructed by adding back the measured or estimated solar generation, which is obtained from solar irradiation data combined with the installed capacity in each zone. In this way, the regression captures the gross consumption of customers before the effect of self-generation. For future projections, distributed generation is subtracted ex post from the projected load, based on specific forecasts of future installed capacity and typical hourly generation profiles for each zone.

Electrification of the transport sector, represented primarily by the adoption of electric vehicles (EVs), is also treated exogenously with respect to the core regression models. PJM incorporates scenarios for EV fleet growth, the associated hourly charging profiles, and the resulting impact on net load by zone. This approach makes it possible to test different charging management strategies, such as night-time charging or on-demand charging, and to evaluate their effects on peak demand and on the overall shape of the load curve.

In the case of industrial electrification, the treatment is more limited. Part of the growth is implicitly captured through projections of industrial output and energy intensity by sector, measured in kilowatt-hours per unit of product. However, specific additions such as new energy-intensive industrial plants or large-scale data centers are addressed through exogenous manual adjustments, developed in consultation with market participants. This decision reflects the difficulty of accurately representing structural shocks with highly specific location and load profiles using purely econometric models.

The forecasts are produced annually with a long-term horizon of up to fifteen years, although the standard reference horizon is generally ten years for regulatory and operational purposes. Updates are carried out once per year, with the Long-Term Load Forecast typically published in the first quarter. In each forecasting cycle, the input variables are updated with the most latest information on climate, macroeconomic conditions, technological adoption, and end-use consumption, and the models are re-estimated as necessary.

Critical assessments, however, highlight inconsistencies in PJM's forecasts for large consumers such as data centers. Market participants have raised concerns, describing the process as speculative and inconsistent, noting that the data provided are undocumented with respect to the actual feasibility of future loads, and therefore result in questionable forecasts. Sectoral evaluations have further suggested that PJM tends to overestimate reserve requirements, leading to over-procurement in the RPM capacity market, derived by an "overpredicted peak demand in 17 out of the last 18 years", raising concerns about the credibility of its projections. This over-procurement has been criticized for artificially inflating costs for end consumers [SMFD25].

2.1.5 ISO-NE methodology

ISO-NE is the Independent System Operator responsible for managing the transmission grid and wholesale electricity markets in the six New England states, namely Connecticut, Maine, Massachusetts, New Hampshire, Rhode Island, and Vermont. Since 2005, ISO-NE has operated as a Regional Transmission Organization (RTO) under the oversight of the Federal Energy Regulatory Commission (FERC). Long-term demand forecasting developed by ISO-NE plays a dual strategic role. On the one hand, it provides the technical foundation for determining the Installed Capacity Requirement (ICR) and the Forward Capacity Market (FCM), which define the level of capacity to be procured in order to ensure future reliability. On the other hand, it guides transmission planning and system resource adequacy assessments, thereby influencing both operational reliability and long-term infrastructure investment decisions.

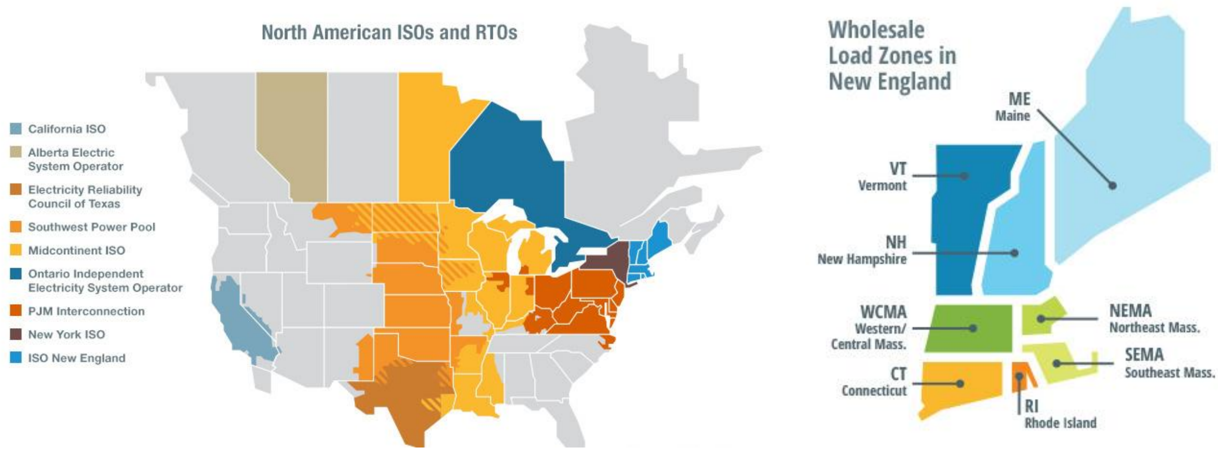

Figure 5. ISO-NE load zones and North America ISOs. [ISON25A]

ISO-NE's load forecast estimates the energy and demand for 10 years for the states they serve, with this forecast been applied for power system planning and reliability studies [FELS21]. The model generates estimates for annual energy (in GWh) and seasonal peak demand (in MW), both calculated before and after the application of reductions. These are defined respectively as gross load, which represents the reconstructed consumption before accounting for policy or distributed resource impacts, and net load, which reflects the effective demand that must be supplied by the centralized system after accounting for distributed energy resources and efficiency programs. Forecast results are published each year in the Capacity, Energy, Loads, and Transmission (CELT) Report, and methodological revisions are continuously discussed in open stakeholder processes such as the Load Forecast Committee.

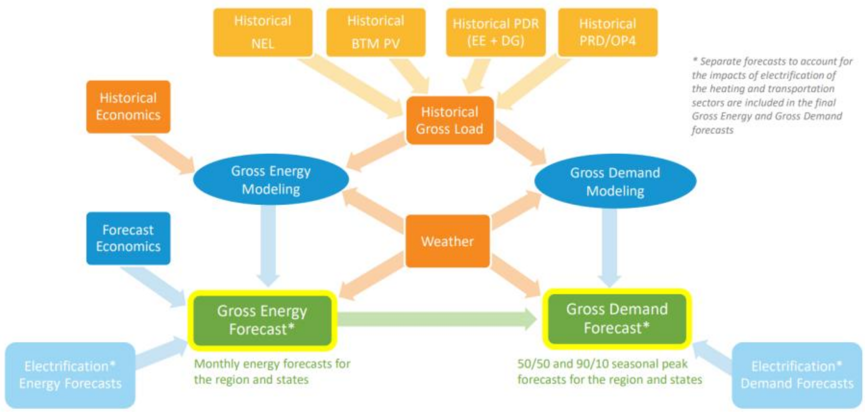

Figure 6. High-Level Process Flow Chart applied by the ISO-NE. [ISON23]

The forecasting process begins with the reconstruction of gross load from the observed Net Energy for Load (NEL), which corresponds to load measured at the transmission interface, adjusted for imports and the charging or discharging cycles of storage units such as pumped hydro facilities. To this reconstructed series, ISO-NE adds back historical hourly series of energy efficiency (EE), passive distributed resources (PDR), and in particular behind-the-meter solar photovoltaic (BTM PV), which is not captured by system-level metering. BTM PV is estimated using quarterly reports of installed capacity, standardized hourly generation profiles, and sampling-based estimation methods. The results are incorporated ex ante into the historical series, ensuring that the forecasting model is calibrated on the true gross load prior to regulatory adjustments. For future projections, EE and BTM PV are subtracted ex post in order to obtain the final net load to be supplied by the wholesale market.

$$Load_{Net} = NEL + PRD$$

$$Load_{Gross} = NEL + PRD + EE + DG + BTMPV$$

NEL = Net Energy for Load, defined as the net generation, plus net interchange across external tie lines, less energy required for storage at energy storage facilities

PRD = Price-responsive demand, which is flexible load that is dispatched in real-time

EE = Net Energy for Load, defined as the net generation, plus net interchange across external tie lines, less energy required for storage at energy storage facilities

DG = Passive (non-dispatchable) distributed generation resources

$BTMPV$ = Behind-the-meter photovoltaic installations that do not participate in wholesale markets but reduce metered load

Equation 3 – Net Energy for Load and Reconstitution of Load applied by the ISO-NE [ISON23]

For the estimation of gross annual energy, ISO-NE employs a log-log ordinary least squares (OLS) model in which the dependent variable is the natural logarithm of NEL for each year, by each of the seven modelled regions. Explanatory variables include real gross domestic product, population, heating degree days (HDD), cooling degree days (CDD), energy prices, and dummy variables capturing atypical years such as 2008, corresponding to the global financial crisis, 2020, reflecting the COVID-19 pandemic, or years with exceptional weather conditions. The inclusion of these dummy variables allows the model to account for transitory shocks without compromising the consistency of the long-term econometric fit. The weather data applied are based on a recent 30-year history and reflect an average monthly degree days by month.

$$Gross\ Energy_{month} = \beta_0 + \beta_1 \cdot Economy + \beta_2 \cdot Weather + \beta_3 \cdot Weather \cdot Trend$$

β_i = Regression model coefficients

$Economy$ = Annual economic variable(s)

$Weather$ = Monthly weather variable(s)

$Trend$ = Annual linear counter from an initial start year

Equation 4 – Gross energy modeling applied by the ISO-NE [ISON23]

For peak demand estimation, ISO-NE adopts a linear regression framework in which the dependent variable is the seasonal peak, defined either as the maximum daily peak or the maximum quarterly peak. The explanatory variables include the gross monthly load, weather data, defined not only by the CDD and HDD, but also weighted temperature-humidity index and effective temperature. A typical specification is expressed as follows:

$$Peak\ Demand_{day} = \beta_0 + \beta_1 \cdot Gross\ Energy_{month} + \beta_2 \cdot Weather + \beta_3 \cdot Weather \cdot Trend\ + \beta_4 \cdot Calendar$$

β_i = Regression model coefficients

$Weather$ = Monthly weather variable(s)

$Calendar$ = Holiday or Day of Week indicators

$Trend$ = Annual linear counter from an initial start year

Equation 5 – Peak demand modeling applied by the ISO-NE [ISON23]

These models generate probabilistic weekly and seasonal distributions, which allow the derivation of percentiles such as P50 (median), P95 (which corresponds to so called "50/50 peak"), and P99 (which corresponds to so called "90/10 peak"). These scenarios are built essentially by the weekly weather distributions, derived using a 30-years period of historical weather data. Such probabilistic outcomes are essential for reserve planning and for determining the Installed Capacity Requirement (ICR), as they provide forward-looking visibility over potential critical capacity scenarios and allow ISO-NE to stress-test the adequacy of system resources under varying conditions.

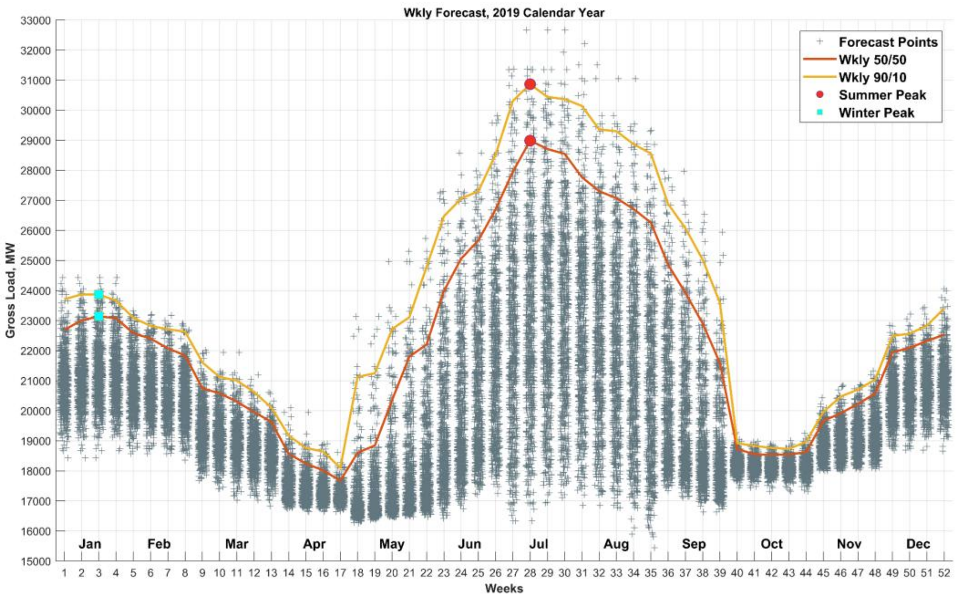

Figure 7. ISO-NE 2019 Forecast Example. [ISON23]

In addition to the econometric core of the long-term load forecast, ISO-NE incorporates exogenous adjustments that capture the structural impacts of energy efficiency programs, photovoltaic development, and passive demand resources. Each year, ISO-NE produces a dedicated forecast of long-term savings in both energy and peak demand resulting from state-sponsored energy efficiency initiatives. The energy efficiency forecast is closely aligned with the methodology used to reconstitute Passive Demand Resources (PDR) into the gross load, ensuring that the underlying regression models are calibrated on a consistent demand baseline. The model relies on state-level budgets provided by regulatory commissions or their representatives, which serve as the primary constraint on the achievable savings. To estimate future reductions, ISO-NE applies assumptions regarding the allocation of program activity across end-uses, evolving over time according to administrator-provided data. Seasonal coincidence factors are used to differentiate summer and winter peak impacts, reflecting the temporal variability of efficiency-driven savings. This approach ensures that the gross-to-net reconciliation accounts for sectoral heterogeneity and the gradual escalation of production costs, while embedding economic indicators such as inflation into the forecast trajectory.

The photovoltaic (PV) forecast follows a policy-based approach, recognizing that distributed solar expansion in New England is largely the outcome of state-level initiatives. ISO-NE does not independently project the introduction of new policies but instead anchors its forecast on the explicit goals already established by state governments. Within this framework, PV resources are disaggregated into three categories: capacity resources that participate in the Forward Capacity Market, energy-only generators outside of the FCM, and behind-the-meter photovoltaic installations. Of particular importance is the treatment of behind-the-meter PV, which is reconstituted into historical gross load by combining installed capacity data with standardized hourly production profiles and solar irradiation metrics. This reconstitution allows ISO-NE to calibrate its econometric models on the unobserved gross demand, avoiding distortions caused by embedded distributed generation. For future projections, BTM PV output is subtracted ex post from the gross forecast, producing the net load used in market operations and transmission planning.

Finally, the methodology also carries out a reconstitution of Passive Demand Resources, instead of simply accounting for all installed measures. Taking into consideration the results from the Capacity Supply Obligations (CSOs) in the most recent Forward Capacity Auction, ISO-NE calibrates the real contribution from the PDR, focusing on the quantity that effectively participates in the capacity market, and in this sense avoiding overestimating demand reductions from expired or non-participating measures. The reconstitution procedure follows a staged process: first, a linear trajectory is established between the inception of PDR participation in 2006 and the most recent CSO values; second, this trajectory is applied separately to summer and winter months; and finally, the resulting monthly megawatt values are used to derive the hourly adjustments incorporated into the gross load. The outcome is a more precise alignment between modeled demand and the market-relevant contributions of PDR, thereby enhancing the transparency and robustness of the long-term load forecast.

Historically, ISO-NE did not generate complete hourly load profiles for the full 8,760 hours of the year. Instead, the methodology relied on historical typical hourly profiles to disaggregate projected monthly loads and daily peaks into approximate hourly patterns. Since 2025, however, the model has evolved to incorporate full hourly forecasts, thereby enabling a more explicit treatment of behind-the-meter photovoltaic generation (BTM PV) and electrification trends with temporal granularity [ISON25B]. Even so, the integration of these hourly projections into the CELT forecasting cycle remains limited. The most recent updates, covering 2024 and 2025, emphasize the enhancement of climatic variables through the inclusion of additional meteorological stations and the explicit integration of the Temperature Humidity Index (THI). They also include refinements in BTM PV estimation and advances in the modeling of residential and transport electrification, particularly through the inclusion of electric vehicles and heat pumps. These factors are incorporated as exogenous adjustments applied at the final stage of the modeling process, maintaining the underlying logic of reconstructing gross load first and subsequently subtracting distributed resources and efficiency measures to obtain the final net load projection.

2.2 SCIENTIFIC LITERATURE REVIEW

The increasing frequency and intensity of extreme weather events, associated with the broader dynamics of global climate change, has attracted growing attention in scientific literature concerning the impacts of climatic variability on the operation, expansion, and reliability of power systems. A growing body of recent studies highlights how the rise in average temperatures, greater interannual variability, and seasonal anomalies can simultaneously affect both electricity demand and supply, thereby undermining traditional planning and operational practices that rely on stationary assumptions. In particular, the conventional presumption that variables such as demand, renewable generation, and thermal generator availability are independent of temperature or follow stable historical patterns has been increasingly challenged by new empirical evidence.

According to [MUSA19], conventional resource adequacy models, as traditionally applied by system operators such as PJM Interconnection in the United States, typically assume that forced outage rates (FOR) of thermal generators are constant and uncorrelated with meteorological variables. While this simplification is operationally convenient, it introduces the risk of systematically underestimating the likelihood of generator unavailability under adverse weather conditions. This limitation becomes especially critical during episodes of extreme temperatures, such as heat waves or cold snaps, where surging demand coincides with deteriorating performance of conventional thermal generation. The compounded effect of higher load and increased forced outage probability places additional stress on the system, leading to potential shortfalls in capacity at the very moments when reliability is most at stake.

Building on this motivation, the same study has investigated empirically the relationship between temperature and the forced outage rates of thermal generating units in the PJM region, one of the largest electricity markets in the world, covering several states across the Northeastern and Mid-Atlantic United States. The authors rely on a comprehensive dataset spanning 23 years from the Generating Availability Data System (GADS), maintained by the North American Electric Reliability Corporation (NERC). This database provides hourly records of unit availability and forced outages for a wide spectrum of thermal technologies, including coal, oil-fired plants, natural gas units operating in both simple and combined-cycle configurations, and nuclear generation.

The methodological framework centers on the estimation of logistic regression models linking the probability of a forced outage to ambient temperature, with the explicit goal of deriving temperature-dependent availability curves for each generator type. The results provide clear and statistically robust evidence of a non-linear relationship between thermal plant performance and external temperature conditions. More specifically, the study demonstrates that once temperature surpasses certain thresholds the forced outage rate increases substantially, signaling heightened vulnerability of thermal generation during extreme heat events, especially for coal- and gas-fired units. Conversely, very low temperatures also raise the probability of outages, particularly in gas-fired generators that rely on non-firm fuel supply contracts, which are prone to disruptions during stress events in the natural gas system. One of the most prominent examples is the Polar Vortex of 2014, which exposed the fragility of gas supply chains and caused significant unavailability in thermal generation precisely at a time of elevated electricity demand.

Such occurrences can lead to correlated failures across multiple thermal generating units, thereby violating the assumption of statistical independence that is often embedded in conventional reliability calculation. Correlated outages imply that the joint probability of unavailability for several plants under particular meteorological conditions may be significantly higher than predicted by models that treat outages as independent and purely stochastic events. These finding challenges one of the most fundamental premises of traditional reliability modeling, underscoring the risks of overlooking common-mode failures induced by weather extremes.

Given this empirical evidence, the author developed a second study [MULA20], in which they explicitly incorporated the climate dependency of thermal unit availability into a system-level resource adequacy model. For this purpose, they employed RECAP (Renewable Energy Capacity Planning Model), an open-source framework calibrated specifically for the PJM system in the 2018/2019 delivery year. RECAP performs hourly simulations of the interactions among thermal generation, renewable generation (wind and solar), and electricity demand, with each component driven by historical records and climate-based projections. By integrating weather-sensitive availability curves into a systemic model, the approach moves beyond static assumptions and captures the operational risks of simultaneous stress across demand and supply.

In representing demand, the study adopted regression models based on heating degree days (HDD) and cooling degree days (CDD), in order to link the daily average temperature to electricity consumption, while adjusting for seasonal and socioeconomic variables. Wind generation was modeled using hourly production profiles derived from the National Renewable Energy Laboratory (NREL) database for representative locations across the PJM footprint. Solar generation relied on the National Solar Radiation Database (NSRDB), which was converted to alternating current output through the GridLab-D model. Thermal generator availability, in turn, was incorporated using the logistic curves estimated in the first study, embedding the hourly variability of forced outage rates as a function of simulated temperature.

The application of RECAP enabled the direct quantification of the impact of climate-dependent thermal availability on system reliability, expressed in terms of the LOLE index. The results are striking: to achieve the industry benchmark of 0.1 LOLE, the required reserve margin increased from 15.9% under the assumption of constant forced outage rates to 22.9% when accounting for climate-dependent failures. In other words, ignoring the weather sensitivity of thermal unavailability can lead to systematic under-procurement of capacity, thereby elevating the risk of load-shedding events or blackouts.

However, the study also notes that in that delivery year PJM procured an even higher reserve margin of 26.6%, which, when evaluated under the climate-dependent model, would correspond to a LOLE below 0.02. According to the authors, this additional procurement implied an incremental cost of approximately 315 million U.S. dollars in capacity payments. The implied value of lost load (VOLL) associated with this decision was estimated at around 700,000 U.S. dollars per megawatt-hour, a figure nearly two orders of magnitude above the VOLL parameters typically employed in operational dispatch and planning studies. While such over-procurement might be interpreted as a precautionary strategy in the face of climate uncertainty, it also exposes the inefficiencies of relying on traditional, climate-insensitive adequacy models. By not fully capturing the weather-dependent risks, system operators may inadvertently commit to capacity levels that overshoot the economically efficient optimum, with significant financial implications for consumers.

In addition to the reliability analysis under different reserve margins, additional analyzes also tested future climate change scenarios characterized by average temperature increases of 1 °C and 2 °C relative to the historical baseline period of 2006–2017. The results demonstrated that such increases in ambient temperature would lead to additional capacity requirements of approximately 0.5% to 1.5% in order to maintain the same reliability target. When combined with scenarios that assume the retirement of coal and nuclear facilities, replaced predominantly by natural gas combined-cycle (CCGT) units, the required reserve margins shift further, decrease slightly the reserve margin required due to the lower forced outage rates of combined-cycle gas generators during the hot critical hours, underscoring the critical importance of properly accounting for the climate sensitivity of newly installed generation resources in long-term expansion planning.

Another significant contribution of the study lies in its proposal to replace the annual capacity procurement paradigm with monthly adequacy targets, motivated by the strong seasonality of risk in the PJM system. Their analysis reveals that the majority of the LOLE is concentrated in the months of July and August, coinciding with the most severe heat waves and associated stress on the thermal fleet. By contrast, the risk of unserved load during the remaining months is relatively limited. Consequently, the authors demonstrate that reducing capacity commitments by up to 16% in the off-peak months would not compromise system reliability, provided that adequacy is maintained during the critical summer period. This adjustment could yield substantial economic efficiency gains by avoiding over-procurement of capacity and would also facilitate the integration of variable renewable energy resources such as solar, wind and demand-responsive loads, whose contributions vary seasonally.

Finally, the authors emphasize that while the RECAP model represents a considerable step forward toward more realistic reliability modeling, it nonetheless retains important limitations, as for example the absence of a fully sequential hourly unit-commitment framework that can represent the chronological interdependence of dispatch decisions and the operational constraints of thermal units during extreme events. RECAP simulates availability and load interactions stochastically but does not explicitly model the intra-day operational dynamics of thermal generation under stress conditions. The authors argue that future work should focus on embedding climate-dependent availability curves into Security-Constrained Unit Commitment (SCUC) models, which would enable a more faithful representation of operational realities.

The assessment of power system reliability under increasing climate variability and the intensification of extreme weather events requires, in addition to a detailed characterization of electricity demand, a realistic representation of the availability of generation resources. In the Brazilian context, although hydropower has historically dominated the generation mix, the growing presence of thermal power plants makes the analysis of their forced outage rates (FOR) particularly critical, especially under adverse climatic conditions. A reference in this debate is the study by [SANT20], which sought to evaluate the reliability of Brazilian thermal units using operational outage data provided by the National System Operator (*Operador Nacional do Sistema Elétrico* - ONS), comparing the results against international benchmarks established by the North American Electric Reliability Corporation (NERC).

The research was based on a comprehensive dataset of historical unavailability compiled by the ONS, encompassing multiple thermal technologies installed within the Brazilian Interconnected Power System (*Sistema Interligado Nacional* - SIN). The central objective was to test the robustness and adequacy of the data and to verify whether the forced outage rates observed in Brazil are comparable to those documented in North America. According to the authors, the results indicate that the reliability statistics of Brazilian thermal plants are generally favorable and broadly consistent with the reference parameters employed by NERC. This finding is particularly significant for the planning and operation of the Brazilian power system because it demonstrates that, despite differences in regulatory frameworks, generation mix structure, and climatic conditions, the technical performance of thermal plants in Brazil is in line with international standards of availability and reliability.

It is important to emphasize, however, that the study did not attempt to identify significant seasonal variations in the forced outage rates of Brazilian thermal units, focusing instead on annual averages. This limitation underscores a promising avenue for future research: the empirical analysis of how temperature and other climatic variables influence the availability of thermal plants in Brazil. Such analysis would require the use of advanced statistical models capable of detecting patterns of correlation, heteroscedasticity, and extreme behavior in outage probabilities. By pursuing this line of investigation, it would be possible to significantly refine the assessment of system reliability in Brazil, particularly under conditions of hydrological scarcity and an increasing reliance on thermal generation in the national energy mix. This refinement would be especially relevant for securing supply during peak hours, when system stress is highest and the contribution of thermoelectric resources becomes most critical.

The relevance of incorporating climate dependence into expansion planning models is also demonstrated in the study conducted by [RCJB21], which focused on estimating the effects of climate change on optimal generation expansion decisions in the southeastern United States. The article presents an integrated approach to evaluating future scenarios of rising temperatures and their repercussions on both electricity demand and the availability of thermal generators.

In this context, the authors developed a framework composed of multiple coupled models, centered on a deterministic expansion model that minimizes the total system costs while accounting for both investment expenditures in new capacity and operating costs at an hourly resolution. With a planning horizon extending to 2050, the model identified, in five-year intervals, which generation technologies should be added to the system. Climate change impacts were endogenously integrated into the model through climate projections from twenty CMIP5 models, under both RCP 4.5 and RCP 8.5 scenarios, spatially and temporally disaggregated.

Electricity demand was modeled using an econometric specification estimated with hourly historical data from FERC (2006–2015), combined with climate variables from the gridMET dataset. Socioeconomic drivers such as population growth and GDP were held constant, with the objective of isolating the direct effects of climate on load. On the supply side, the authors incorporated multiple climate-driven effects, including the reduction in available capacity of thermal plants under high ambient air and water temperatures, as well as changes in hydroelectric potential resulting from shifts in streamflow patterns. The performance of thermal units under different environmental conditions was derived from response curves generated by the Integrated Environmental Control Model (IECM), which links local meteorological variables with the performance of cooling technologies in thermal power plants.

The results showed that, even when disregarding CO_2 emissions constraints, the explicit inclusion of climate impacts in the expansion model led to a 35% increase in total installed capacity by 2050 compared with the reference scenario without climate change. This expansion was driven primarily by up to a 16% increase in summer peak demand and, to a lesser extent, by the efficiency losses in conventional thermal units. Solar generation emerged as particularly advantaged, given its temporal alignment with the new summer peak hours, partially offsetting the decline in performance of the thermal fleet.

An important aspect of the findings is the convergence between mitigation and adaptation strategies. The expansion of the electricity system to cope with climate impacts indirectly drives a reduction in carbon emissions by shifting the technology mix toward renewable sources. Thus, the study suggests that integrating climate risks into energy planning can generate dual benefits, avoiding underinvestment in system reliability while simultaneously contributing to environmental decarbonization goals.

The authors also acknowledged several limitations of the study. The most important was the assumption of stationarity in socioeconomic variables, in addition to the exclusion of new load types such as those associated with large-scale electrification of transport. The analysis also did not consider emerging technologies such as battery storage, hydrogen, or small modular nuclear reactors, which could play a significant role in future scenarios. Furthermore, climate impacts on renewable resources such as wind and solar radiation, as well as transmission network constraints, were not modeled, given the greater uncertainty associated with such projections.

The results obtained by [RCJB21] corroborate the findings of earlier studies by [MULA20], reinforcing the argument that the incorporation of climate variability is not only desirable but essential to avoid systematic errors such as the underestimation of required installed capacity or the overvaluation of less reliable resources under thermal stress conditions. The main innovation of the former work lies in the concrete application of CMIP climate projections to guide expansion decisions, thereby bridging the gap between technical literature and integrated climate–energy system modeling.

The relevance of this approach to the Brazilian case is evident, particularly given the increasing vulnerability of the national power system to extreme events such as prolonged droughts and heatwaves. While traditional expansion models used by Brazilian planners do consider hydrological scenarios and demand projections, the systematic incorporation of robust climate projections that affect both supply and demand simultaneously remain limited. The implementation of methodologies similar to those abovementioned, adapted to Brazil's institutional and technical context, could represent a significant step forward in improving the quality of national energy planning. This is especially critical in the context of rising thermal participation in the generation mix, coupled with the accelerated expansion of solar and wind power.

Electricity demand forecasting in medium-term horizons constitutes a fundamental component of energy planning, with direct implications for generation expansion, the definition of operating reserves, and the evaluation of system reliability. The growing climatic variability and the intensification of extreme events impose additional challenges to this task, making it imperative to incorporate meteorological variables, particularly temperature, into predictive models. Recent studies have sought to refine forecasting methodologies by integrating traditional statistical approaches with machine learning techniques, aiming to improve the accuracy of estimates and capture nonlinearities in the relationship between climate and energy consumption. In this context, the articles by [BAFR23], focused on Italy, and [AVMA18], focused on the city of Sydney, Australia, offer significant contributions both from the methodological perspective and from the analysis of climatic impacts on electricity load.

The role of temperature as an explanatory variable for electricity consumption has become increasingly relevant in the load forecasting literature, particularly in contexts marked by growing climatic variability and the intensive penetration of cooling and heating systems. Medium-term demand forecasting (covering horizons from day to months) involves specific challenges, such as uncertainty about the future behavior of temperature and the need to preserve model interpretability in operational and regulatory environments. Overly complex models may deliver statistical gains but become difficult to apply in planning agencies, where transparency and reproducibility are essential. In this regard, the abovementioned stand out by proposing methodological solutions that reconcile econometric rigor with practical applicability, exploring different ways of including temperature as a predictive factor.

The study by [BAFR23] has as its central objective the comparative assessment of the performance of linear econometric models and artificial neural networks in forecasting daily electricity demand in Italy, for the period 2016-2019, considering different strategies for incorporating temperature. The main motivation of the article lies in the observation that, while short-term forecasting benefits from reliable meteorological projections, medium-term horizons face substantial limitations in anticipating climatic variables, which may compromise the accuracy of load estimates. To overcome this limitation, the authors test different representations of future temperature, ranging from a “perfect” forecast to more realistic approximations such as historical averages and random walk models.

The methodological approach is based on two main classes of models: linear regressions (both static and ARMA/ARMAX specifications) and feed-forward artificial neural networks (FNN) with a single hidden layer and sigmoid activation function. In both classes, the authors incorporate seasonal variables and binary dummy variables to control structural patterns in the load. Specifically, they use indicator variables for Saturdays, Sundays, Mondays, holidays, and months of the year. This structure makes it possible to capture the influence of recurrent factors related to the calendar and to the seasonality of consumption.

With respect to temperature modeling, the article adopted an asymmetric linear spline with a turning point at 60°F (approximately 15.5°C), reflecting the asymmetric effect of cold and hot days on consumption. This representation allows the model to adequately capture the differentiated use of energy for heating and cooling as the temperature moves away from the thermal comfort point. The study tests four strategies for forecasting temperature: (i) a “perfect” future temperature, used as a theoretical benchmark; (ii) the observed temperature from the previous day (t-1); (iii) the average of the last five years for the same day of the year; and (iv) a random walk model, in which future temperature is assumed to be equal to the most recent observation. These strategies are applied both in regressions and in neural networks, allowing for a systematic comparison of the impacts of temperature on the predictive accuracy of each class of models.

The empirical results are evaluated using metrics such as RMSE (Root Mean Square Error) and MAPE (Mean Absolute Percentage Error), in addition to statistical tests of predictive significance. The inclusion of temperature significantly improves forecasts, especially in the first days of the prediction horizon. When perfect temperature is used, the gains are evident across all horizons. In more realistic scenarios, the benefits are statistically significant up to the fourth day for regressions and up to the third day for neural networks.

Neural networks demonstrate superior performance compared to linear regressions in horizons of two to seven days. However, beyond one month, the gains become marginal and linear models, equipped with seasonal dummies and exogenous variables, return to showing competitive results. This observation suggests that although FNNs are more effective at capturing the nonlinearity of the load’s response to temperature, their advantage is more pronounced in short horizons, where transient shocks in temperature still strongly affect demand. In longer horizons, climatic variability tends to smooth out, and simpler models with seasonal controls become more effective.

Additional robustness tests are carried out with alternative estimation windows and with regional samples (with a focus on Northern Italy), confirming the generalization of the results. The authors conclude that although future temperature cannot be predicted with precision, even simplified estimates of this variable, such as historical averages or random walk models, contribute positively to demand forecasting. This reinforces the importance of interpretable and robust models that incorporate relevant explanatory variables, particularly in environments where analytical justification is required for decision making.

Complementarily, the article [AVMA18], adopts a distinct approach focused on analyzing the impacts of climate change on per capita electricity demand in the city of Sydney. The research begins with the hypothesis that the increase in average temperature, accompanied by changes in correlated climatic variables such as humidity, evaporation, solar radiation, and wind, will significantly affect energy consumption patterns over the coming decades. The methodology integrates Pearson correlation analysis, the calculation of degree days (CDD and HDD), and multiple linear regression with backward elimination to quantify these impacts.

Initially, the study characterizes the global and regional climate scenarios projected by the IPCC and CSIRO, estimating that Sydney's temperature will increase between 0.9°C and 3.0°C by 2070, with repercussions on evaporation (increase), humidity (decrease or stability), and precipitation (reduction). Based on historical data from AEMO and the Bureau of Meteorology (1999-2010), the authors conduct a correlation analysis between temperature and the other climatic variables. Evaporation shows a positive correlation with temperature, while humidity and precipitation display a negative correlation.

Subsequently, the study applies the concept of balance point temperature (BPT), defined as the temperature at which energy consumption for climate control is minimized. Although many international studies adopt the standard value of 18.4°C, empirical analysis indicates that the BPT for Sydney is 14.3°C. From this value, the CDD (Cooling Degree Days) and HDD (Heating Degree Days) indicators are calculated, quantifying the need for cooling or heating over time and thus making it possible to measure the sensitivity of electricity demand to temperature variation.

The multiple linear regression model is estimated using the backward elimination technique. The process begins with an initial set of climatic variables (CDD, HDD, humidity, evaporation, precipitation, and wind speed), and at each step, the variable with the lowest statistical significance ($p > 0.05$) is excluded. In the final specification, only three variables remain: CDD, wind speed, and evaporation. HDD, despite its theoretical relevance in colder regions, proved to be statistically irrelevant for Sydney and was discarded in the first step. The final model achieved an R^2 of 81.6%, indicating good explanatory power for the historical data.

With the estimated coefficients, the authors simulate the impact of global warming on per capita electricity demand through 2070, combining the econometric model with climate projections from the IPCC's A1B, B1, and A1F1 scenarios. The results indicate an expected increase of 6% in demand per capita by 2030 and between 11.2% and 21.6% by 2070, depending on the scenario. These projections assume that there will be no significant advances in energy efficiency or behavioral changes, thereby isolating the pure climatic effect.

However, in system reliability analyses, it becomes imperative to also consider the distribution of demand scenarios rather than only their expected value. The article [HYFA10] represents a significant advance by proposing a probabilistic approach to forecasting peak electricity demand. The methodological proposal presented by the authors stems from the recognition that electricity demand, especially in its peak form, is subject to multiple sources of uncertainty, among them climatic variations, economic fluctuations, and demographic factors, which cannot be adequately captured by traditional deterministic forecasts.

The structure of the model developed is semiparametric and additive, composed of two main components: an annual model and a half-hourly model. The annual model is responsible for capturing the long-term trend of peak demand, using as explanatory variables the State Gross Product (GSP), the average electricity price lagged one year, and the sum of Cooling Degree Days (CDD) during the summer. These variables were selected based on the Corrected Akaike Information Criterion (AICc), which seeks a balance between parsimony and quality of fit, particularly important given the limitation of available annual data. The results of the model indicate interpretative coherence: GSP and CDD are positively related to demand, while electricity price shows a negative relationship, reflecting load elasticity in response to marginal costs.

The half-hourly model, in turn, consists of 48 distinct regressions, one for each half-hour period throughout the day, each with a specific set of explanatory variables. The selection of these variables is carried out through an iterative elimination procedure similar to the backward stepwise method, based on cross-validation. Among the variables considered are current temperature and its lags, maximum and minimum values of the last 24 hours, weekly averages, and calendar variables such as day of the week, holidays, and relative position within summer. The methodology ensures that only variables with statistically significant contribution to reducing the mean squared error (MSE) remain in the final model.

One of the main innovations of the article lies in the generation of future temperature scenarios to feed the calibrated models. To this end, the authors propose the use of the double seasonal block bootstrap, an adaptation of the traditional block bootstrap method that allows preserving both the daily and annual seasonality of the historical temperature series. This technique consists of extracting moving blocks of 7 to 11 days of length, with displacements of up to three days in the calendar, and adding light stochastic noise, simulating synthetic series that maintain the statistical coherence of historical data from 1900 to 2008. The use of two levels of seasonality makes it possible to capture more realistic temperature patterns, which are essential for sizing peak demand in future contexts.

By applying this technique, the authors generate 2000 hourly temperature scenarios for each year of the forecast horizon (2008 to 2018), which, combined with GSP and electricity price projections (under three economic scenarios), feed into the previously calibrated models. The hourly demand for each scenario is then estimated, allowing the construction of complete distributions of weekly and annual peak demand. The analysis of these distributions is conducted through probability of exceedance (PoE) metrics, with emphasis on the 10%, 50%, and 90% percentiles, representing respectively the demand values that are exceeded in 10%, 50%, and 90% of the simulated scenarios. The validation of the model was carried out using data from the summer of 2007–2008, the last year not included in the calibration. Both the ex-ante forecast (using only data up to 2007 and the synthetic temperature scenarios) and the ex-post forecast (with real temperature and explanatory variables) showed high adherence to the observed values.

The study also discusses sources of uncertainty that remain in the forecasting process, even with the use of advanced simulations. In addition to climatic variability, which represents the largest share of uncertainty captured by the synthetic temperature series, the article highlights economic uncertainty, especially in longer horizons, where projections of GSP and electricity prices become more volatile. Even so, the model demonstrated stability and effectiveness, being able to provide probabilistic forecasts in reduced computational time (less than one hour on conventional computers). The authors acknowledge that future extensions of the model may explicitly include climate change trends in the temperature series and the use of more climate measurement points in order to increase the geographic representativeness of the modeling.

The methodological contribution from this paper is significant for offering a tool that combines predictive capacity and statistical transparency, allowing the planner not only to know the expected forecast but also the risk distribution associated with peak demand. The model is particularly valuable for decisions related to firm capacity contracting, expansion planning, and operational risk management, since it provides PoE estimates that can be directly integrated into the security and reliability criteria adopted by operators and regulators.

Complementarily, the article [SDZC23] proposes an alternative approach based on deep learning techniques. Although less transparent than the semiparametric model previously presented, the proposal in this article stands out for its ability to capture complex and nonlinear patterns of the electricity load series through the decomposition of demand into two distinct components: base load and seasonal load. The base component is modeled with a two-layer MLP (Multi-Layer Perceptron) neural network, having as explanatory variables time and daily average temperature, while the seasonal component is treated by an LSTM (Long Short-Term Memory) network, capable of capturing short- and long-term temporal dependencies. This structural separation allows each part of the load to be modeled with techniques appropriate to its spectral nature, with the MLP being more suitable for low-frequency trends and the LSTM for high-frequency oscillations.

The empirical results presented are promising: the model was tested in three regions of the United States (CAISO, BPA, and PACW), with hourly forecasts for the years 2018, 2019, and 2020. The MAPE (mean absolute percentage error) values were below 5% in the first two years across all regions, meeting the electricity industry's requirements for medium-term forecasts. However, performance was negatively impacted in 2020, especially in the CAISO region, due to abrupt changes in consumption patterns caused by the COVID-19 pandemic.

Despite predictive effectiveness, the model presents limitations regarding interpretability. The internal mechanisms of LSTM networks, composed of input, output, and forget gates, make causal analysis or auditing of results difficult, often being described as "black boxes". To mitigate this limitation, the authors adopt a modular architecture in which the MLP assumes an interpretable and simple role, while the LSTM captures the remaining complexity. Even so, this hybrid structure represents a trade-off between accuracy and explainability, being more suitable for operational applications that require high predictive accuracy, even at the expense of lower transparency.

In summary, from a methodological perspective, there is a clear duality between traditional statistical models and deep learning techniques. Among the former, multiple linear regressions (OLS), ARMAX models, and additive semiparametric structures stand out. These methods prove to be robust and transparent, especially when the goal is to provide causal justification and statistical clarity in forecasts. In linear models, electricity demand is estimated based on climatic variables (such as temperature and humidity), economic variables (GDP, income, electricity price), temporal variables (month, day of the week, hour), and demographic variables. This structure allows for direct interpretation of the effect of each variable on load. Such models usually show good performance in short- and medium-term horizons, provided they are properly calibrated to the local reality.

Variable selection proves to be a key component in these approaches. Recent studies adopt strategies such as stepwise selection with cross-validation, as well as penalizations based on AICc. In general, statistical criteria are combined with theoretical foundations, ensuring that the included variables have both empirical relevance and interpretative coherence. Finally, additive models, such as those used in [HYFA10], add flexibility by allowing nonlinearities and complex interactions to be captured. The decomposition of load into different temporal scales, such as annual and half-hourly, enables separate analysis of climatic and economic effects and allows the construction of probabilistic distributions of peak demand, facilitating long-term decision-making.

In the field of deep learning, the works of [SDZC23] and [BAFR23] portrays examples of employing architectures such as MLP (Multi-Layer Perceptron) and LSTM (Long Short-Term Memory). These networks are effective at detecting complex temporal patterns but are less transparent from a statistical standpoint. In the former model, which separates base load (via MLP) and seasonal load (via LSTM), represents an attempt at modularization aimed at increasing interpretability. Nevertheless, the internal mechanisms of LSTM remain difficult to audit or explain intuitively.

The inclusion of temperature as an explanatory variable is nearly unanimous. The way it is incorporated varies according to the approach: from daily and monthly averages, to more sophisticated derived metrics such as Cooling Degree Days (CDD), lags, moving windows, and weekly aggregated statistics. Regarding the origin of climate data, the use of historical observed series, usually obtained from meteorological stations, prevails. Some authors also employ synthetic simulations through techniques such as the double seasonal block bootstrap, which preserve statistical patterns such as autocorrelation and seasonality. Although global climate models, such as those from CMIP, are not yet widely incorporated in the reviewed studies, this application is recognized as a promising methodological extension, as exemplified by [RCJB21].

The time horizon directly influences the methodological choice. Long-term models, such as [HYFA10], are more suitable for expansion planning and reliability assessment, while those of

[SDZC23] and [BAFR23] are more appropriate for operation and commercialization strategies over horizons of days to weeks. The performance metrics include MSE, MAE, and MAPE, the latter being preferred in applications with hourly load, as it indicates relative accuracy in percentage terms. In the case of probabilistic forecasts, quality is assessed by the adherence between the predicted density and the observed data, including the analysis of confidence intervals and probability of exceedance (PoE) quantiles.

Despite their high performance, deep learning models face limitations regarding interpretability, which hinders their application in regulatory contexts. On the other hand, statistical models, while more transparent, may have difficulties in capturing nonlinear dynamics in systems with high renewable penetration or greater climatic variability. Regardless of the approach, there is consensus on the importance of temperature in load projections. Whether through derived variables such as CDD and HDD, or through direct interpolation of hourly series, climate data are essential for anticipating load peaks, seasonal variations, and the impacts of extreme events.

In addition, temporal granularity (monthly, daily, hourly, or sub-hourly) conditions both the complexity of the models and the need for specialized treatment of climatic variables. Models with fine granularity, such as those of Hyndman and Fan and Sun et al., require greater attention to the temporal correlation of variables, justifying more sophisticated scenario simulation techniques. In contrast, approaches with lower temporal frequency operate with thermal aggregates, with less sensitivity to short-term fluctuations.

Finally, the growing interest of the literature in quantifying uncertainty in demand projections is highlighted. Probabilistic models not only provide point forecasts but also complete distributions, enabling more comprehensive risk analyses. This focus is essential for energy planning in contexts marked by climatic uncertainties and structural transformations in electricity consumption and supply.

3 METHODOLOGY

The methodology proposed in this study seeks to develop in the first stage a medium-term electricity demand forecasting framework, including hourly profiles for critical days, that is simultaneously transparent, interpretable, and adaptable. This framework will seek to treat the temperature as an explicitly variable, in order to incorporate the impacts originating from the climate into the demand behavior. To this end, the proposed framework adopts a modular approach based on an open programming language (Python), which favors the replicability of results and the flexibility to adapt to different geographic or regulatory contexts. The central objective consists of two main stages: (i) projecting medium-term monthly demand; and (ii) generating representative hourly profiles for critical load days, usually corresponding to monthly peak days, based on the monthly projections. The articulation between these two stages allows not only for estimating the total expected load, but also for providing a detailed assessment of the system's ability to meet extreme hourly consumption patterns, which is particularly relevant in contexts of tight capacity margins, growing penetration of intermittent resources, and the need for operational modernization.

In the first stage, related to monthly demand forecasting, the proposal involves comparing different classical statistical and econometric methods, with emphasis on ARIMAX (AutoRegressive Integrated Moving Average with eXogenous variables), SARIMAX (Seasonal ARIMAX), and multiple linear regression using Ordinary Least Squares (OLS). The focus is on evaluating the predictive performance of each class of models, but also on exploring their capacity for generalization and interpretation of the effects of explanatory variables on load. In order to avoid a high-dimension model and multicollinearity between the variables, the models are tested with different variable selection techniques, including stepwise elimination with OLS and regularization via Lasso (Least Absolute Shrinkage and Selection Operator). Also, independent variables are also considered, by consideration of macroeconomic indicators, such as Gross Domestic Product (GDP) and industrial production, as well as climate variables.

Temperature variables are treated with special attention, given their recognized influence on electricity demand, especially at thermal extremes. To increase the spatial adaptability of the methodology, geographical clustering of meteorological data is carried out in order to adequately represent the climatic heterogeneity of the study areas. Each zone or subsystem is characterized by multiple climate clusters. As an alternative to the simple inclusion of temperature, heating degree days (HDD) and cooling degree days (CDD) indicators are calculated based on a reference temperature. This reference value can be optimized individually by region, using search algorithms that minimize predictive error. In addition, dummy variables indicating the occurrence of months with CDD or HDD above extreme percentiles (such as the 90th or 95th) are tested, allowing the model to capture nonlinear effects associated with heat waves or extreme cold events.

Subsequently the methodology foresees a stage of generating hourly load profiles for the critical days of each month, defined as those with the highest predicted aggregate demand. This modeling builds on the monthly values obtained in the previous stage and seeks to disaggregate them to hourly granularity, while maintaining consistency with historical patterns. For this purpose, ARIMAX models and OLS models with harmonic decomposition (via Fourier series) are tested, enabling a more precise capture of daily and weekly seasonal patterns. The independent variables also includes weather variables, such as the maximum and minimum temperature for the critical day, the fully hourly temperature data and the heating degree hour (HDH) and cooling degree hour (CDH) indicators, as well as the total monthly demand, which serves as an anchor for the hourly profile. Complementary dummy variables are added for extraordinary events, such as the impact of the COVID-19 pandemic, which significantly altered hourly consumption patterns in various power systems worldwide.

Each model developed will be evaluated in terms of its predictive capacity based on the RMSE (Root Mean Squared Error) metric, which measures the square root of the mean squared error and provides a robust estimate of the magnitude of forecast errors. However, recognizing that statistical performance is not the only relevant criterion, especially in contexts where interpretability and robustness are central requirements for decision-making, several diagnostic tests will also be applied to the regression residuals. The White test will be used to detect the presence of heteroskedasticity, that is, non-constant variance of the residuals, which compromises the validity of inferences obtained from the model. The presence of heteroskedasticity may indicate omitted relevant variables or incorrect model specification. The Shapiro-Wilk test, in turn, will be used to assess the normality of residuals, an important condition for the validity of confidence intervals and significance tests in OLS models. The absence of normality may indicate the need for transformations in the dependent variable or adjustments in the model structure. Finally, tests of residuals such as Durbin-Watson and Ljung-Box will be applied to check for autocorrelation, which is especially relevant in time series, where its presence may signal the omission of autoregressive terms or poor specification of the temporal model.

The application of the methodology will be carried out for the Brazilian case, focusing on the four main operating regions of the National Interconnected System (SIN): Southeast/Central-West, South, Northeast, and North, as well as the state of Roraima (RR), which currently operates in isolation but whose integration is scheduled for October 2025. For this purpose, the official hourly load database made available by the National Electric System Operator (ONS) will be used, containing disaggregated information by subsystem. Temperature data will be obtained from the National Institute of Meteorology (INMET), covering all available automatic and conventional weather stations. This data will be processed, standardized, and interpolated to ensure temporal and spatial consistency, and subsequently aggregated according to the climate clusters defined for each region of the power system.

4 DEMAND FORECAST

The National Interconnected System (SIN) is responsible for meeting almost all of Brazil's electricity demand, with the exception of the state of Roraima, which still operates in isolation. The operation of the SIN is coordinated by the National Electric System Operator (ONS), a technical entity established by Law No. 9,648/1998 and regulated by the Brazilian Electricity Regulatory Agency (ANEEL). The ONS holds central responsibilities such as coordinating the real-time operation of electricity generation and transmission, optimizing the available energy resources, and minimizing operating costs, while simultaneously ensuring supply reliability.

Figure 8. Brazilian transmission system. [OPER25A]

From a geographical and operational standpoint, the SIN is subdivided into four major subsystems: Southeast/Central-West (SE/CO), South (S), Northeast (NE), and North (N). This segmentation, which reflects electrical and operational correlations, is widely used both for the centralized dispatch of power plants and for expansion planning and demand forecasting. Each subsystem presents distinct characteristics in terms of load structure, climatic variability, socioeconomic profile, and generation mix, which underscores the need for a regionalized approach in demand analyses.

In the specific case of Roraima, the state is still not integrated into the SIN, operating with predominantly thermal generation and costs significantly higher than the rest of the country. However, interconnection is planned through the construction of the "Linhão de Tucuruí," a direct current transmission line that will connect the capital, Boa Vista, to the Manaus electrical system. The commissioning of this infrastructure is scheduled for October 2025 and is expected to enable the replacement of diesel-based generation with more economical and cleaner sources, while also providing greater security and stability to the local system.

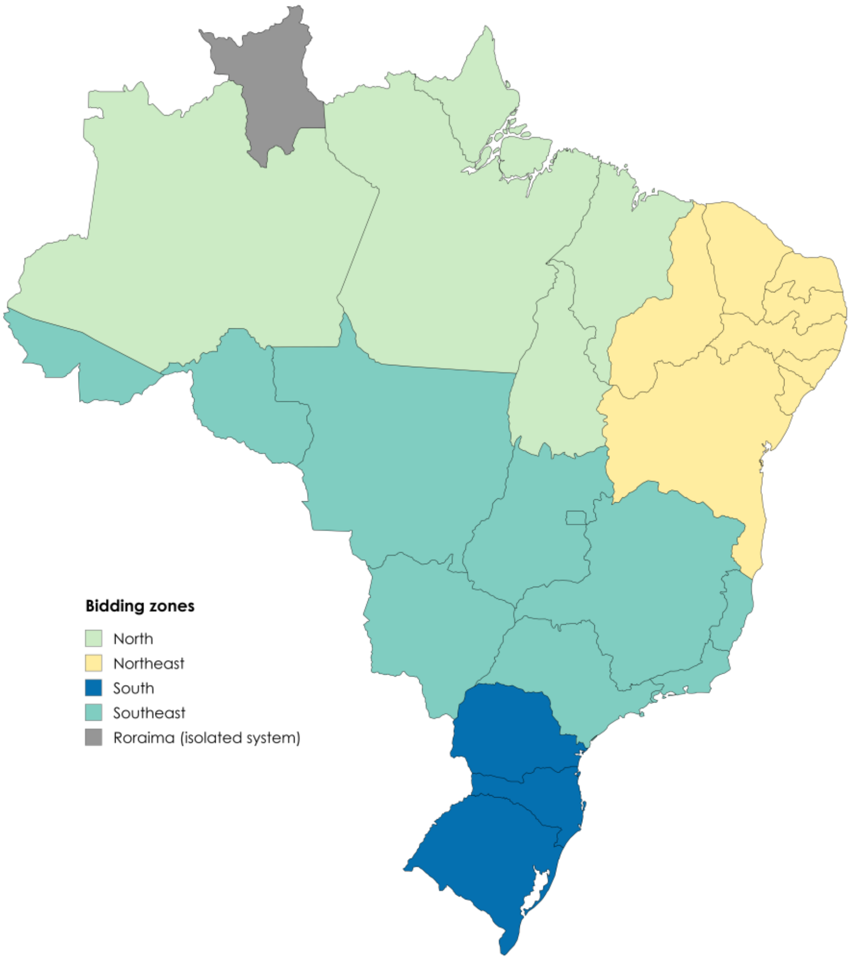

Figure 9. Brazilian bidding zones. Own work.

4.1.1 Historical Demand

In this study, a detailed and historically consistent database of electricity demand for the SIN and the state of Roraima was compiled. For this purpose, semi-hourly records made available by ONS through its public application programming interface (API) were used. The extracted series include, among others, consolidated global load, supervised load, unsupervised load, and the load associated with distributed micro and mini generation (MMGD), reconstructed by the Operator. For analytical purposes, the main variable adopted was the consolidated global load, which represents the total energy consumed at each moment, encompassing all demand components.

The data extraction process was automated through successive HTTPS requests to the ONS API, respecting the three-month interval limitation per request. All officially recognized load areas were considered, organized into three levels: the four subsystems (SE/CO, S, NE, and N), as well as intermediate geo-electrical areas – although, in the latter case, only Roraima data was effectively used. The files returned in JSON format were converted into CSVs and processed to remove inconsistencies and null values, ensuring the homogeneity and completeness of the database.

To adapt the data to the proposed modeling, the first processing step consisted of converting semi-hourly values into hourly averages, consolidating the two records per hour (e.g., 01:00 and 01:30) into a single average value. Subsequently, the data was aggregated on a monthly scale by calculating the average hourly load for each month and each load area.

In addition to the monthly series, representative hourly profiles of criticality were identified for each month and load area. Two days were selected: the one with the highest daily average load and the one with the highest hourly load recorded (monthly peak). For each of these days, the 24-hour series was extracted, allowing for a detailed analysis of demand behavior during moments of greatest system stress, which is crucial to assess the generating fleet's ability to meet demand during critical periods. For the purposes of this thesis, the hourly profile of the day with the highest hourly load (maximum demand) will be used for historical analysis, future projection, and subsequent assessment of system exposure.

An interesting point concerns the possibility of decomposing historical demand into three components: long-term trend (related to economic growth, expansion of the consumer base, and structural changes), seasonal component (related to monthly and annual cycles and climate patterns), and residual component (atypical events, noise, and high-frequency fluctuations). Figure 10 clearly illustrates this decomposition for Brazilian monthly load between 2016 and 2025. The trend shows consistent growth over the period, with a slight negative inflection in 2020 associated with the economic recession caused by the Covid-19 pandemic, and a sharper recovery from 2021 onwards, as well as strong growth in 2023 and 2024. The seasonal component reveals recurring annual variation patterns, with peaks in the warmer summer months, especially in the first quarter of the year, and reductions in the winter months, consistent with the use of air conditioning equipment and the dynamics of industrial consumption. The residual component highlights shocks not explained by the first two factors, such as abrupt negative oscillations observed in 2020 due to the pandemic, and positive spikes in some months of 2023 and 2024, caused, for example, by the intense heat waves observed during this period.

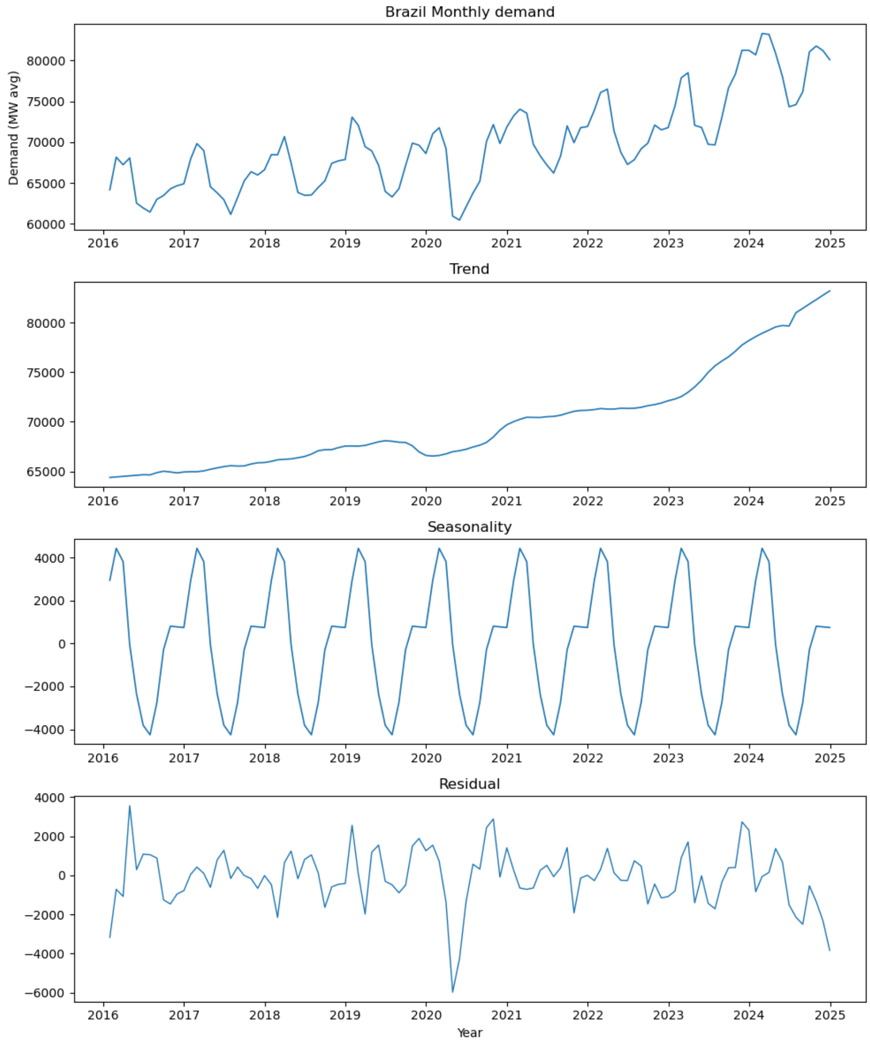

Figure 10. Brazil monthly demand – original and decompose time series. Own work.

4.1.2 Economic data

For the medium-term demand modeling, economic variables were selected based on their relevance to economic activity and, consequently, to the behavior of aggregate electricity load. The data were compiled from the Statistics Portal of the Central Bank of Brazil (BACEN), which systematically and publicly provides a set of historical data, as well as consolidated macroeconomic projections of market expectations, for a range of temporal indicators.

Although higher-frequency economic series exist, such as monthly economic activity indicators, including breakdowns by states and regions, this study opted to use annual indicators for which official projections are available for horizons of up to five years. This choice aims to ensure the applicability of the methodology in the context of medium-term electricity demand forecasting, aligning the explanatory variables with the horizons effectively used in energy planning processes. Thus, the main economic variables adopted were the Central Bank's Economic Activity Index (IBC-Br) and the sectoral indicators of value added for industry, services, and agriculture, all expressed in real terms (annual percentage variation) on a national scale.

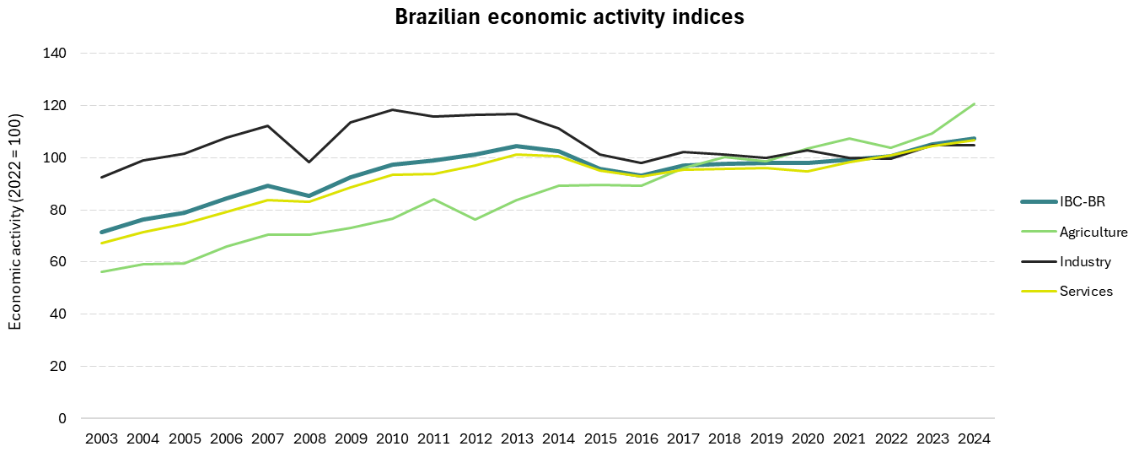

Figure 11. Brazilian historical economic activity indices [BACE25]

The IBC-Br, due to its scope and calculation methodology, is widely used as a monthly proxy for the evolution of the Brazilian Gross Domestic Product (GDP), aggregating contributions from industry, trade, services, and agriculture. Although its official release is monthly, the Central Bank provides annual projections of the IBC-Br up to five years ahead. Similarly, the sectoral indicators, which reflect the performance of industry, services and agricultural sectors, also have annual projections within the same horizon. These forecasts are displayed in the Figure 12. The choice of these sectoral indicators is justified by the possibility of capturing the differentiated influence of each economic segment on electricity demand, especially given the high heterogeneity across Brazilian regions.

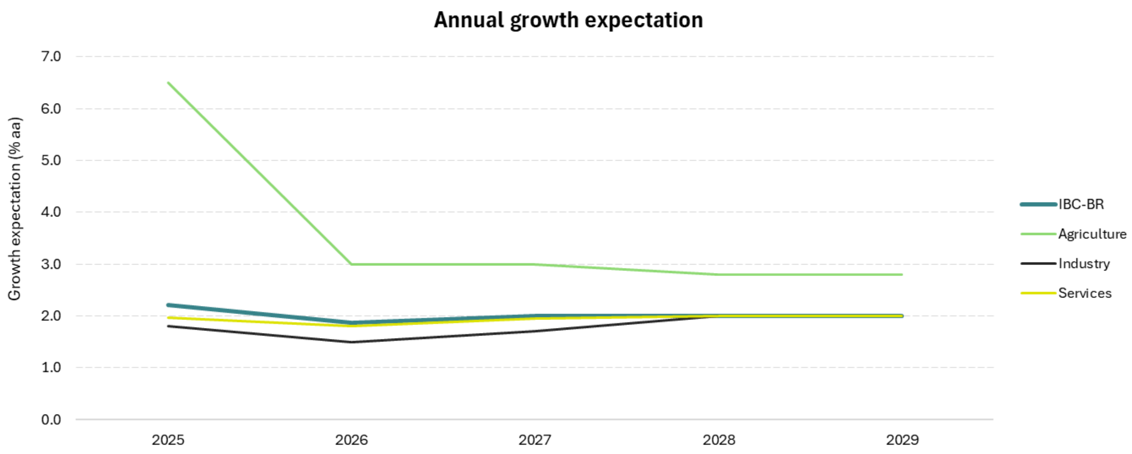

Figure 12. Brazilian annual growth expectation in 26/06/2025 [BACE25]

By prioritizing broad economic indicators with annual periodicity and official projections released by a recognized institution, as the Central Bank of Brazil (BCB), in the present case study, the proposed methodology not only ensures consistency with the planning practices adopted in the country but also enhances the generalization and replicability of the model for other regions and national contexts. The use of aggregated variables, such as the IBC-Br and sectoral indicators (industry, services, and agriculture), whose future expectations are periodically updated by official market sources, avoids excessive specificity of the model to the Brazilian case and reduces the need for in-house forecasts, which would otherwise be required if regional or state-level indicators were used, since, although available historically, they do not have periodically updated projections..

4.1.3 Temperature data

The use of climatic variables for electricity demand forecasting represents an important advance in statistical modeling of the energy sector, especially in contexts of strong thermal sensitivity, as occurs in urban regions of Brazil. The consolidation and processing of the meteorological database is therefore a critical step for the success of any forecasting application or reliability assessment based on temperature.

In this study, an hourly historical database of meteorological data was developed, with emphasis on air temperature, using the meteorological stations of the Brazilian National Institute of Meteorology (INMET). The process involved multiple stages: (i) acquisition and organization of raw data, (ii) consolidation into single files per station, (iii) filtering and selection of stations based on quality criteria, (iv) statistical treatment of missing data using the KNNImputer algorithm, and (v) geoclimatic clustering of stations by subsystem.

4.1.3.1 Acquisition and organization of raw data

Unlike automated systems of API requests or bulk downloads, the initial process of data collection was conducted manually by downloading the files made available by INMET on its official portal. These files, distributed by station and by month in .rar format, were fully downloaded, covering the entire period available for automatic stations: from 2004 to the beginning of 2024.

After manual decompression, the data were organized into directories structured by year. From this structure, a Python script was developed to recursively scan the folders, identify the files corresponding to the same meteorological station across the years, and consolidate the data into a single file per station. This consolidation was particularly challenging due to the lack of complete standardization in the file layouts over the decades: subtle variations in the number of columns, changes in field names, and even differences in character encoding required the code to be written with defensive and robust logic, enabling exception handling and adaptation to different formats. Routines were applied for column normalization, standardization of date and time, and removal of duplicates, ensuring that each final file contained a complete, continuous, and standardized hourly series per station.

From the structure of the processed files, the chronological merging of all months for each station into a single DataFrame was carried out. This process ensured the creation of a continuous hourly series for each station, stored in unique .csv files named according to the station code. The variables maintained for each station were:

- Air temperature (°C)
- Relative humidity (%)
- Date and time (ISO 8601 standard)
- Station identifier (code and name)

During this process, filters were applied to remove aberrant values (e.g., temperatures above 60 °C or negative in tropical locations) and records with invalid or duplicated timestamps. Records with all variables missing were discarded. In addition, basic coverage statistics were computed, such as the percentage of hours filled per year and the proportion of valid records for each variable.

4.1.3.2 Filtering and selection of stations

With the consolidated files, the next step was the selection of the stations that would actually be used in the modeling. Considering that the objective of the study includes adequately representing the spatial variability of temperature across the SIN's electrical subsystems, a minimum historical coverage criterion was established for the inclusion of a station in the final database. Thus, only stations that met the following requirements were selected: (i) Provided continuous data since at least the year 2011, and (ii) contained, within this period, at least 20% coverage of the expected records for the variables of air temperature and relative humidity.

The analyzes results from each meteorological station of each subsystem are presented below, in the Figure 13 to Figure 17. The application of these criteria ensured the exclusion of stations with overly recent records, highly fragmented series, or a high presence of gaps, which could compromise the quality of imputation and the subsequent statistical models. However, it was necessary to make an exception to this rule for the states of Acre and Roraima, whose stations did not meet the minimum criteria defined. To ensure national climatic representativeness, it was decided to include, in these cases, at least one station per state, prioritizing those located in the capitals Rio Branco and Boa Vista, respectively.

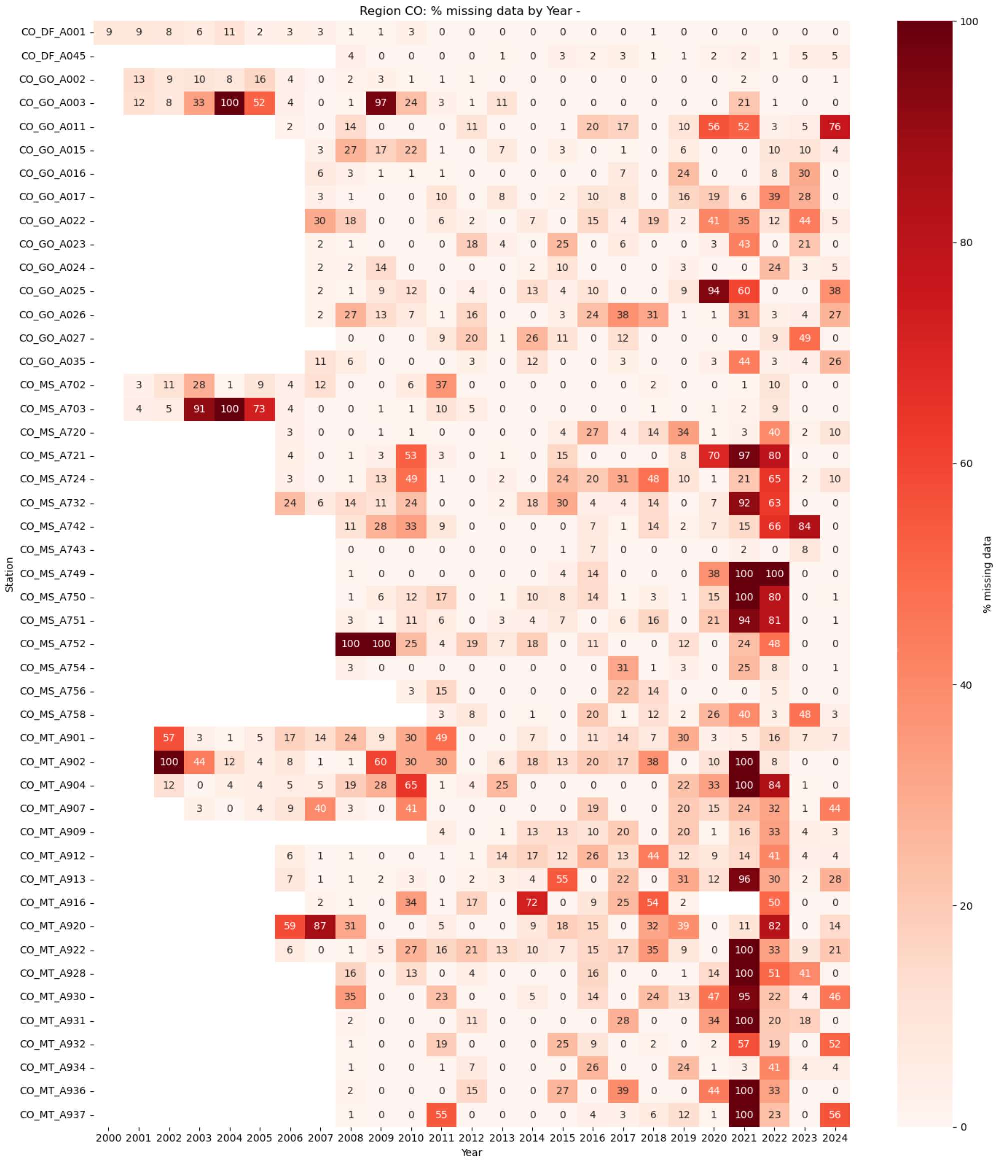

Figure 13. Missing data for selected meteorological stations in the Central-West Region. Own work.

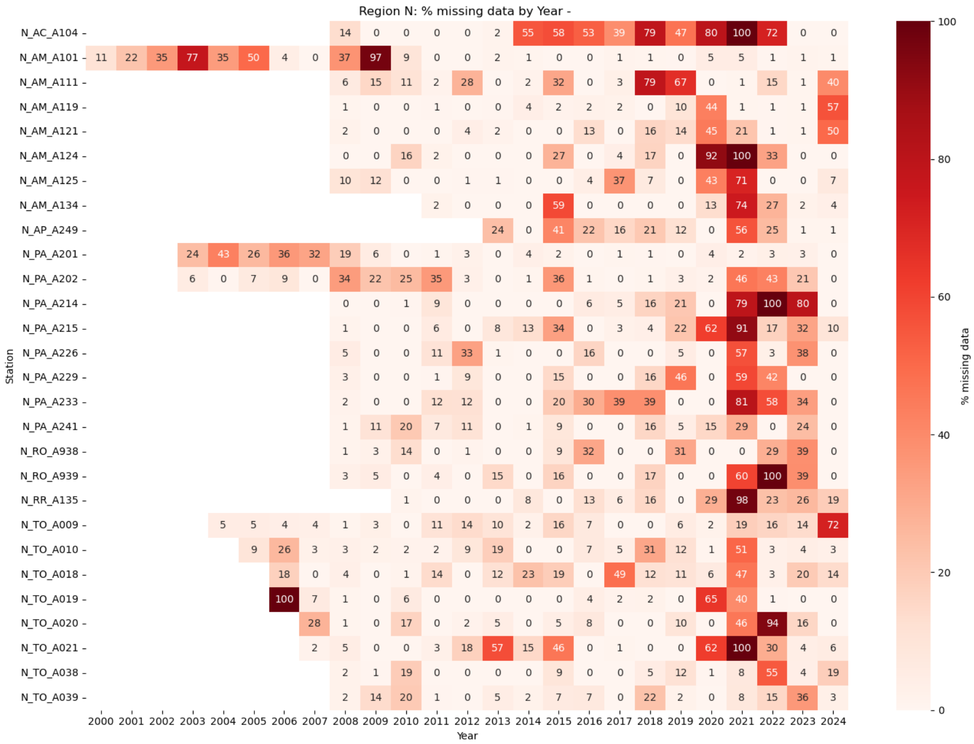

Figure 14. Missing data for selected meteorological stations in the North Region. Own work.

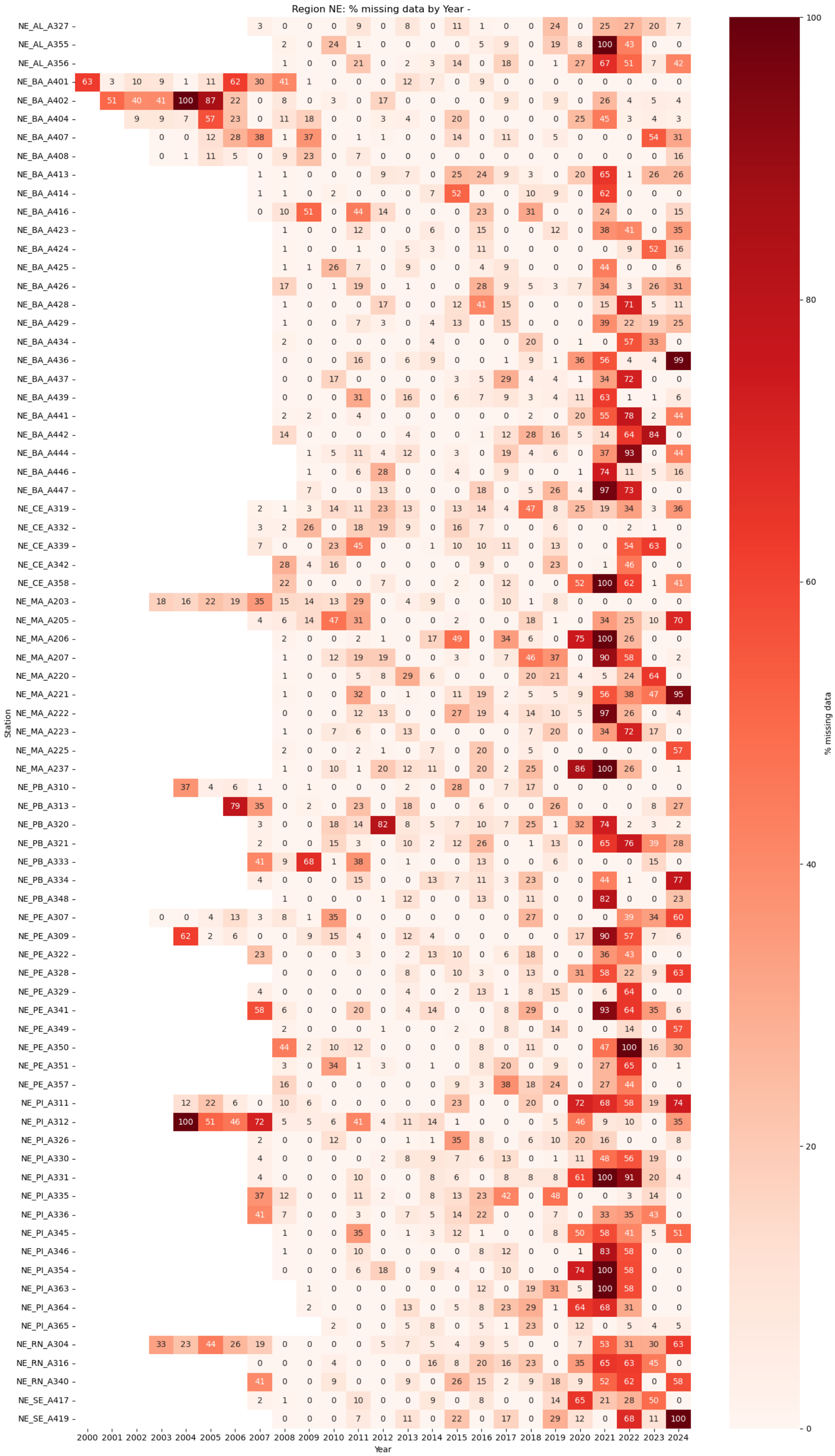

Figure 15. Missing data for selected meteorological stations in the Northeast Region. Own work.

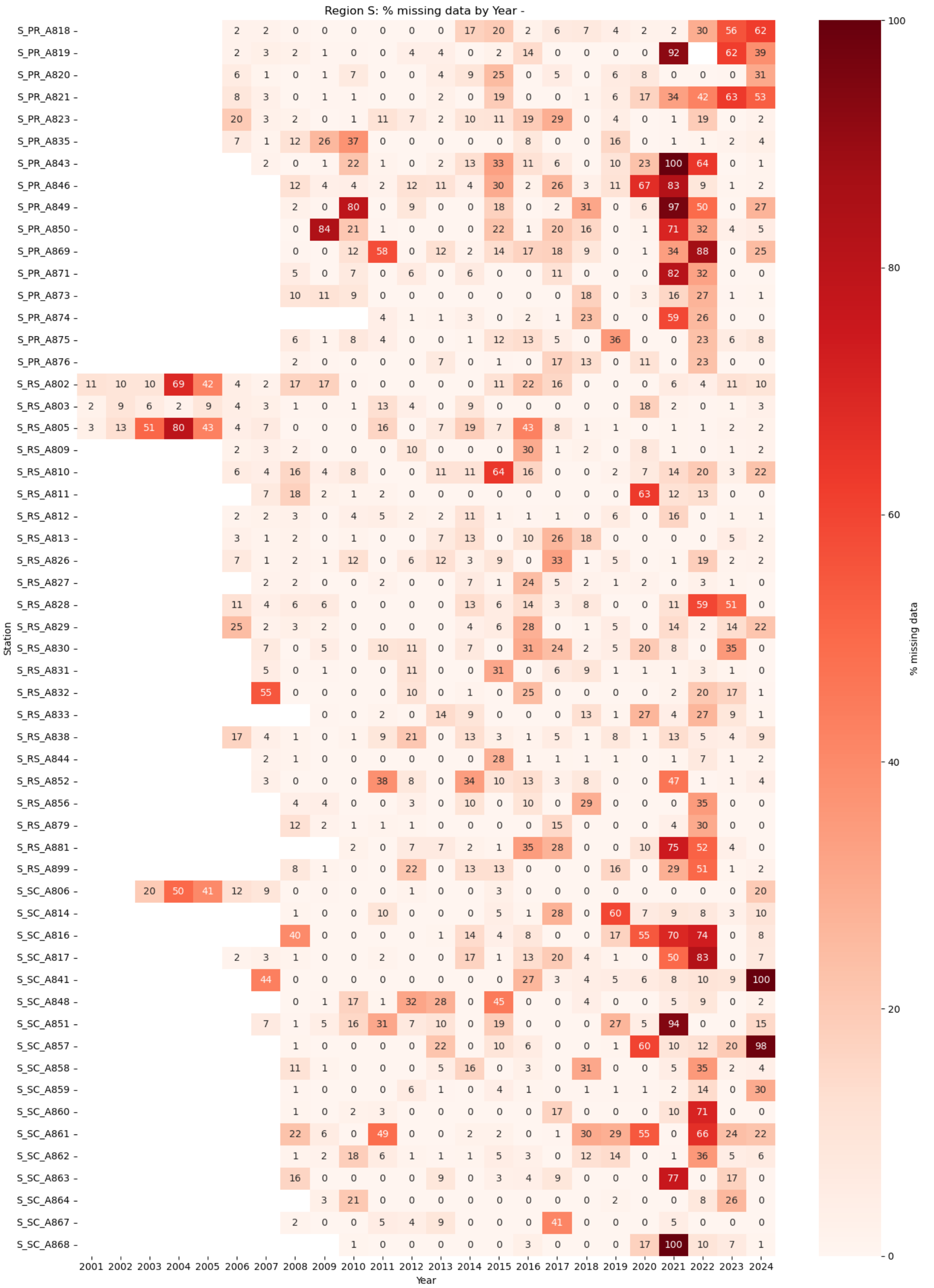

Figure 16. Missing data for selected meteorological stations in the South Region. Own work.

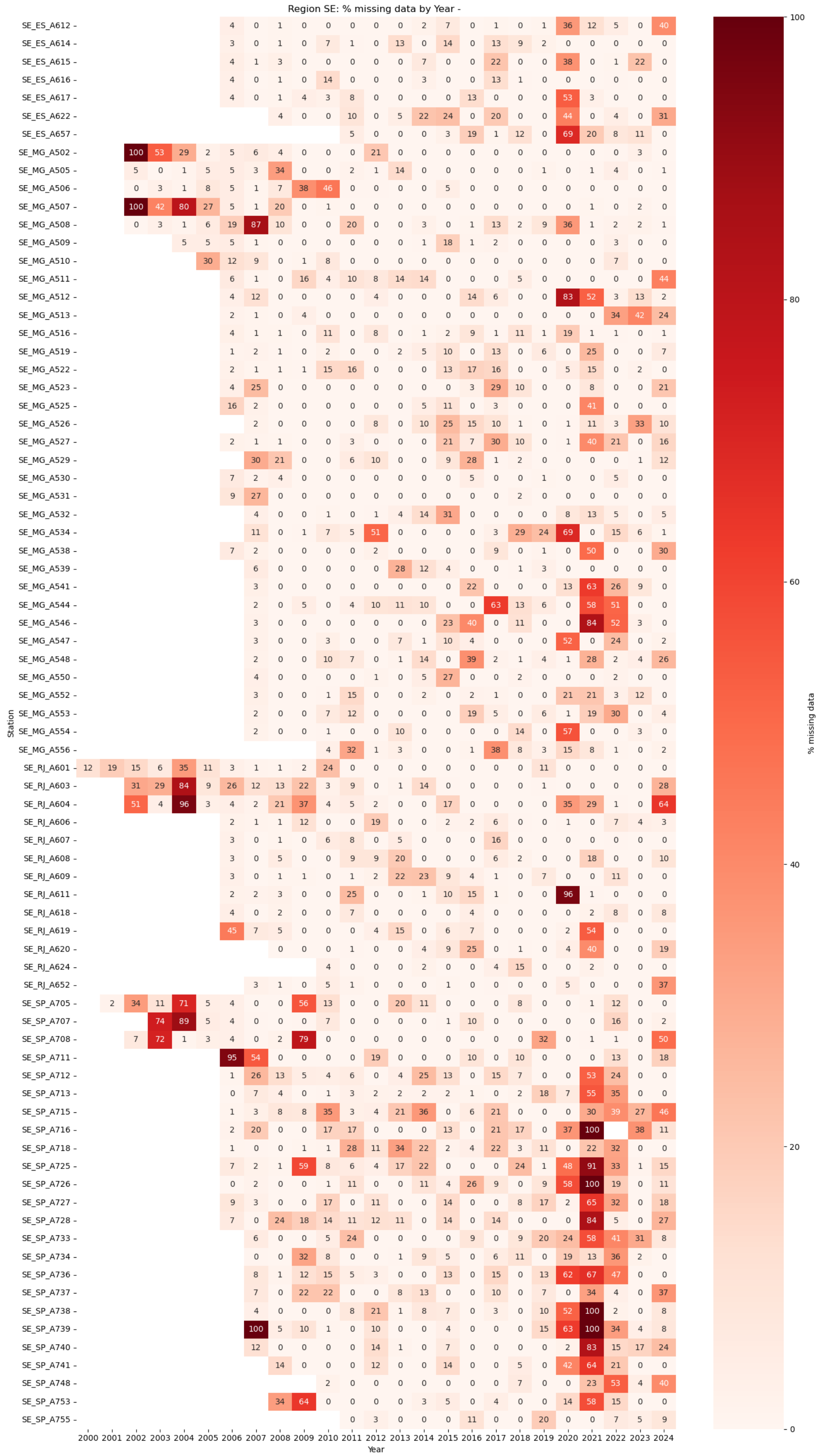

Figure 17. Missing data for selected meteorological stations in the Southeast Region. Own work.

4.1.3.3 Statistical treatment of missing data

Even after applying the minimum coverage filter, the remaining series still presented significant gaps, requiring the imputation of missing data. For this purpose, the KNNImputer algorithm was employed, an implementation of the k-nearest neighbors technique for filling missing values, available in the Python *scikit-learn* library. The choice of this method was due to its robustness in imputing continuous values in time series and multivariate datasets, particularly when there is spatial redundancy among correlated variables.

The method works by calculating, for each instance with missing values, the distance (in this case, the Euclidean distance adapted for missing data) between that incomplete observation and all others in the dataset. From this, a fixed number of neighbors is selected, and a weighted average (with weights inversely proportional to the distance) of the known values among the neighbors is computed, imputing the missing values in a way that is consistent with the spatial and temporal patterns of the series.

Although this study did not carry out systematic performance tests or benchmarking of the method across different datasets, its use is supported by previous studies that have demonstrated high accuracy of the method in applications involving meteorological data. A particularly relevant example is the study by [SDCB22]. In this work, it was shown that the KNNImputer achieved high precision in imputing meteorological variables in hourly series, with accuracy above 90% in series with up to 10% missing data. According to the study, performance remained consistent even in scenarios with up to 50% missing data, with gradual degradation of statistical indicators (F1-score, precision, MSE) in a predictable manner. In this dissertation, parameters were chosen based on recommended best practices recommended in the study. This configuration proved efficient in ensuring coherence in imputation, even in regions with low station density.

4.1.3.4 Geoclimatic clustering of stations by subsystem

With the imputed and consolidated data per station, the next step involved dimensionality reduction and representative selection of climatic variables. As is well known, multivariate regression modeling with an excessive number of highly correlated variables, as occurs with multiple nearby stations, can lead to multicollinearity problems, inflating the Variance Inflation Factors (VIFs) and compromising the interpretability of the models [DAOU18].

To mitigate this risk, an unsupervised clustering technique of the k-means type was applied, with the aim of grouping similar meteorological stations within each electrical subsystem of the SIN. The algorithm was implemented using the *scikit-learn* library, considering as input variables the (i) Latitude and longitude of the station, and (ii) the monthly average temperatures aggregated by station throughout the available historical period, as displayed in the Figure 18.

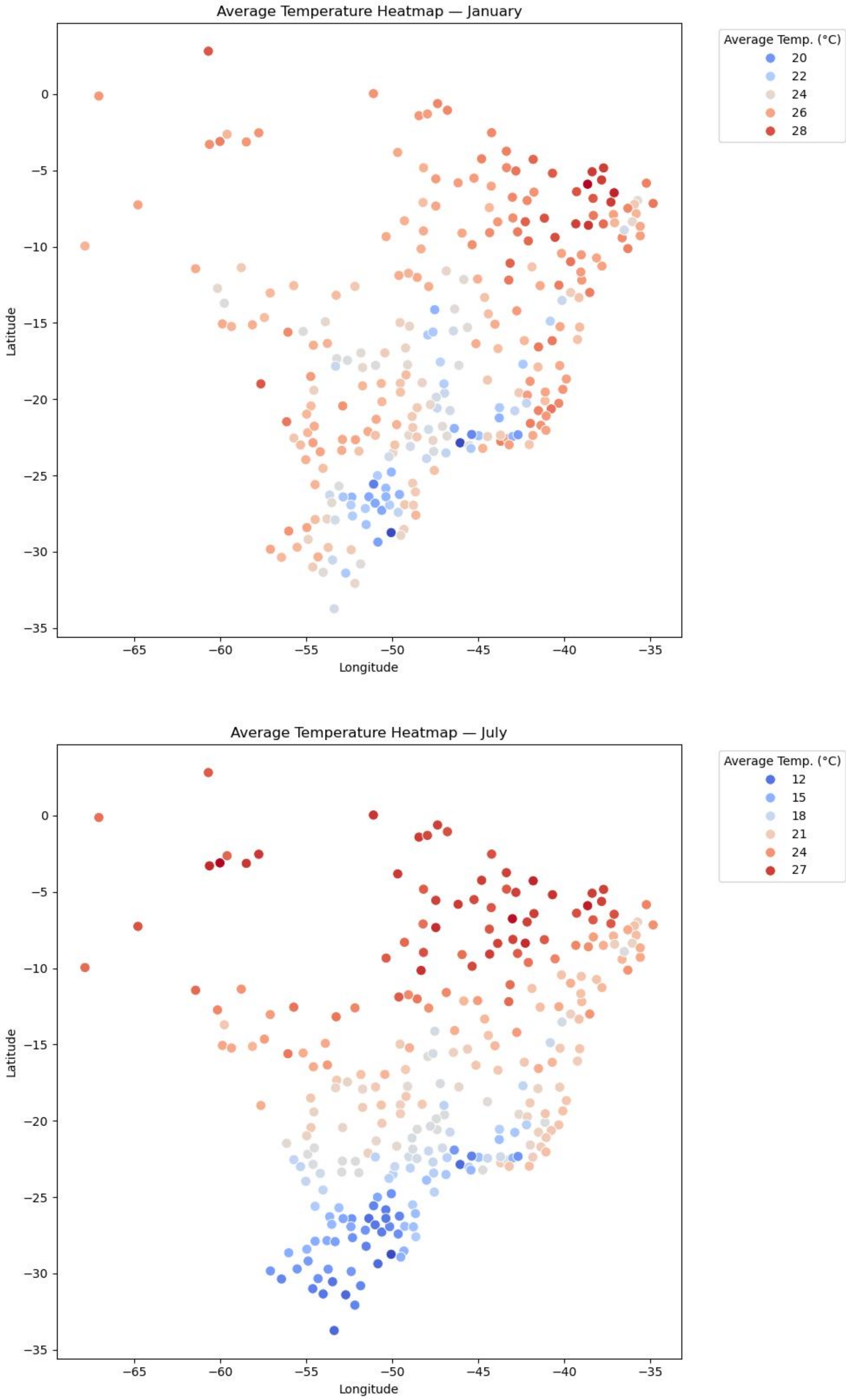

Figure 18. January and July average temperature for all INMET selected stations. Own work.

This choice was motivated by the fact that spatial distribution (geographic coordinates) and seasonal thermal patterns are the main determinants of climatic heterogeneity among stations. By using these variables, the algorithm was able to form groups that were coherent both spatially and thermally, allowing for the selection of a representative station for each group (the station most central relative to the centroids of each cluster).

This process was repeated for each subsystem, also considering the isolated system of Roraima. The final result was a compact set of meteorological stations representative of each region, reducing the dimensionality of the regression problem while maintaining the climatic diversity necessary to capture the effects of temperature on electricity demand. The results are presented in the Figure 19.

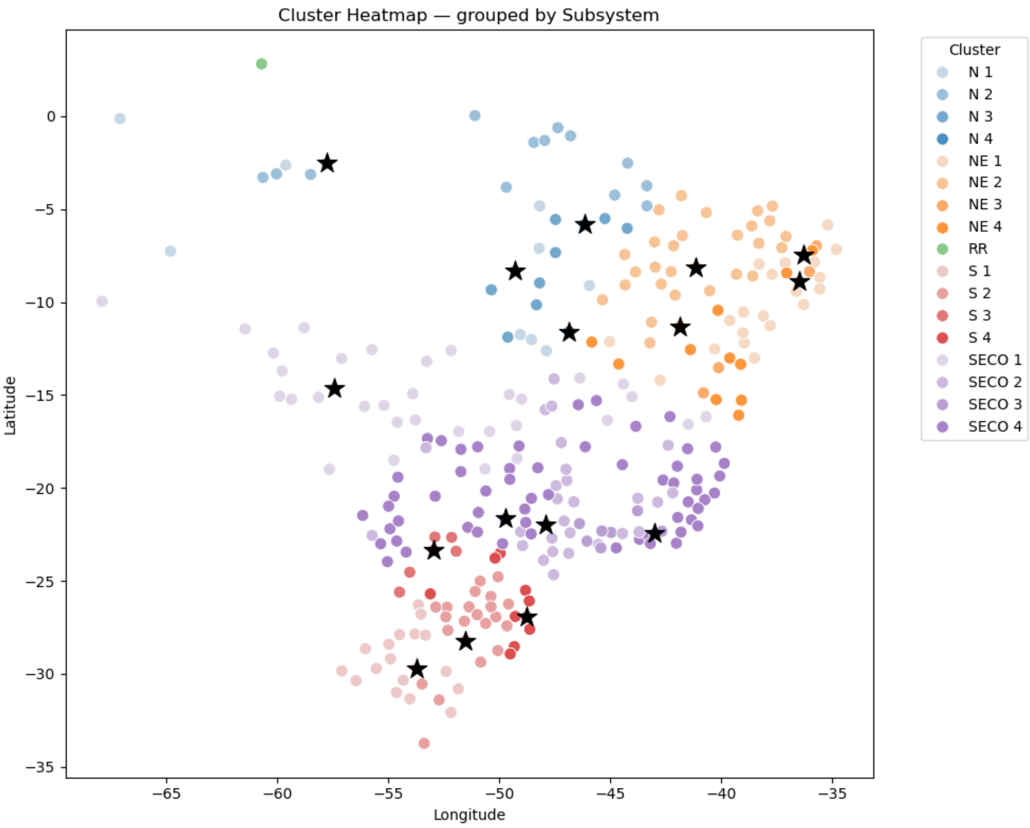

Figure 19. Clustered meteorological stations and representatives for each zone. Own work.

4.2 MONTHLY DEMAND CALIBRATION

As a first step in conducting the projections, it is necessary to calibrate the different possible models to the historical information. Based on the quality of fit of these models, it becomes possible to choose the one that best represents the specific characteristics of the Brazilian electricity system.

For calibration and subsequent forecasting, this thesis considers two different approaches for projecting monthly demand: the OLS method and the use of Time Series models. The OLS method seeks to estimate the linear relationship between electricity demand and a set of explanatory variables, such as economic indicators, climatic variables (heating and cooling degree days), and seasonal effects. The formulation is based on the principle of ordinary least squares, in which the sum of the squared errors between observed and predicted values is minimized, resulting in consistent estimates and coefficients that are straightforward to interpret. In this way, it is possible to identify the magnitude and direction of the impact of each factor on electricity demand, ensuring transparency and interpretability of the results. In addition, OLS models allow for the incorporation of lagged variables, which increases their capacity to capture short-term patterns and seasonality, albeit in a simplified manner.

$$y_t = \sum_{i=0}^{k} \alpha_i \cdot x_{i,t} + \varepsilon_t$$

Equation 6 – OLS regression

On the other hand, the use of Time Series models seeks to incorporate dynamic effects and temporal dependencies, explicitly representing the correlations present in the historical demand data. The ARIMA model and its extensions are particularly relevant in this context, as they allow the combination of autoregressive, moving average, and differencing components in order to adequately represent trend, seasonality, and short-term shocks. The ARIMAX version extends this structure by including exogenous variables, such as economic indicators and meteorological variables, thus enabling a more comprehensive capture of the determinants of electricity demand. This ability to incorporate external factors is fundamental, since electricity consumption is directly sensitive to variations in temperature and economic activity.

$$\phi(B)\nabla^d x_t = c + \theta(B) w_t$$

Equation 7 – ARIMA Times Series method [TIBS23]

In this context, two alternative strategies were applied and evaluated: the SARIMAX method, which explicitly represents seasonality through the inclusion of seasonal autoregressive and moving average terms, and the ARIMAX method, in which seasonality is represented by monthly dummy variables or by harmonic series. The first alternative has the advantage of providing an intrinsic representation of seasonality, although with greater computational complexity. The second alternative, on the other hand, is more parsimonious and interpretable, allowing for a more direct capture of recurring seasonal patterns, in addition to offering faster execution, a particularly useful feature in multiple scenario analyses.

$$\phi(B)\Phi(\mathrm{B}^s)\nabla^d x_t \nabla_s^D x_t = c + \theta(B)\Theta(\mathrm{B}^s)w_t$$

Equation 8 – Representation of the seasonality in the SARIMA method [TIBS23]

On the other hand, regarding the ARIMAX method, two different strategies were applied for the representation of seasonality: (i) the use of monthly dummy variables, or (ii) the use of harmonics. In this way, the model is able to capture seasonal behaviors commonly inherent to monthly electricity consumption, while also offering the advantages of faster execution and greater transparency and interpretability of results when compared to the SARIMA method.

$$\sum_{k=1}^{K} \cos\left(\frac{2\pi kt}{m}\right) + \sin\left(\frac{2\pi kt}{m}\right)$$

Equation 9 – Harmonics series in the ARIMAX method [GBWM23]

A relevant point pursued in this thesis concerns an optimized validation of the best model, aiming to provide the user with the optimal model in a simple manner. In the ARIMAX/SARIMAX methods, the optimal model selection essentially consists of choosing the coefficients p, d, and m (in addition to P, D, and M for the seasonal components of the SARIMA model). To perform this step, the *auto_arima* function from the *pmdarima* library was used. This method conducts an optimal model search through a stepwise strategy that minimizes the objective function. In this thesis, the Hannan-Quinn information criterion (HQIC) was adopted, as it represents an intermediate solution between the tendency of the AIC to overfit the model and the tendency of the BIC to select excessively parsimonious models [IANT22, LOBV24].

$$HQIC = -2 \cdot ln(L) + 2 \cdot k \cdot ln(ln(T))$$

Equation 10 – HQIC method

Due to the sizable number of variables that can be considered in the models, it becomes important to perform a variable selection prior to the regression. This step is essential in order to limit multicollinearity among the variables, as well as to allow for better interpretability and simplicity of the models, which are primary objectives of this work. According to [MIRA24] backward selection methods are an effective alternative for variable selection, relying on the significance of the model and/or the individual variables. Moreover, the use of penalization methods, such as the Lasso method, is also mentioned [CHAN17]. As a final result, the Lasso method continuously reduces the value of the variables (shrinking) through first-order penalization on the size of the coefficients, thus obtaining a final reduced list of variables.

$$\beta = arg\ min\left\{\frac{1}{2n}\sum_{i=1}^{n}(y_i - x_i \cdot \beta)^2 + \lambda \cdot \sum_{j=1}^{p}\left|\beta_j\right|\right\}$$

Equation 11 – LASSO regression [MIRA24]

In the case of applying LASSO, it was necessary to pay attention to the regularization of exogenous variables in order to ensure that penalization occurred appropriately. Since variables with distinct magnitudes could be disproportionately penalized, two regularization strategies were evaluated: traditional standardization through logarithmization and the use of the Robust Scaler, which adjusts variables considering measures that are robust to the presence of outliers, such as the median and interquartile range. This approach is particularly relevant given the intrinsic occurrence of extreme CDD/HDD values, which could have their analysis negatively affected if other regularization methods were applied.

$$x_i^{scaled} = \frac{x_i - Median(X)}{IQR(X)}$$

$$IQR\ (X) = Q_3(X) - Q_1(X)$$

Equation 12 – Robust scaler regularization [AMCC22]

In this context, the present thesis assesses the application of twenty-four different models for the representation of monthly demand. As previously mentioned, each method will be assessed separately for each subsystem, using the training period corresponding to data from 2016 to 2023 and the validation period conducted with 2024 data. All 24 methods will be tested under three different approaches: (i) without considering associated temperature data, (ii) considering temperature data through HDD/CDD with optimized base temperature selection, and (iii) considering temperature by isolating the occurrence of extreme CDD/HDD, using one variable capped at P90 and another capturing the excess above this threshold. Model selection will be based on RMSE (Root Mean Square Error), with the final model also being subsequently analyzed for its statistical consistency.

Table 1 – Models assessed for the monthly demand

Number	Variable selection	Exogenous Regularization	Seasonality representation	Method
1	Back	log	Monthly dummies	ARIMAX
2	Back	robustscaler	Monthly dummies	ARIMAX
3	Back	log	Harmonics	ARIMAX
4	Back	robustscaler	Harmonics	ARIMAX
5	Back	log	SARIMAX	SARIMAX
6	Back	robustscaler	SARIMAX	SARIMAX
7	Lasso	log	Monthly dummies	ARIMAX
8	Lasso	robustscaler	Monthly dummies	ARIMAX
9	Lasso	log	Harmonics	ARIMAX
10	Lasso	robustscaler	Harmonics	ARIMAX
11	Lasso	log	Monthly dummies	OLS
12	Lasso	robustscaler	Monthly dummies	OLS
13	Lasso	log	Harmonics	OLS
14	Lasso	robustscaler	Harmonics	OLS
15	Lasso	log	Lags	OLS
16	Lasso	robustscaler	Lags	OLS
17	Lasso	log	SARIMAX	SARIMAX
18	Lasso	robustscaler	SARIMAX	SARIMAX
19	Back	log	Monthly dummies	OLS
20	Back	robustscaler	Monthly dummies	OLS
21	Back	log	Harmonics	OLS
22	Back	robustscaler	Harmonics	OLS
23	Back	log	Lags	OLS
24	Back	robustscaler	Lags	OLS

4.2.1 Historical calibration results

Table 2 presents the results for the validation period (2024) for all the methods analyzed, displaying (i) methods without temperature, presented as "RMSE sT", (ii) methods applying temperature, through the calculation of CDD and HDD, presented as "RMSE T base" and methods applying temperature with the consideration of a capping of CDD and HDD and consideration of dummies, to signal months that exceed the historical percentile, presented as "RMSE T Cap". As a first major finding, it is possible to highlight the poor performance during the validation period of the OLS methods when combined with LASSO variable selection – there is a significant deterioration between the training and validation periods, indicating that the selection method may have made the model short-sighted in cases of changes in the out-of-sample dataset. A second noteworthy result of poor performance is characteristic of the OLS models when combined with explicit lag consideration for representing seasonality, which perform worse compared to the other OLS methods, as well as showing significant deterioration when temperature-related variables are added. On the other hand, the time series methods, particularly the ARIMAX models (even more so than the SARIMAX ones), stand out for their good performance across all classes, especially when temperature-related variables are considered. It is worth noting the robust scaler's good relative performance when applied to the Lasso method, which is consistent with this selection method. However, there is no consistency in the robust scaler's application across methods, depending on the temperature consideration method used. Similarly, in methods that apply OLS (whether through the backward selection method or in the final selection itself), the logarithmization method tends to yield better results. Finally, it is noted that the strategy of considering a capped and excess CDD/HDD did not necessarily translate into accuracy gains for the model, although improvements did occur in certain cases.

Table 2 – RMSE for the validation period for all methods

Number	Variable selection	Exogenous Regularization	Seasonality representation	Method	RMSE sT	RMSE T base	RMSE T Cap
1	Back	Log	Monthly dummies	ARIMAX	1260	1142	1205
2	Back	robustscaler	Monthly dummies	ARIMAX	1326	1281	1243
3	Back	Log	Harmonics	ARIMAX	1558	1493	1655
4	Back	robustscaler	Harmonics	ARIMAX	1763	1812	1384
5	Back	log	SARIMAX	SARIMAX	2313	1576	827
6	Back	robustscaler	SARIMAX	SARIMAX	2390	1143	947
7	Lasso	log	Monthly dummies	ARIMAX	1156	987	744

8	Lasso	robustscaler	Monthly dummies	ARIMAX	943	688	1953
9	Lasso	log	Harmonics	ARIMAX	1108	829	803
10	Lasso	robustscaler	Harmonics	ARIMAX	957	702	1276
11	Lasso	log	Monthly dummies	OLS	3784	1370	1679
12	Lasso	robustscaler	Monthly dummies	OLS	3495	1070	1221
13	Lasso	log	Harmonics	OLS	3843	1485	1615
14	Lasso	robustscaler	Harmonics	OLS	3562	1274	1260
15	Lasso	log	Lags	OLS	2248	3615	---
16	Lasso	robustscaler	Lags	OLS	2146	1756	1580
17	Lasso	log	SARIMAX	SARIMAX	2104	850	1010
18	Lasso	robustscaler	SARIMAX	SARIMAX	2296	887	1420
19	Back	log	Monthly dummies	OLS	1572	869	1050
20	Back	robustscaler	Monthly dummies	OLS	1138	1538	1502
21	Back	log	Harmonics	OLS	1587	948	885
22	Back	robustscaler	Harmonics	OLS	1160	1451	1679
23	Back	log	Lags	OLS	2399	4562	---
24	Back	robustscaler	Lags	OLS	2295	4009	---

Overall, it is observed that the inclusion of temperature-related variables reduces the RMSE by around 38%. When excluding the OLS methods with explicit lags, the reduction compared to the sample medians reaches 44%. The best-performing method is method 8, which corresponds to the ARIMAX model with monthly dummies, combined with LASSO variable selection and regularization of exogenous variables using the robustscaler.

The Figure 20 and Figure 21 presents the forecast versus actual data for the consolidated system, comparing the approaches with and without temperature for method 8. The corresponding plots by subsystem can be viewed in Appendix A.

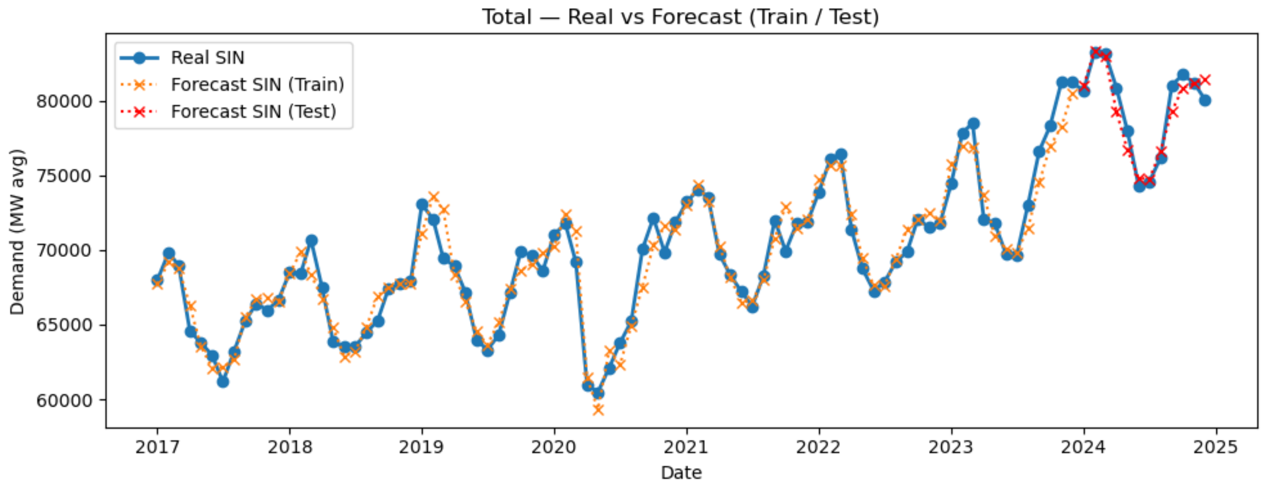

Figure 20. Method 8 results without temperature. Own work.

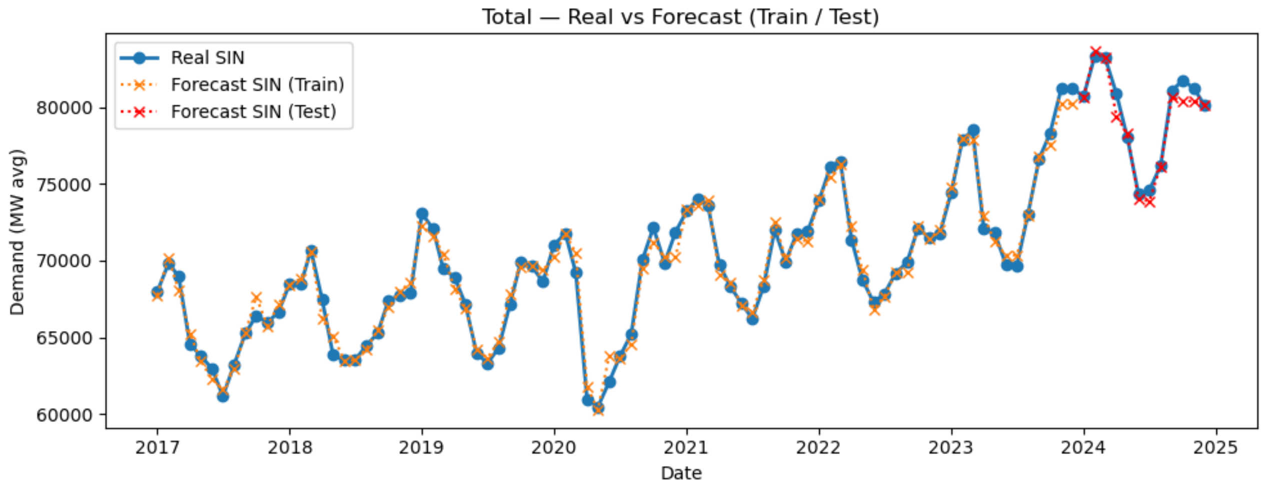

Figure 21. Method 8 results with base temperature. Own work.

4.2.2 Statistical robustness

In addition to model accuracy, represented by the RMSE, it is equally important to assess the statistical robustness of the chosen model, particularly when the objective is to analyze the statistical significance of the estimated coefficients.

For this evaluation, a set of statistical tests was applied to the final selected model. The tests performed were:

- Heteroskedasticity tests, conducted using the White Test and the Breusch-Pagan Test, available through the *het_white* and *het_breuschpagan* methods in the statsmodels library, respectively.

- Normality test of the residuals, performed using the Shapiro-Wilk Test, available through the *shapiro* method in the *scipy* library.
- Autocorrelation tests, performed using the Durbin-Watson Test and the Ljung-Box Test of order 3, available through the *durbin_watson* and *acorr_ljungbox* methods in the *statsmodels* library, respectively.

The final results are presented in the Table 3 below. It is noted that all subsystems passed the five tests performed under the aforementioned conditions, with special emphasis on the SECO subsystem, by far the most significant.

Table 3 – Statistical test results for the final model

Subsis	**WT status**	**BP status**	**SW status**	**LB status**	**DW status**
SECO	Approved	Approved	Approved	Approved	Approved
S	Approved	Approved	Approved	Approved	Approved
N	Approved	Approved	Approved	Approved	Approved
NE	Approved	Approved	Approved	Approved	Approved
RR	Approved	Approved	Approved	Approved	Approved

4.2.3 Detail results for the final model

A key factor that can be highlighted concerns the model's ability to capture the specific characteristics of each region. This is initially exemplified by the optimal temperature used to calculate CDD and HDD: while the SECO and South subsystems register lower optimal temperatures, the other regions present higher thresholds.

This temperature sensitivity is also reflected in the coefficients of the selected temperature variables. A stronger sensitivity is observed with respect to variables associated with cooling needs, which is expected given the climatic conditions across all regions. However, there is also evidence of a significant share of electricity demand related to heating requirements. This feature is particularly salient in the South subsystem, the region that tends to record the lowest temperatures in the country, with colder winters, usually associated with increased heating needs, such as from electric showers.

Another relevant aspect relates to the behavior of demand in relation to economic variables. As noted in Section 4.1.2, this study employs aggregated data on national economic activity, in addition to sectoral indices. Furthermore, two dummy variables are included: one related to the incidence of COVID-19 for April and May 2020, when electricity demand dropped sharply due to social isolation and lockdown policies; and a continuous time dummy variable.

First, the analysis allows us to infer the impact of COVID-19, with particularly strong effects in the Southeast and North regions, both characterized by higher shares of industrial activity that were significantly curtailed during the period. Additionally, it is observed that, with the exception of the SECO region, the time-trend dummy shows greater relevance compared with the economic activity variables, consistent with the stronger economic dynamics of SECO relative to the other subsystems. The detailed coefficient-level results are presented in the Appendix B.

Table 4 – Detail results for the final model

Subsis	Base Temp (º C)	Arima Order	RMSE calibration (MW avg)	R^2 calibration	RMSE 2024 (MW avg)	R^2 2024
SECO	24	(2, 1, 2)	464.5	0.9637	377.2	0.9631
S	18	(1, 1, 0)	170.3	0.9708	341.4	0.8510
N	26.5	(0, 1, 0)	84.4	0.9839	317.8	0.3622
NE	25	(1, 1, 0)	149.5	0.9644	307.7	0.6232
RR	28	(1, 1, 1)	6.2	0.9104	5.4	0.9346

4.3 CRITICAL DAY HOURLY PROFILE CALIBRATION

As in the previous step, the projection of the critical day also applies two different approaches: OLS regression and time series, both using harmonics to represent seasonality, an approach more suitable for analyzing daily cycles.

As noted earlier, a variable selection method is applied for the projection of the critical day in order to provide greater control over the selection of variables due to the higher criticality of this stage. In this step, only the backward selection is applied. Furthermore, for the optimal model selection in the ARIMAX method, the same automatic choice algorithm is applied.

As pointed out in Section 4.1.1, the critical days of each month were extracted from the historical series based on the day with the highest hourly load (maximum demand), and these were used to build the historical series for training and calibration. However, it is important to note that the methodology was designed with flexibility: for example, it allows the creation of a complete hourly profile for each year, should the user so desire.

A key factor for projecting the critical day concerns the treatment and proper consideration of temperature data. First, three distinct strategies are applied for incorporating temperature in the calibration period: (i) including as exogenous variables the maximum and minimum temperatures recorded at each station on the day of highest demand, (ii) explicitly considering the hourly temperature profile or (iii) using the hourly profile to calculate the CDH and HDH, as the difference between the current temperature and the reference temperate, as calculated in the monthly step. The different models assessed are presented in the Table 5.

Table 5 – Models assessed for the critical day demand

Number	Variable selection	Temperate Application	Seasonality representation	Method
1	Back	Max / Min	3 Harmonics	ARIMAX
2	Back	Max / Min	6 Harmonics	ARIMAX
3	Back	Max / Min	8 Harmonics	ARIMAX
4	Back	Hourly profile	3 Harmonics	ARIMAX
5	Back	Hourly profile	6 Harmonics	ARIMAX
6	Back	Hourly profile	8 Harmonics	ARIMAX
7	Back	Max / Min	3 Harmonics	OLS
8	Back	Max / Min	6 Harmonics	OLS
9	Back	Max / Min	8 Harmonics	OLS
10	Back	Hourly profile	3 Harmonics	OLS
11	Back	Hourly profile	6 Harmonics	OLS
12	Back	Hourly profile	8 Harmonics	OLS
13	Back	CDH / HDH	3 Harmonics	OLS
14	Back	CDH / HDH	6 Harmonics	OLS
15	Back	CDH / HDH	8 Harmonics	OLS

4.3.1 Historical calibration results

The Table 6 presents the results for the testing period (2016–2023) and the validation period (2024) for all the methods analyzed. Although showing better results in the testing period across all models, the ARIMAX method tends to produce significantly worse results in the validation stage, indicating possible overfitting to the training data.

On the other hand, the models analyzed using the OLS method appear more stable, with consistent results between the training and testing periods. It is also observed that as the number of harmonics increases, there is a relative improvement in the results, although with diminishing incremental gains as the number of harmonics grows.

Regarding the incorporation of temperature data, the method of application does not lead to significant discrepancies in the results. Focusing on the OLS models with eight harmonics, for instance, the difference between the three models is only 2.8%. Given the superior performance achieved by Model 15, which combines degree-hours with eight harmonics, this model was chosen for the final forecast.

Table 6 – Models results for the critical day demand profile

Number	Variable selection	Temperate Application	Seasonality representation	Method	RMSE Train	RMSE Test
1	Back	Max / Min	3 Harmonics	ARIMAX	1269	3715
2	Back	Max / Min	6 Harmonics	ARIMAX	1274	8994
3	Back	Max / Min	8 Harmonics	ARIMAX	1289	11743
4	Back	Hourly profile	3 Harmonics	ARIMAX	1279	3027
5	Back	Hourly profile	6 Harmonics	ARIMAX	1290	34939
6	Back	Hourly profile	8 Harmonics	ARIMAX	1114	3029
7	Back	Max / Min	3 Harmonics	OLS	2359	2271
8	Back	Max / Min	6 Harmonics	OLS	2175	2097
9	Back	Max / Min	8 Harmonics	OLS	2164	2090
10	Back	Hourly profile	3 Harmonics	OLS	2336	2287
11	Back	Hourly profile	6 Harmonics	OLS	2168	2140
12	Back	Hourly profile	8 Harmonics	OLS	2157	2127
13	Back	CDH / HDH	3 Harmonics	OLS	2313	2236
14	Back	CDH / HDH	6 Harmonics	OLS	2141	2083

15	Back	CDH / HDH	8 Harmonics	OLS	2131	2069

Although the different methods of incorporating temperature do not produce significant differences among the models studied, a critical point of analysis lies in the comparison with a method where temperature is not considered. For this purpose, taking the model with eight harmonics, performance was compared between the version with and without temperature, as was also done for the monthly demand projection methods. An improvement in forecasting accuracy of approximately 16% is observed for the testing period, once again demonstrating the robustness gained by including temperature in demand projections. Notably, when analyzing the system's maximum requirements under monthly peak demand, shown in the Figure 22 and Figure 23, it is also evident that the model with temperature provides better results, as the model without temperature routinely tends to underestimate such critical moments. Other graphs and additional analyses of Model 15 are presented in the Appendix C.

Table 7 – Critical day demand profile results with and without temperature

Number	Variable selection	Temperate Application	Seasonality representation	Method	RMSE Train	RMSE Test
15	Back	CDH / HDH	8 Harmonics	OLS	2131	2069
16	Back	---	8 Harmonics	OLS	2337	2453

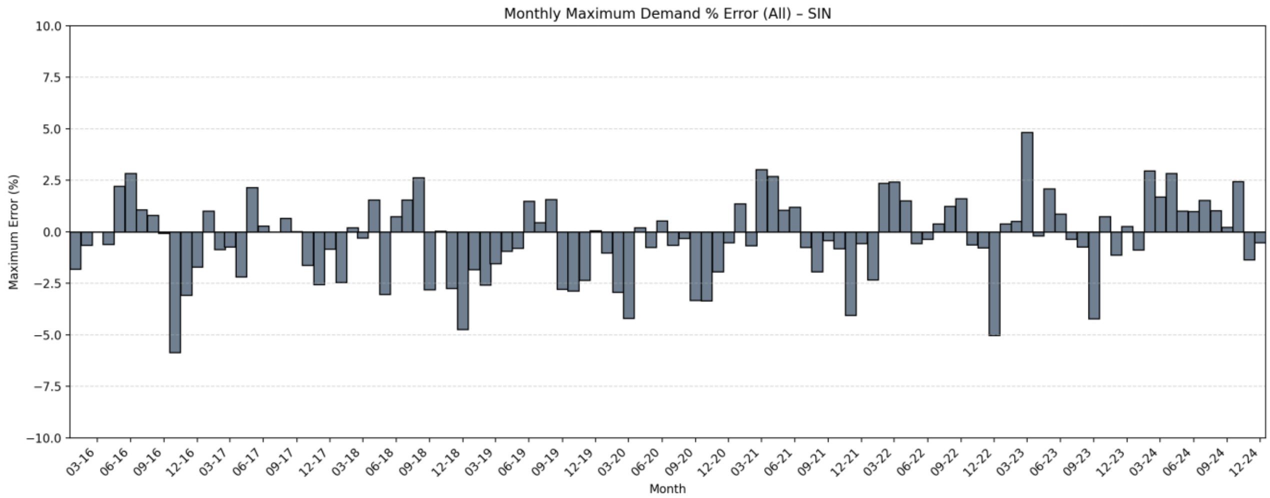

Figure 22. Monthly maximum demand error without temperature consideration. Own work.

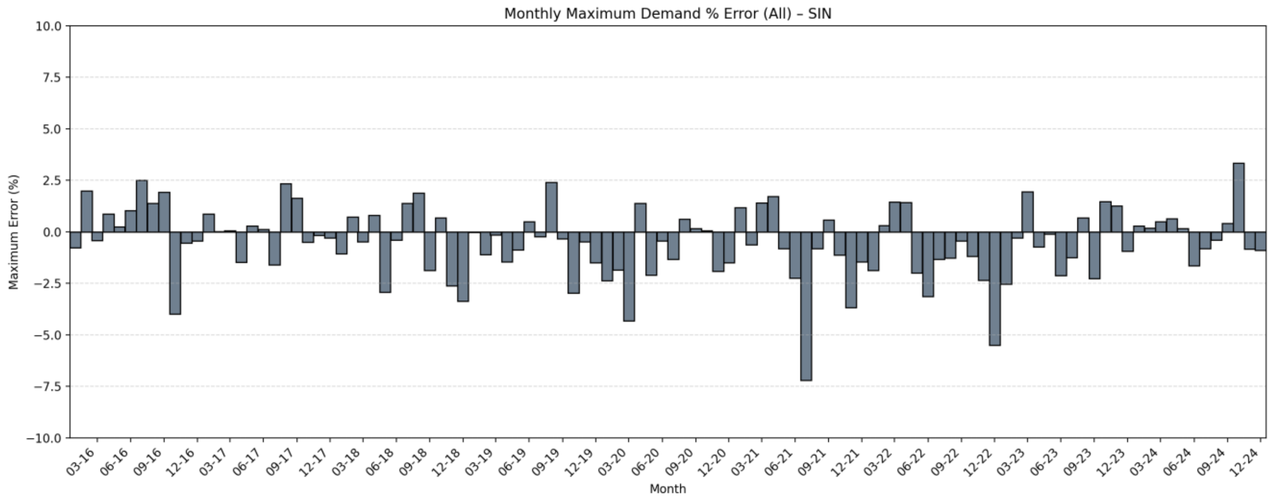

Figure 23. Monthly maximum demand error with temperature consideration. Own work.

4.4 DEMAND FORECAST

In the analyses conducted in the previous sections, temperature was already a compiled dataset: the exact temperatures for each month were known in the case of monthly demand calibration, as well as the recorded temperatures on peak demand days. However, in order to carry out projections that incorporate both variables, it becomes necessary to implement a strategy for their application. Due to the stochastic nature of temperature, it is not possible, for example, to reliably project what the temperature will be on the day of peak demand, and simply repeating the last observed value would make the analysis less robust.

To address this issue, a double bootstrap strategy is applied to generate stochastic temperature scenarios based on historical data, while preserving the temporal correlation among different stations. As noted in [HYFA10] this strategy consists of:

- Dividing the historical series into daily blocks of fixed duration; in this way, each year will have the same number of blocks, which will be temporally aligned. For instance, with a block length of 7 days, Block 1 will consist of January 1 to January 7 for all years in the historical record.
- Randomly drawing a year from the historical record. In this study, the historical period considered the historical record from 2011 to 2024.
- Randomly drawing a day-shift for each block, thereby significantly expanding the number of scenarios that can be generated. For example, if a maximum shift of ±6 days is applied, the start and end of each block can be displaced by up to six days in either direction.

- Additionally, the method allows for the inclusion of a linear annual warming trend, enabling a simplified analysis of the potential impacts of climate change on temperature increases.

Applying this abovementioned methodology, the results for one of the selected stations are displayed in the Figure 24 and Figure 25. As can be seen, the distribution profile of the projected temperature data are very similar to the historical record, maintaining in this sense the coherence between the two series.

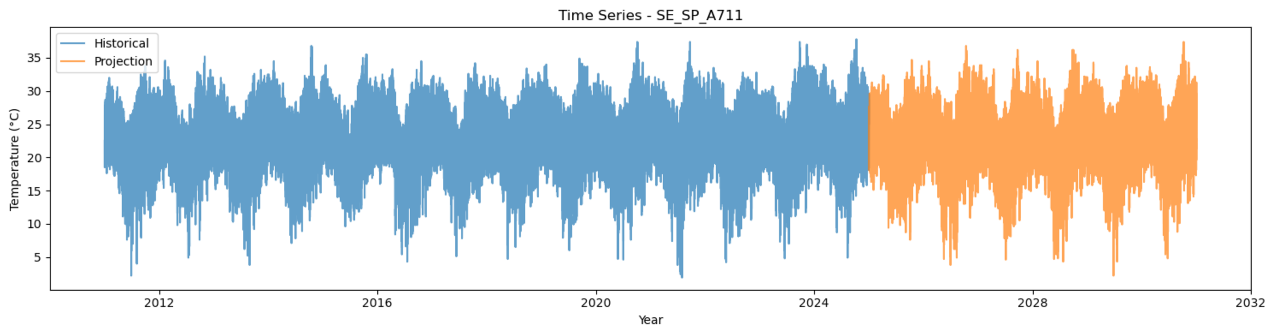

Figure 24. Double bootstrap time series for the SE_SP_A711 station with one scenario. Own work.

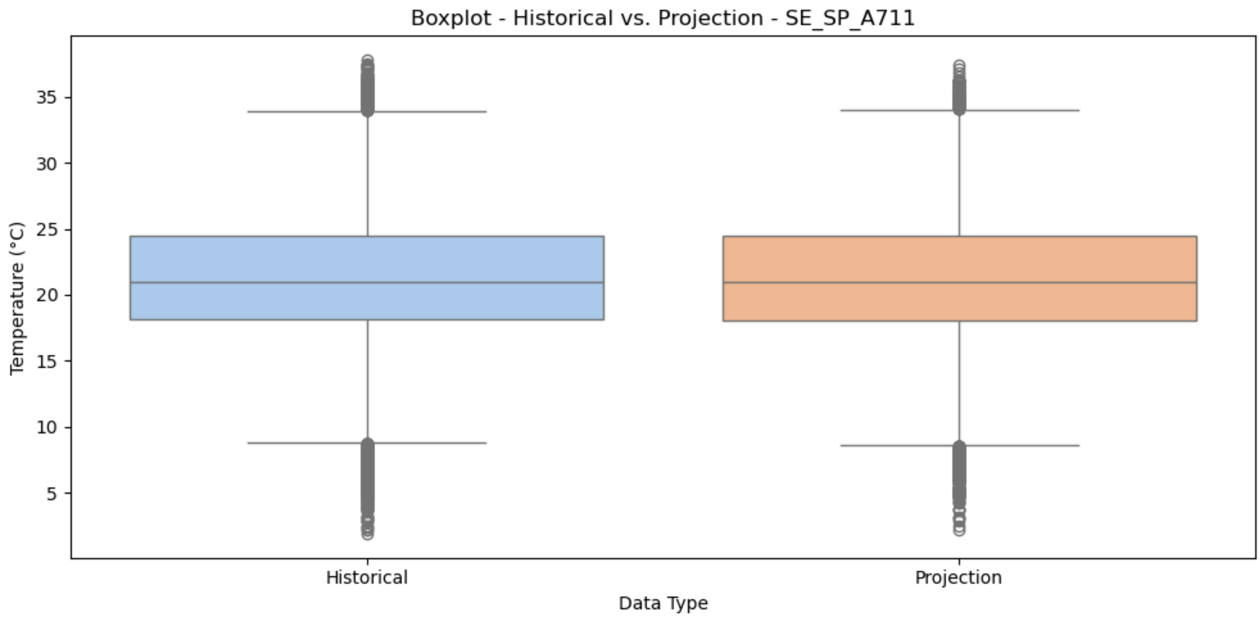

Figure 25. Double bootstrap box-plot for the SE_SP_A711 station with one scenario. Own work.

From the generation of temperature scenarios, it becomes equally possible to generate future demand scenarios. To this end, a scenario tree is employed to create correlated scenarios. For the monthly demand projection, five different temperature scenarios are used. Subsequently, for the hourly peak demand projection, twenty different days are randomly drawn for each month, resulting in a total of one hundred different demand scenarios. This approach can be expanded as needed, thus allowing for a conditional analysis of the relationship between demand and temperature.

4.4.1 Monthly demand forecast

According to the proposed methodology, the average total aggregate demand evolves with a growth rate of around 2.1% in the long term, considering the load on the Roraima system, a result consistent with projected economic growth. The impact of temperature is notable, especially in years with higher average temperatures and during transition periods to summer - while December 2026 presents a difference of over 5% between the scenarios, June 2028 presents a difference of only 0.5% between the scenarios.

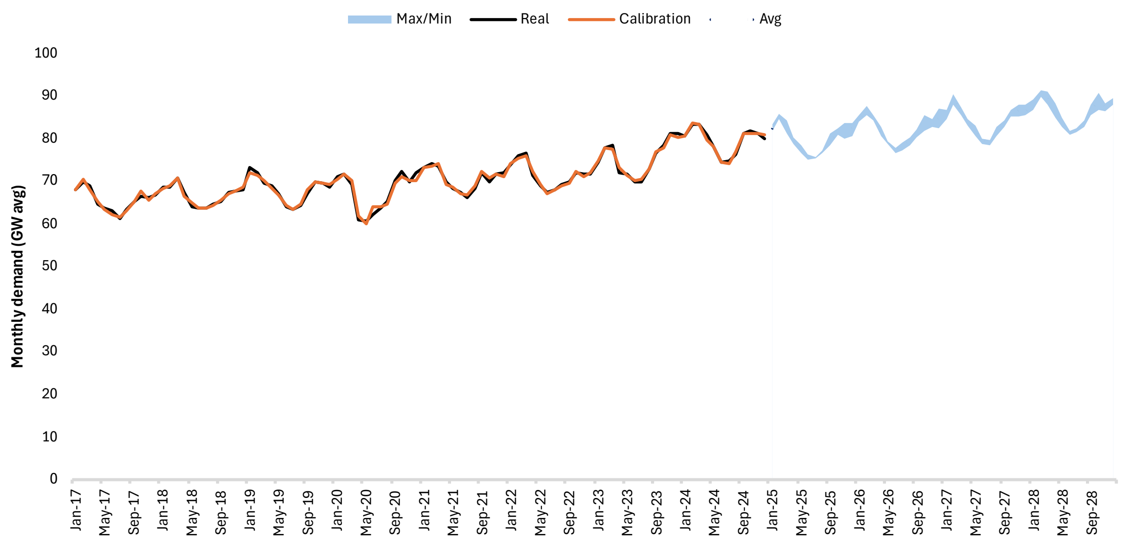

Figure 26. Monthly demand – historical data and forecast. Own work.

The impact of temperature also becomes notable when analyzing the hourly demand profile. In the warmer months, a significant difference in projected load results is observed, which can exceed 10% when comparing the 5% and 95% percentiles.

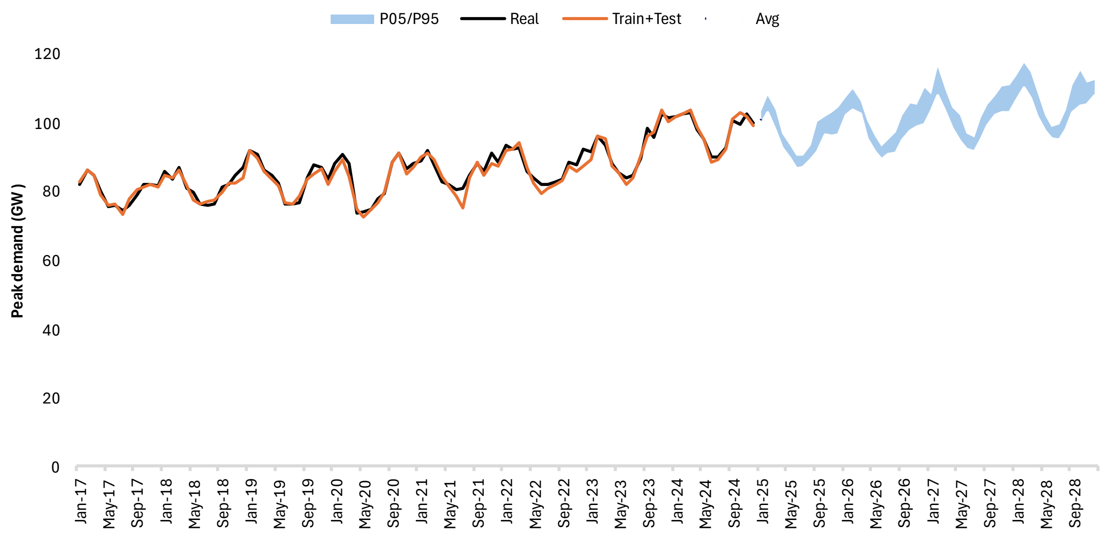

Figure 27. Peak demand – historical data and forecast. Own work.

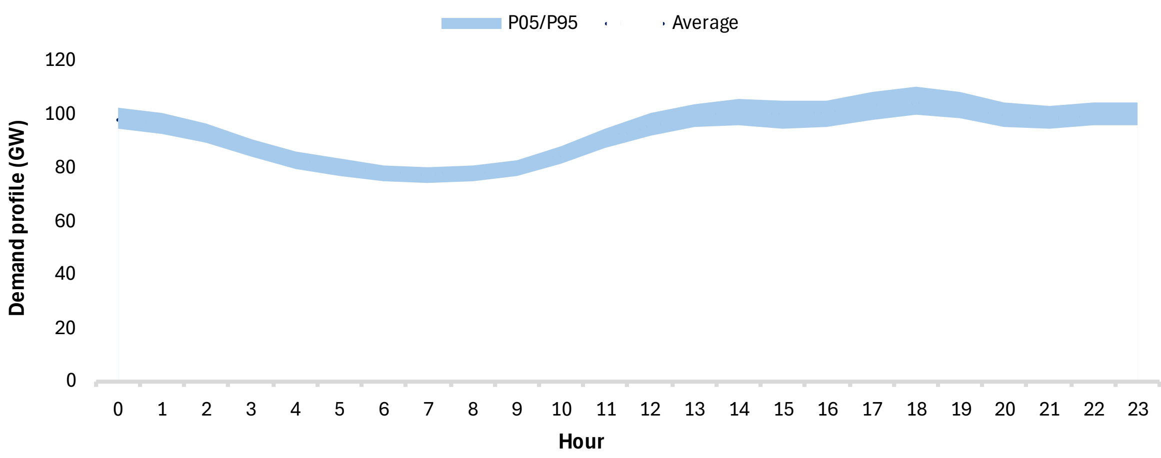

Figure 28. Critical day demand profile – December 2026. Own work.

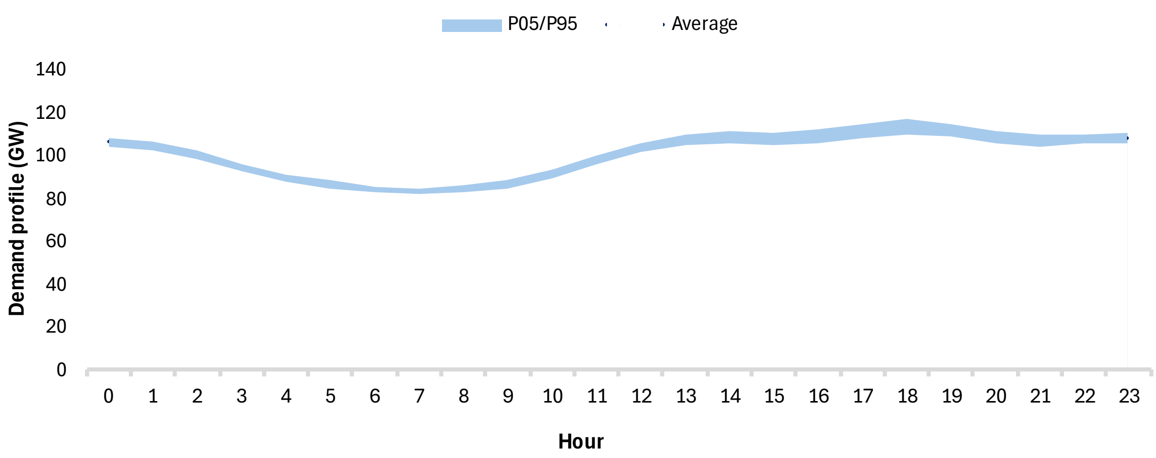

Figure 29. Critical day demand profile – February 2028. Own work.

Table 8 – Detail results for forecasted peak demand

Year	Average	P05	P90	P95	P99
2025	105.3	103.0	107.2	107.9	108.7
2026	106.6	103.6	109.1	110.2	110.6
2027	111.1	108.0	113.9	116.3	116.6
2028	113.5	110.1	116.6	117.2	118.3

5 RELIABILITY ASSESSMENT OF THE BRAZILIAN POWER SYSTEM

Taking into account the compiled temperature data and the hourly demand forecast considering temperature effects conducted in the previous step, the reliability of the Brazilian interconnected system will be analyzed for a target year (e.g., 2028). In addition to the temperature-dependent demand scenarios, the relationship between the availability of generators and this climate variable will also be considered, both in relation to the decrease in efficiency and the possible increase in their failure rate in extreme temperature events [MULA20]. This analysis will be carried out with a focus on thermal power plants, which are the main technology listed by the Brazilian Government to provide firm capacity support to the system, having had the largest number of products offered in the latest version of the 2025 Capacity Mechanism. This mechanism, although listed as essential to the guarantee of supply in the short and medium term for the Brazilian system, had a call for proposals proposed and later canceled due to legal issues, with a relaunch scheduled for 2026 [MINI25].

5.1 SYSTEM MODELING AND DATA INTEGRATION

In order to analyze the reliability of the system while explicitly considering temperature, this thesis adopts a systemic reliability assessment approach based on the probabilistic analysis of cuts of the Brazilian power system, evaluating jointly the entire system and the different permutations among its subsystems. In this way, beyond the energetic perspective, it becomes possible to analyze the probability of failure also as a function of the interconnection between subsystems, which in the Brazilian system is characterized by the existence of large transmission backbones [CENT20].

As the starting point of the analysis, and in order to incorporate the official planning framework, the Monthly Operation Plan (PMO) of ONS/CCEE with reference date of August 2025 is used [OPER25B]. This allows for a detailed representation of the entire national generation fleet, including the thermal and hydroelectric plants, their hydraulic restrictions and the detailed modeling of plants through head–storage curves, which are essential for the correct representation of the available capacity of each unit. In addition, the expectations of the operator regarding renewable penetration, both centralized and distributed generation, mainly solar, as well as the availability of interchanges between subsystems, are incorporated.

In the case of hydroelectric plants, the particular feature of Brazil having large reservoirs requires careful treatment in order to avoid overestimating their firm contribution. The criterion adopted follows the principle that, when the usable storage of a reservoir allows regulation greater than 14 days, its available capacity is considered, adjusted by the head–storage curve that relates available capacity to storage level. When the regulation capacity is below this threshold, only the estimated effective generation for the period is considered. This procedure, with adaptations, is officially adopted by ONS as well as by other institutions of reference in the Brazilian system, ensuring that only reservoirs with significant storage capacity are treated as relevant contributors to firm capacity [OPER24].

$$Useful\ storage\ duration_{t,hp}(h) = \frac{\left(Storage_{t,hp}(hm^3) - Minimum\ Storage_{t,hp}(hm^3)\right) \cdot 10^6}{Maximum\ Turbining_{t,hp} \cdot 3600}$$

Equation 13 – Assessment of regularization capacity by plant

For renewable generation, the database provided by ONS considers average generation profiles, without representing the intrinsic stochasticity of renewable output and its availability. In order to incorporate this key component into the dataset, and consequently into the present analysis, the production of stochastic series generated by the TSL tool is included [PSR25A]. This tool produces wind and solar radiation series from ERA5 reanalysis climate data, calibrated with historical production factors, ensuring spatial and temporal consistency among plants located in different regions. Combined with the generation of synthetic scenarios of hydro inflows, different stochastic scenarios of renewable generation are also considered, reflecting a broader range of possible climatic conditions. In this thesis, one hundred distinct production scenarios are taken into account, with the system operation set with the same methodology as applied by the Operator, using in this case the SDDP model [PSR25B].

As detailed in the previous sections, demand is explicitly modeled as a function of temperature, in contrast to the representation provided and considered by ONS. To avoid excessive computational effort, the analysis focuses on the critical hours of system supply, between 5 p.m. and 2 a.m., which historically concentrate the highest risk of deficit. As mentioned in section 4.4, one hundred scenarios of hourly peak demand are generated, reflecting different combinations of temperature, economic growth, and seasonal variations.

In order to represent the stochasticity of thermal availability, this analysis includes its availability as conditional on temperature, taking into account the average hourly temperature for each subsystem. For this purpose, a gamma distribution is adopted to represent the total amount of unavailable capacity in each subsystem, conditional on temperature. This distribution approximates the results obtained from Monte Carlo simulations but with significantly reduced computational effort [ALBI96]. The gamma distribution is a continuous probability distribution frequently used to represent positive and asymmetric phenomena, such as the magnitudes of aggregated events. Its flexibility derives from the presence of two parameters, generally called shape (k) and scale (θ), which allow the adjustment of the asymmetry and dispersion of the distribution.

$$f(x,k,\theta) = \frac{1}{\Gamma(k) \cdot \theta^k} x^{k-1} \cdot e^{-x/\theta}$$

Equation 14 – Gamma distribution [PRSS13]

The application of the gamma distribution in this context is supported by previous studies in the reliability literature. In [KISI98] the use of the gamma distribution was proposed to approximate capacity outage probabilities in generation systems, demonstrating its efficiency in representing the aggregation of failures in environments with multiple units. Other applications in reliability studies are listed in [MURP19, WKLT24]. In the present study, the function FOR(t) is taken as already known, parameterized from international empirical studies, as shown in Table 9. The approach applied avoids the need for individual simulations, reduces computational complexity, and at the same time captures the systemic effect of correlated failures, whose probability increases under extreme temperature conditions. Due to the more stable characteristics of hydroelectric units, in addition to the presence of multiple generating units per plant, which does not always correspond to the same behavior observed in thermal plants, temperature-dependent failure rates are not considered for hydroelectric plants.

Table 9 – Forced-outage as a function of the temperature [MUSA19]

	Temperature (Celsius)	**CC**	**CT**	**DS**	**HD**	**NU**	**ST**
Temperature-dependent forced outage rates	-15	14.90%	19.90%	21.20%	7.00%	1.90%	13.30%
	-10	8.10%	9.90%	17.00%	4.30%	1.80%	11.20%
	-5	4.80%	5.10%	13.70%	3.20%	1.70%	9.90%
	0	3.30%	3.10%	11.60%	2.70%	1.80%	9.10%
	5	2.70%	2.40%	10.60%	2.60%	1.80%	8.60%
	10	2.50%	2.20%	10.20%	2.60%	1.90%	8.30%
	15	2.80%	2.40%	10.40%	2.70%	2.10%	8.40%
	20	3.50%	2.70%	13.60%	2.70%	2.70%	8.60%
	25	3.50%	3.10%	13.50%	2.50%	3.70%	9.40%
	30	4.10%	3.90%	14.30%	2.90%	6.60%	11.40%
	35	7.20%	6.60%	17.50%	8.20%	12.40%	14.00%
Unconditional forced outage rates	All	3.30%	2.80%	10.90%	2.40%	2.60%	9.40%

The reliability assessment is carried out using the minimum cut framework to identify the critical states of the system. All possible permutations of groupings of the four subsystems of the SIN (Southeast/Central-West, South, Northeast, and North) are generated, forming subsets that represent potential points of vulnerability. This approach makes it possible to isolate whether a subsystem, or a combination of them, presents greater fragility, allowing for a more detailed analysis by considering possible import dependencies from neighboring systems. For each scenario, the net capacity of each cut is calculated, defined as the sum of the available capacity of the subsystems in the group plus the import capacity from the others, minus demand and the sampled unavailable thermal capacity. Among all cuts, the worst result is recorded, that is, the one that presents the largest deficit or the smallest reserve margin. In total, the process combines one hundred inflow and renewable scenarios with one hundred peak demand scenarios, resulting in ten thousand system states evaluated, with the process conducted for each hour of the critical period.

$$\begin{gathered} Net\ Available\ Capacity_{t,s,c} = \\ Hydro\ available\ capacity_{t,s,c} +\ Renewable\ generation_{t,s,c} + \\ Thermal\ Available\ capacity_{t,s,c} -\ Demand_{t,s,c} \end{gathered}$$

Equation 15 – Available capacity assessment by cut and scenario

To demonstrate the methodology, the thesis analyzes its application for February 2028, the month marked by the highest projected peak demand, driven especially by the higher temperatures during the period. We compare its application with the explicit consideration of the temperature-dependent failure rate and a second case with only the invariable failure rates.

5.2 RELIABILITY RESULTS

Figure 30 presents the hourly evolution of average deficits for percentiles p90, p95, and p99. It is evident that the most critical period occurs precisely between 5 p.m. and 7 p.m., when the deficit reaches values above 10 GW and even exceeds 13 GW in the most extreme scenarios. This time window coincides with the transition from late afternoon to evening, when solar generation decreases sharply while demand remains high or increases due to the return of residential loads. The result is a strong need for backup from dispatchable and flexible sources, such as hydroelectric plants with intraday regulation capacity or fast-start thermal plants. It is also evident that even after this initial peak, between 8 p.m. and 10 p.m., the deficit remains at elevated levels, only consistently receding after 11 p.m., when demand starts to decline. This persistence suggests that the problem is not limited to an instantaneous ramp shock in net load but extends for several hours, requiring sustained reserves, which is consistent with analyses carried out by [OPER24].

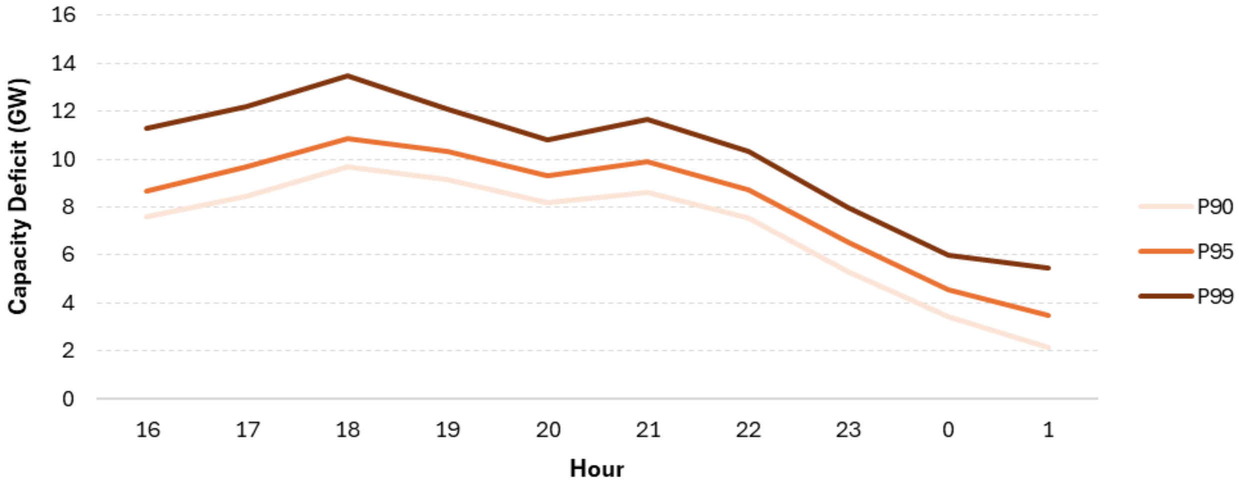

Figure 30. Capacity deficit percentiles for February 2028, by hour. Own work.

The Figure 31, which shows the probabilistic distribution of deficits across percentiles for each critical hour between 4 p.m. and 1 a.m., reinforces the view that the problem is structural and not restricted to rare scenarios. At times such as 5 p.m., 6 p.m., and 7 p.m., the distribution of deficits systematically shifts upward, so that even the median of the distribution already indicates deficits greater than 5 GW. In other words, even under “central” conditions and not only in extreme scenarios, the system presents significant deficits, characterizing a systemic situation of capacity shortfall. Another relevant point is the concentration of larger deficits precisely during the early evening hours (4 p.m. to 8 p.m.), while after 11 p.m. and especially at midnight and 1 a.m. the distribution approaches zero or even shows negative values in some percentiles, reflecting surplus capacity in scenarios of greater renewable availability, which is not present during the early evening hours.

Thus, when jointly analyzed, the results highlight a situation of system vulnerability, even though there is relative renewable surplus in some hours. However, such surplus is not compensated by sufficient reserves at sunset, which in addition to being significantly higher must also be flexible in order to handle load ramps. This situation emphasizes the need for expansion and reliability policies that must consider the system’s requirement for new flexible plants capable of supplying demand at sunset, but that must also account for the impact of temperature on their operation to ensure their availability when needed under these tight conditions.

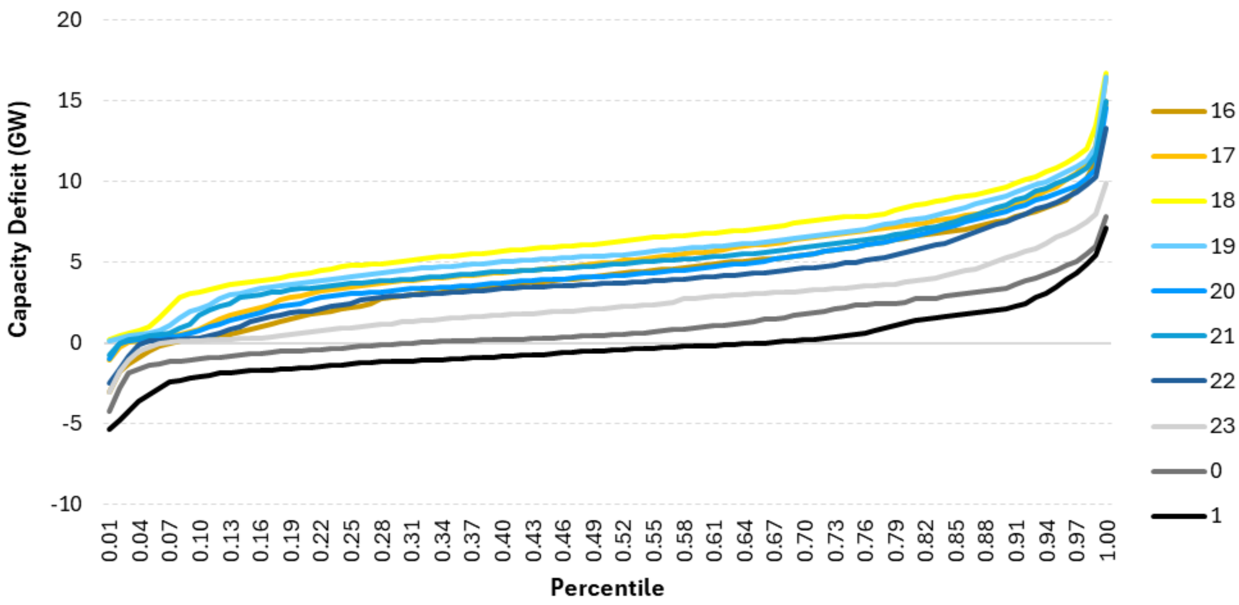

Figure 31. Capacity deficit Probability distribution for February 2028, by hour. Own work.

Finally, the Figure 32 presented below shows the impact of considering the dependence of thermal forced outage rates on temperature. When unavailability is modeled as independent, the capacity deficits observed for percentiles P90, P95, and P99 are 9.7 GW, 10.8 GW, and 13.0 GW, respectively. When climate dependence of outages is included, the values increase to 10.2 GW, 11.2 GW, and 13.6 GW. The difference is therefore around 500 MW across the three severity levels, representing a non-negligible structural increase in the reserve capacity requirement.

It is important to highlight that this comparison was made under the same demand scenarios, which are already temperature dependent. If failure scenarios were instead modeled as stochastic and independent of temperature, the difference would likely be even greater, as the coincidence of high temperatures (which raise demand) with increased thermal outage rates would amplify the risk of deficits.

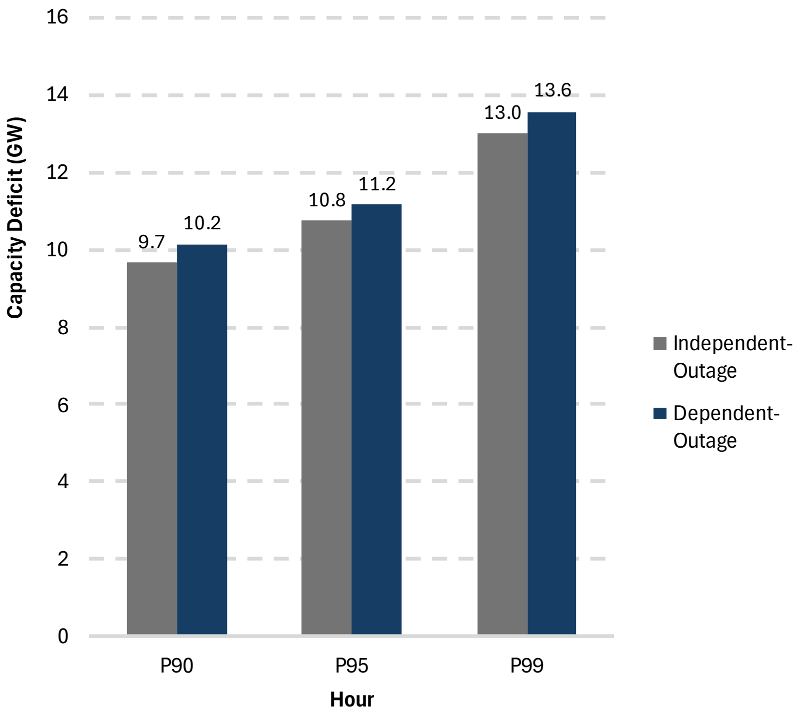

Figure 32. Comparison between scenarios for the capacity deficit percentiles for February 2028. Own work.

From an economic perspective, this difference of approximately 500 MW can be valued using the Marginal Cost of Expansion (CME) for capacity, the = first capacity auction, carried out in 2021, resulted in an average price of R$ 824/kW-yr [EMPR21]. Applying this value, the additional required capacity would cost around R$ 412 million per year (in 2021 values).

If, however, the procurement of this additional capacity was left to an emergency auction, the cost could be much higher. As evidenced by the 2021 Emergency Auction, energy prices were more than five times higher than those in regular new energy auctions, reflecting the urgency and risks associated with last-minute procurement [MINI21]. In such a sensitivity scenario, the reference value could reach approximately R$ 2,000 million per year (in 2021 values), representing a substantial burden on consumers and on sector planning.

6 CONCLUSIONS

This thesis investigated the impacts of explicitly incorporating temperature as a determinant factor in both electricity demand forecasting and generator availability when assessing the long-term reliability of the Brazilian power system. A comprehensive methodology was developed, combining econometric and time-series models for medium-term demand forecasting with a probabilistic reliability framework that accounts for temperature-dependent outage probabilities of thermal plants. The analysis was supported by a robust historical database of electricity demand and climate data, structured to capture the spatial and temporal heterogeneity of the Brazilian Interconnected Power System (SIN).

The results demonstrate that temperature is a critical explanatory variable. In monthly demand forecasts, its inclusion reduced RMSE by more than 38% on average, while in hourly projections its effect was also pronounced, with deviations exceeding 10% for certain hours in specific months, such as February. This not only underscores the sensitivity of demand to thermal discomfort but also highlights the systemic nature of evening peaks, where elevated temperatures simultaneously drive consumption and stress generation adequacy. The stochastic framework revealed that the distribution of hourly demand varies significantly with temperature, which in the current expansion expectations would produce structural deficits above 5 GW even in central scenarios, and exceeding 13 GW in extreme conditions.

On the supply side, the results confirm that ignoring the climate dependency of thermal outages leads to underestimation of system risks. When thermal forced outages are modeled as temperature-dependent, the capacity requirement increases structurally by about 500 MW compared to the independent assumption. This adjustment, while seemingly modest, translates into substantial economic consequences, valued at R$ 412 million annually under the official marginal cost of firm capacity, and potentially rising to nearly R$ 2 billion if procurement were postponed to emergency auctions, as observed in Brazil in 2021.

The findings highlight the dual role of climate: it increases the demand for electricity while simultaneously reducing the availability of thermal plants. This interaction highlights systemic vulnerabilities during sunset hours, when solar generation declines sharply, and emphasizes the need for additional flexible and dispatchable resources to maintain reliability under intensifying climate variability.

As avenues for future work, three directions emerge naturally from the present study. First, extending the demand forecasting framework to generate a full-year projection rather than focusing only on critical days would enable the integration of unit commitment constraints into the reliability analysis, reflecting operational limits of the existing thermal fleet. This would provide a more granular representation of system flexibility, especially under tight reserve margins. Second, although the framework developed here can accommodate warming trends, the present study employed only historical temperature records. Incorporating climate change scenarios and incremental warming would provide a more forward-looking assessment of long-term risks, although estimating this trend may be difficult. Furthermore, counting not only forced outages but also incorporating in the analyzes efficiency losses in thermal and renewable energy sources can lead to even higher capacity requirements. Finally, the reliability analysis could be refined by moving from subsystem-level outage modeling to the unit level, which would allow quantifying the contribution of each thermal plant under extreme conditions and determining the amount of operating reserves required to address correlated failures.

In summary, this work confirms that explicitly accounting for temperature substantially improves demand forecasting accuracy, reveals significant structural vulnerabilities in the evening hours, and shows that the reliability of the Brazilian power system is materially affected by the climate sensitivity of both demand and thermal availability. The proposed methodological framework thus provides a valuable tool to support planning decisions, guide new capacity procurements, and anticipate the systemic challenges that will arise as the country transitions to a more renewable-dominated and climate-sensitive electricity sector.

7 APPENDIX A

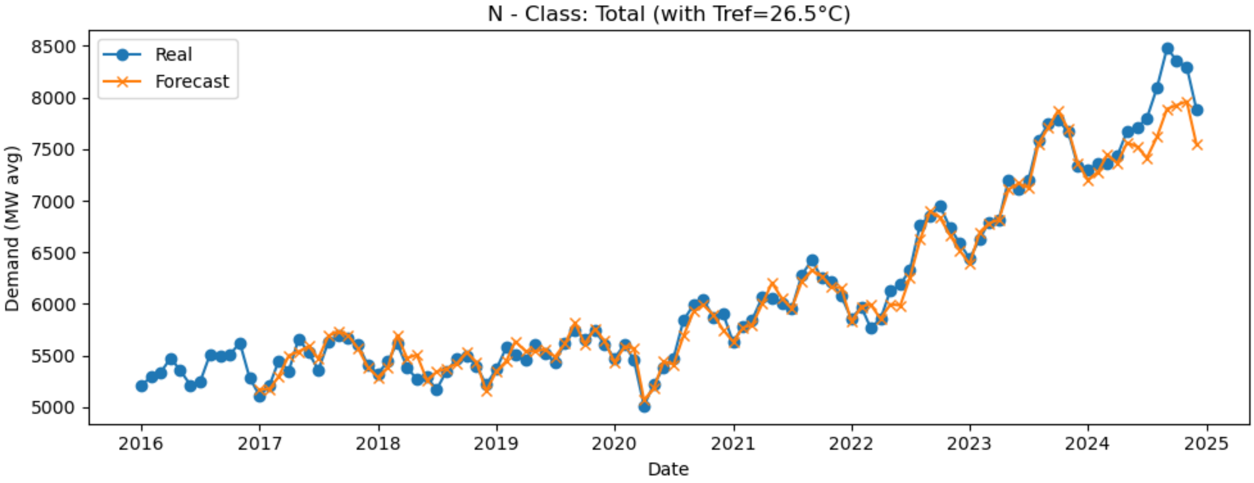
N - Class: Total (with Tref=26.5°C)
Real
Forecast
Demand (MW avg)
Date

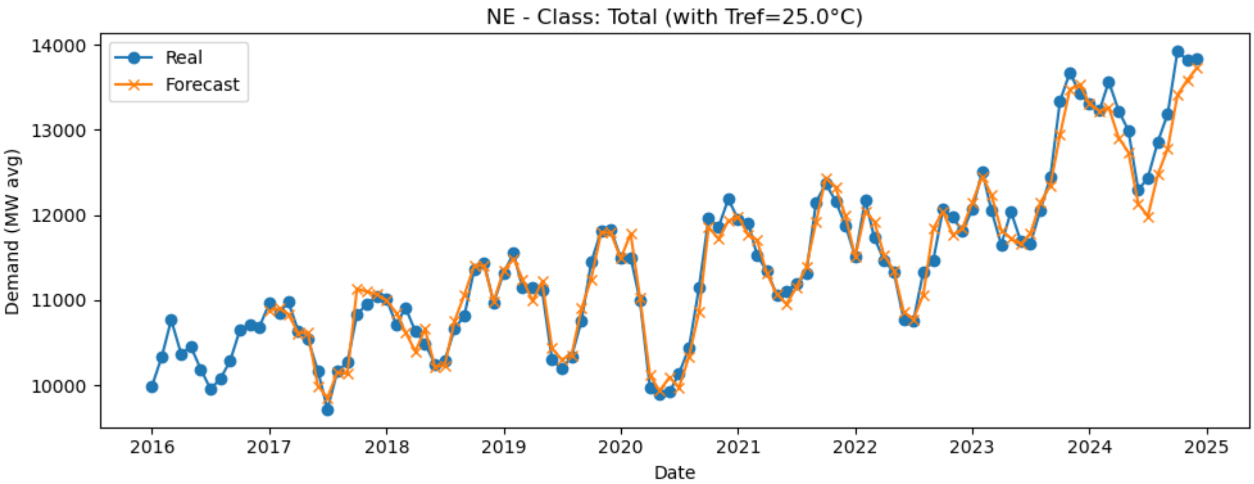
NE - Class: Total (with Tref=25.0°C)
Real
Forecast
Demand (MW avg)
Date

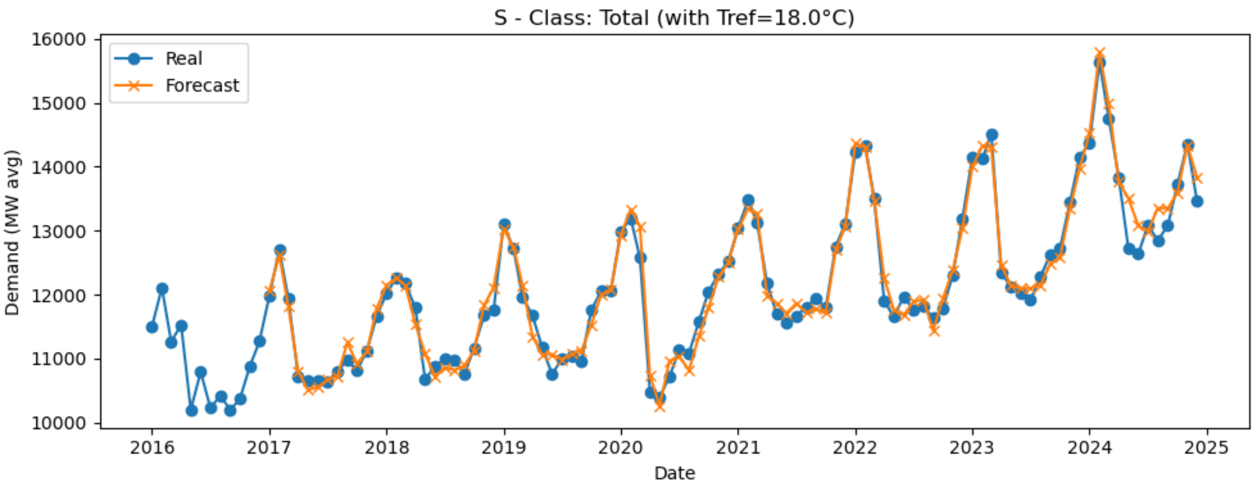
S - Class: Total (with Tref=18.0°C)
Real
Forecast
Demand (MW avg)
Date

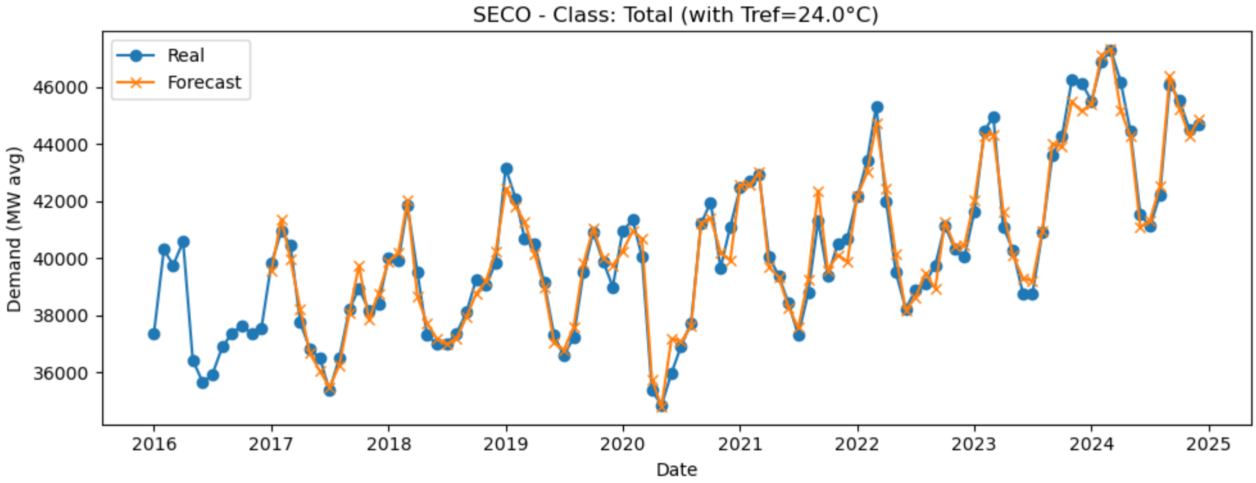
SECO - Class: Total (with Tref=24.0°C)
Real
Forecast
Demand (MW avg)
Date
46000
44000
42000
40000
38000
36000
2016
2017
2018
2019
2020
2021
2022
2023
2024
2025

8 APPENDIX B

Table 10 – Coefficients for the economic variable of the monthly demand final model

Subsis	Brasil	Agro	Industry	Services	dummy_COVID	var_time_dummy
SECO	0.007	0.005	-0.006	0.007	-0.076	0.029
S	-0.005	0.002	0.002	-0.003	-0.040	0.138
N	0.101	-0.023	-0.037	-0.115	-0.060	0.156
NE	0.054	-0.004	-0.012	-0.074	-0.053	0.109
RR	-0.043	0.012	0.017	0.037	-0.036	0.233

Table 11 – Coefficients for the monthly dummies of the monthly demand final model

Subsis	dummy_1	dummy_2	dummy_3	dummy_4	dummy_5	dummy_6	dummy_8	dummy_9	dummy_10	dummy_11	dummy_12
SECO	---	0.028	0.032	0.021	0.015	-0.008	0.006	-0.009	---	0.003	-0.013
S	0.023	0.078	0.042	0.014	0.012	---	---	-0.006	---	0.014	-0.017
N	-0.015	---	0.008	---	0.012	0.012	---	-0.023	-0.025	-0.003	-0.006
NE	-0.010	0.005	-0.012	-0.020	-0.005	-0.012	0.006	---	---	0.009	-0.002
RR	0.069	0.119	0.097	0.099	0.039	---	0.074	0.128	0.146	0.140	0.097

Table 12 – Coefficients for the temperate variables of the monthly demand final model

Subsis	CDD CO_MT_A902	HDD CO_MT_A902	CDD SE_RJ_A618	HDD SE_RJ_A618	CDD SE_SP_A711	HDD SE_SP_A711	CDD SE_SP_A727	HDD SE_SP_A727
SECO	0.0023	0.0053	0.0001	-0.0313	0.0115	-0.0338	0.0138	0.0133

Subsis	CDD S_PR_A869	HDD S_PR_A869	CDD S_RS_A803	HDD S_RS_A803	CDD S_RS_A844	CDD S_SC_A868	HDD S_SC_A868
S	0.0340	0.0028	0.0372	0.0214	0.0214	0.0320	0.0044

Subsis	CDD N_AM_A124	HDD N_AM_A124	CDD N_MA_A207	CDD N_PA_A241	HDD N_PA_A241	CDD N_TO_A038	HDD N_TO_A038
N	0.0087	-0.0088	0.0298	0.0064	0.0009	-0.0030	-0.0068

Subsis	CDD NE_BA_A424	HDD NE_BA_A424	CDD NE_PB_A348	HDD NE_PB_A348	CDD NE_PE_A322	CDD NE_PI_A330	HDD NE_PI_A330
NE	0.0036	-0.0311	0.0300	0.0035	-0.0001	0.0147	0.0006

Subsis	CDD RR_RR_A135	HDD RR_RR_A135
RR	0.0444	0.0061

9 APPENDIX C

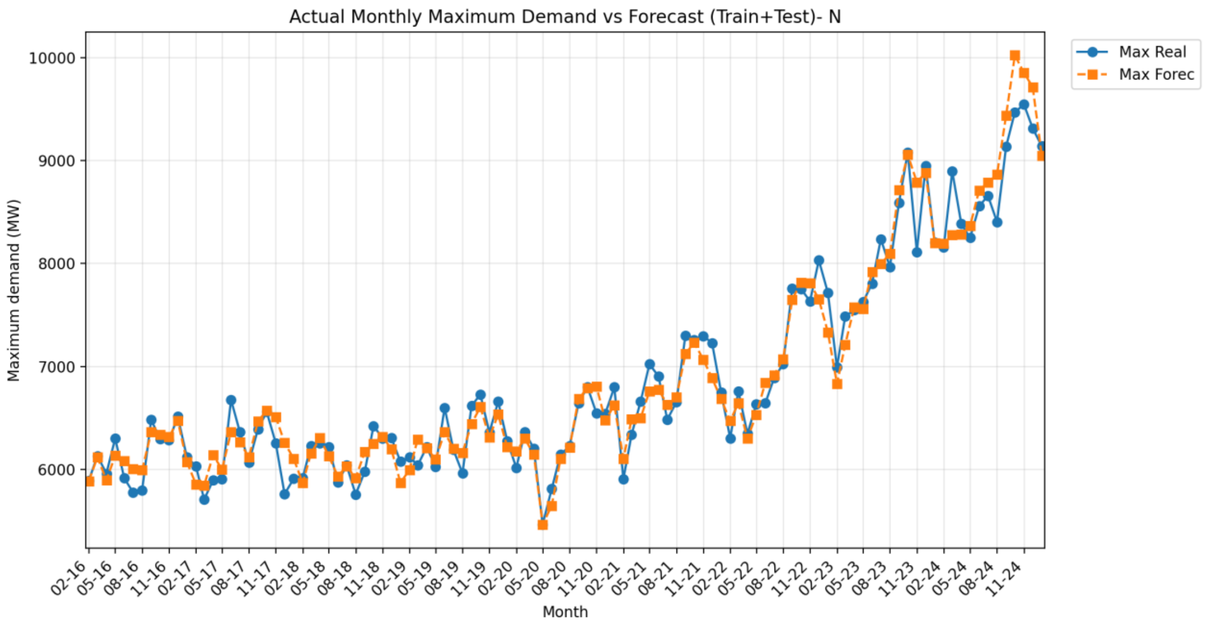
Actual Monthly Maximum Demand vs Forecast (Train+Test)- N
Max Real
Max Forec
Maximum demand (MW)
Month
10000
9000
8000
7000
6000
02-16
05-16
08-16
11-16
02-17
05-17
08-17
11-17
02-18
05-18
08-18
11-18
02-19
05-19
08-19
11-19
02-20
05-20
08-20
11-20
02-21
05-21
08-21
11-21
02-22
05-22
08-22
11-22
02-23
05-23
08-23
11-23
02-24
05-24
08-24
11-24

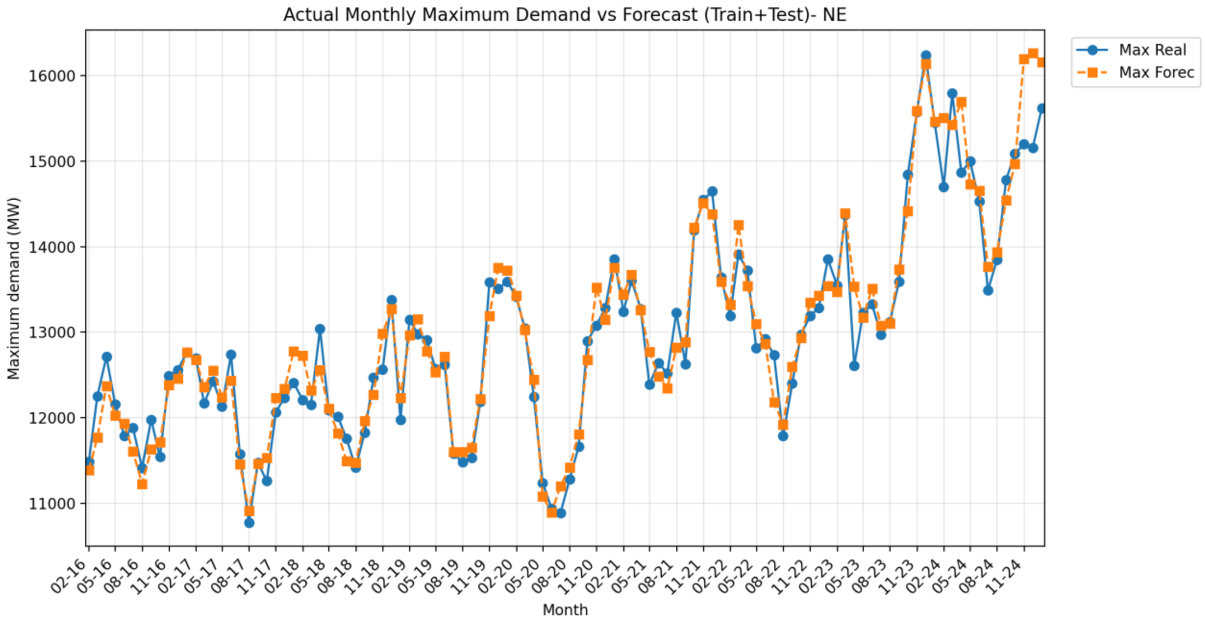
Actual Monthly Maximum Demand vs Forecast (Train+Test)- NE
Max Real
Max Forec
Maximum demand (MW)
Month
16000
15000
14000
13000
12000
11000
02-16
05-16
08-16
11-16
02-17
05-17
08-17
11-17
02-18
05-18
08-18
11-18
02-19
05-19
08-19
11-19
02-20
05-20
08-20
11-20
02-21
05-21
08-21
11-21
02-22
05-22
08-22
11-22
02-23
05-23
08-23
11-23
02-24
05-24
08-24
11-24

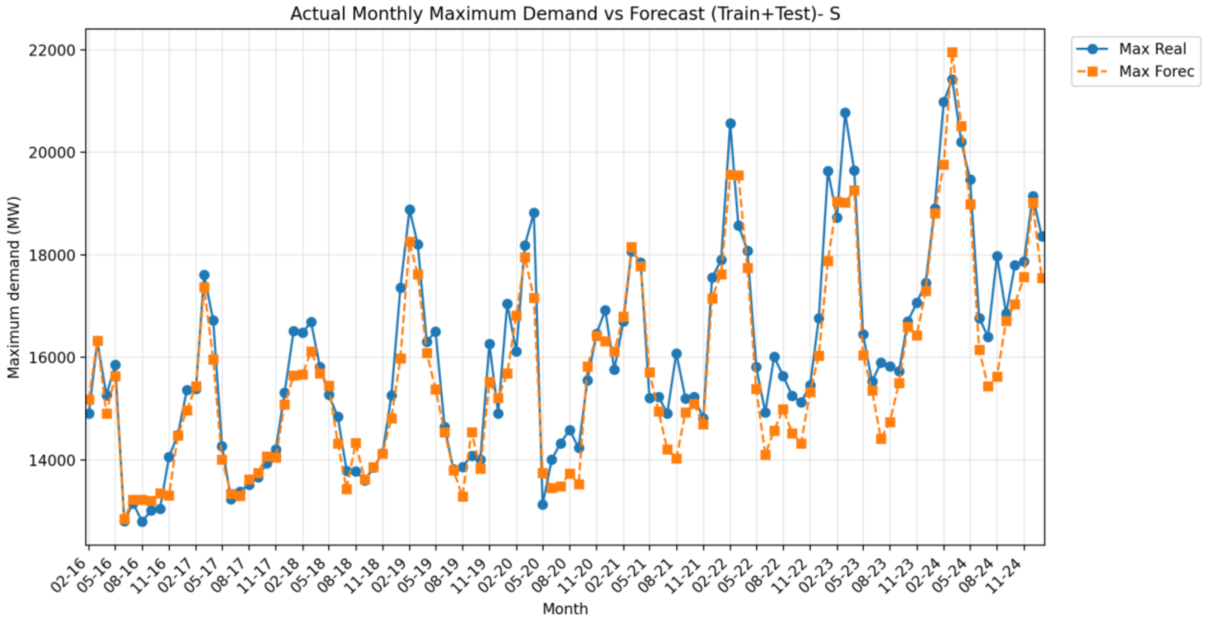
Actual Monthly Maximum Demand vs Forecast (Train+Test)- S
Max Real
Max Forec
Maximum demand (MW)
22000
20000
18000
16000
14000
02-16
05-16
08-16
11-16
02-17
05-17
08-17
11-17
02-18
05-18
08-18
11-18
02-19
05-19
08-19
11-19
02-20
05-20
08-20
11-20
02-21
05-21
08-21
11-21
02-22
05-22
08-22
11-22
02-23
05-23
08-23
11-23
02-24
05-24
08-24
11-24
Month

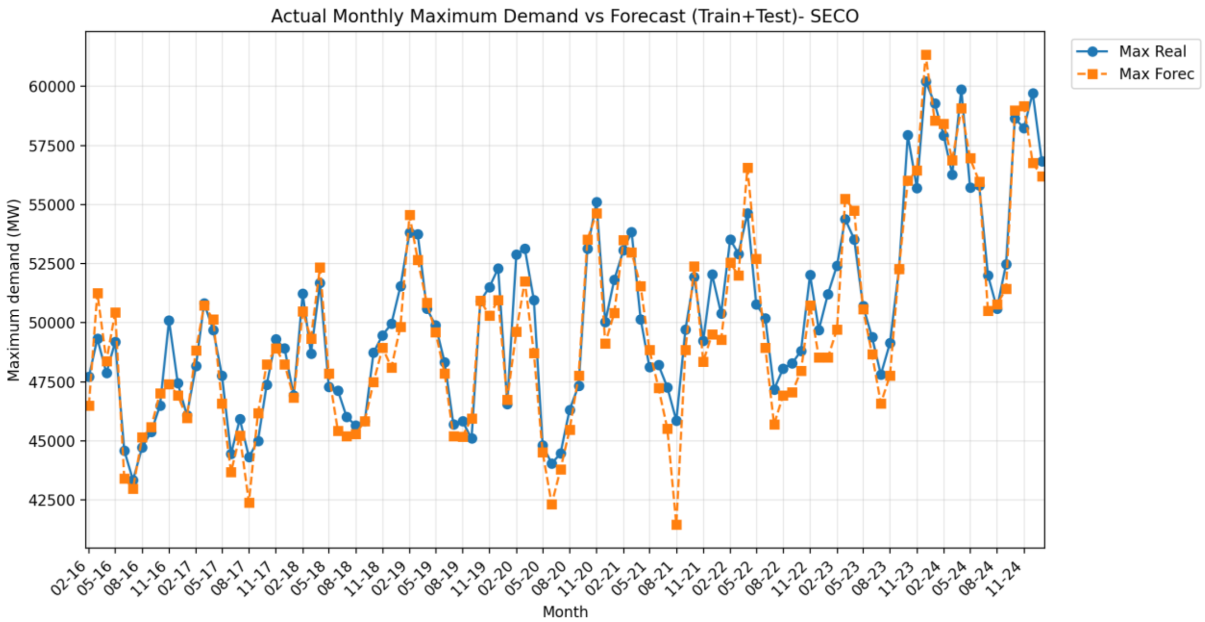
Actual Monthly Maximum Demand vs Forecast (Train+Test)- SECO
Max Real
Max Forec
Maximum demand (MW)
60000
57500
55000
52500
50000
47500
45000
42500
02-16
05-16
08-16
11-16
02-17
05-17
08-17
11-17
02-18
05-18
08-18
11-18
02-19
05-19
08-19
11-19
02-20
05-20
08-20
11-20
02-21
05-21
08-21
11-21
02-22
05-22
08-22
11-22
02-23
05-23
08-23
11-23
02-24
05-24
08-24
11-24
Month

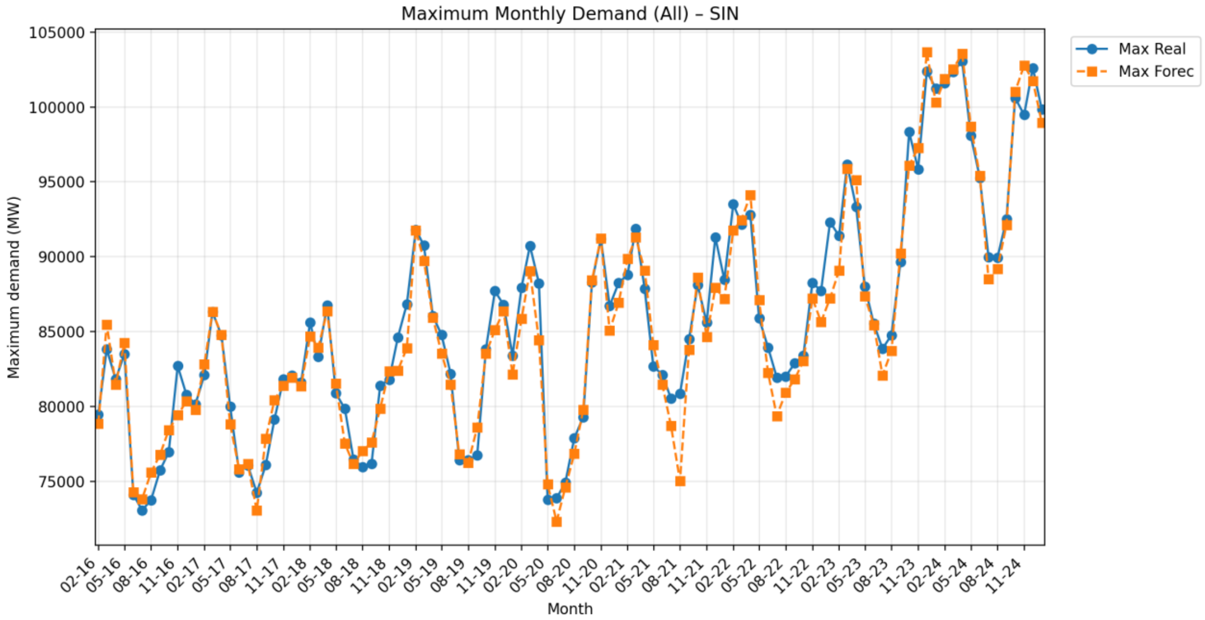
Maximum Monthly Demand (All) – SIN
Max Real
Max Forec
Maximum demand (MW)
Month
105000
100000
95000
90000
85000
80000
75000
02-16
05-16
08-16
11-16
02-17
05-17
08-17
11-17
02-18
05-18
08-18
11-18
02-19
05-19
08-19
11-19
02-20
05-20
08-20
11-20
02-21
05-21
08-21
11-21
02-22
05-22
08-22
11-22
02-23
05-23
08-23
11-23
02-24
05-24
08-24
11-24

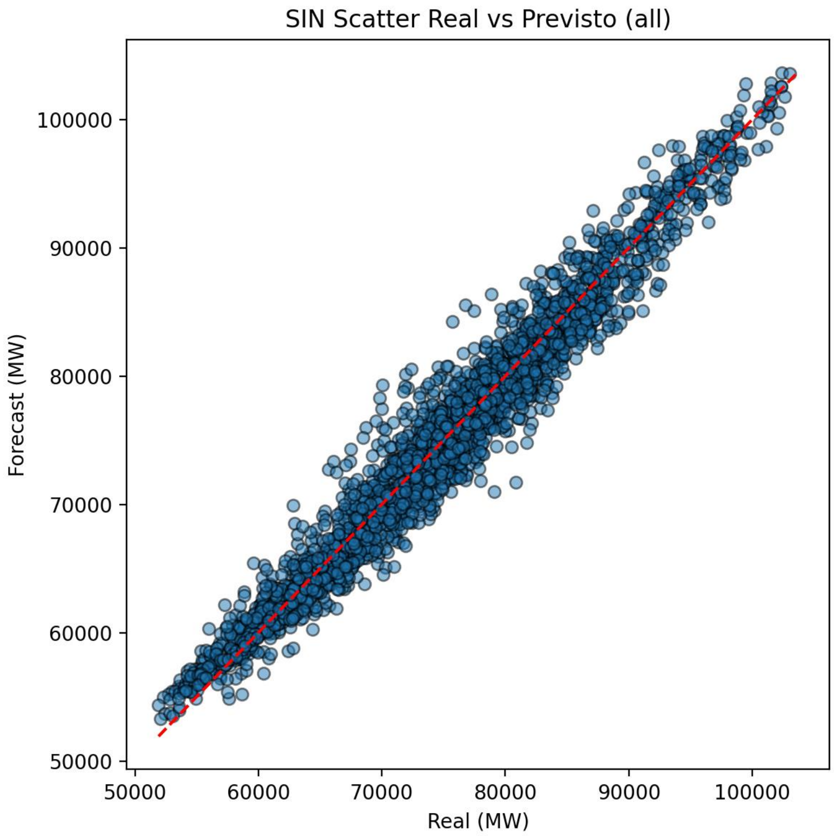
SIN Scatter Real vs Previsto (all)
Forecast (MW)
Real (MW)
100000
90000
80000
70000
60000
50000
50000
60000
70000
80000
90000
100000

10 BIBLIOGRAPHY

[ALBI96] ALLAN, R. N.. ; BILLINTON, R..: *Reliability Evaluation of Power Systems* : Plenum, 1996 — ISBN 0306452596

[AMCC22] DE AMORIM, LUCAS B. V. ; CAVALCANTI, GEORGE D. C. ; CRUZ, RAFAEL M. O.: The choice of scaling technique matters for classification performance (2022)

[AVMA18] AHMED, T. ; VU, D. H. ; MUTTAQI, K. M. ; AGALGAONKAR, A. P.: Load forecasting under changing climatic conditions for the city of Sydney, Australia. In: *Energy* Bd. 142, Elsevier Ltd (2018), S. 911–919

[BACE25] BACEN: *SGS - Sistema Gerenciador de Séries Temporais*. URL https://www3.bcb.gov.br/sgspub/localizarseries/localizarSeries.do?method=prepararTelaLocalizarSeries. - abgerufen am 2025-07-17

[BAFR23] BASHIRI BEHMIRI, NIAZ ; FEZZI, CARLO ; RAVAZZOLO, FRANCESCO: Incorporating air temperature into mid-term electricity load forecasting models using time-series regressions and neural networks. In: *Energy* Bd. 278, Elsevier Ltd (2023)

[BUEN24] BUENOS AIRES TIMES: *Record-breaking energy demand, power cuts in Argentina amid high temperatures*. URL https://www.batimes.com.ar/news/argentina/record-breaking-energy-demand-due-to-the-high-temperatures-50000-households-with-power-cuts.phtml. - abgerufen am 2025-04-25

[CAMP17] CAMPO DALL'ORTO, CELSO EDUARDO RAMOS: *Análise da Redução do Horizonte de Planejamento da Operação no Modelo Computacional de Médio Prazo*, UNIVERSIDADE FEDERAL DE ITAJUBÁ, 2017

[CENT20] CENTRO DE PESQUISAS DE ENERGIA ELÉTRICA: *Cálculo do Critério Geral de Garantia de Suprimento para Aferição da Adequabilidade no Atendimento à Potência no Sistema por meio da Análise de Confiabilidade de Sistemas Interligados utilizando o Modelo CONFINT*, 2020

[CHAN17] CHAN-LAU, JORGE A: *Lasso Regressions and Forecasting Models in Applied Stress Testing*, 2017

[COMI25] COMITÉ DE OPERACIÓN ECONÓMICA DEL SISTEMA INTERCONECTADO NACIONAL: *Pronóstico de la Demanda de Mediano Plazo del SEIN*, 2025

[COOR24] COORDINADOR ELÉCTRICO NACIONAL: *Proyección de Demanda de Largo Plazo del Sistema Eléctrico Nacional: Periodo 2024-2044*, 2024

[DAOU18] DAOUD, JAMAL I.: Multicollinearity and Regression Analysis. In: *Journal of Physics: Conference Series*. Bd. 949 : Institute of Physics Publishing, 2018

[DIAM18] DIMOULKAS, ILIAS ; AMELIN, MIKAEL: Medium and Long-term Probabilistic Heat Demand Forecasting in District Heating. In: *EuroHeat&Power* (2018)

[EMPR20] EMPRESA DE PESQUISA ENERGÉTICA: *NT Metodologia Projeção Carga Horária_EPE-NT-EPE-DEA-005-2020*, 2020

[EMPR21] EMPRESA DE PESQUISA ENERGÉTICA: *LEILÃO DE RESERVA DE CAPACIDADE 2021*, 2021

[FEAC15] DE FELICE, MATTEO ; ALESSANDRI, ANDREA ; CATALANO, FRANCO: Seasonal climate forecasts for medium-term electricity demand forecasting. In: *Applied Energy* Bd. 137, Elsevier Ltd (2015), S. 435–444

[FELS21] FRICK, NATALIE MIMS ; ECKMAN, TOM ; LEVENTIS, GREG ; SANSTAD, ALAN: *Methods to Incorporate Energy Efficiency in Electricity System Planning and Markets*, 2021

[GBWM23] GODAHEWA, RAKSHITHA ; BERGMEIR, CHRISTOPH ; WEBB, GEOFFREY I. ; MONTERO-MANSO, PABLO: An Accurate and Fully-Automated Ensemble Model for Weekly Time Series Forecasting (2023)

[HYFA10] HYNDMAN, ROB J. ; FAN, SHU: Density forecasting for long-term peak electricity demand. In: *IEEE Transactions on Power Systems* Bd. 25 (2010), Nr. 2, S. 1142–1153

[IANT22] IACONE, FABRIZIO ; NIELSEN, MORTEN ØRREGAARD ; TAYLOR, A. M.ROBERT: Semiparametric Tests for the Order of Integration in the Possible Presence of Level Breaks. In: *Journal of Business and Economic Statistics* Bd. 40, American Statistical Association (2022), Nr. 2, S. 880–896

[ISON23] ISO NEW ENGLAND: *Long-Term Load Forecast Methodology Overview*, 2023

[ISON25A] ISO NEW ENGLAND: *Maps and Diagrams*. URL https://www.iso-ne.com/about/key-stats/maps-and-diagrams/. - abgerufen am 2025-08-17

[ISON25B] ISO NEW ENGLAND: *2025 Final Draft Energy and Seasonal Peak Forecasts*, 2025

[KISI98] KIM, J O ; SINGH, C: Comparative study of continuous distribution models for power system reliability evaluation. In: *IEE Proceedings Generation, Transmission and Distribution*, 1998

[LOBV24] LOMBARDI, STEFANO ; VAN DEN BERG, GERARD J. ; VIKSTRÖM, JOHAN: Empirical Monte Carlo evidence on estimation of timing-of-events models. In: *Econometric Reviews* Bd. 44, Taylor and Francis Ltd. (2024), Nr. 1, S. 90–118

[MBBR13] MASTROPIETRO, PAOLO ; BATLLE, CARLOS ; BARROSO, LUIZ A ; RODILLA, PABLO: *ELECTRICITY AUCTIONS IN SOUTH AMERICA: TOWARDS CONVERGENCE OF SYSTEM ADEQUACY AND RES-E SUPPORT*, 2013

[MBBR16] MASTROPIETRO, PAOLO ; BATLLE, CARLOS ; BARROSO, LUIZ A. ; RODILLA, PABLO: The evolution of electricity auctions in South America. In: *Energy Sources, Part B: Economics, Planning and Policy* Bd. 11, Taylor and Francis Inc. (2016), Nr. 12

[MINI21] MINISTÉRIO DE MINAS E ENERGIA: *Relatório de Gestão 2021*, 2021

[MIRA24] MIRANDA, GUSTAVO MACEDO: *Comparative Analysis of Variable Selection Techniques*. Belo Horizonte, Federal University of Minas Gerais, 2024

[MULA20] MURPHY, SINNOTT ; LAVIN, LUKE ; APT, JAY: Resource adequacy implications of temperature-dependent electric generator availability. In: *Applied Energy* Bd. 262, Elsevier Ltd (2020)

[MUSA19] MURPHY, SINNOTT ; SOWELL, FALLAW ; APT, JAY: A time-dependent model of generator failures and recoveries captures correlated events and quantifies temperature dependence. In: *Applied Energy* Bd. 253, Elsevier Ltd (2019)

[NIMC19] NICK MACMACKIN ; MILLER, LINDSAY ; CARRIVEAU, RUPP: Modeling and disaggregating hourly effects of weather on sectoral electricity demand. In: *Energy* Bd. 188, Elsevier Ltd (2019)

[OPER23] OPERADOR NACIONAL DO SISTEMA ELÉTRICO: *Temperaturas elevadas aumentam a carga nacional em 16,8% na comparação com o início de novembro*. URL https://www.ons.org.br/Paginas/Noticias/details.aspx?i=9734. - abgerufen am 2025-04-25

[OPER24] OPERADOR NACIONAL DO SISTEMA ELÉTRICO: *PLANO DA OPERAÇÃO ENERGÉTICA 2024/2028 (PEN 2024): RELATÓRIO DAS CONDIÇÕES DE ATENDIMENTO*, 2024

[OPER25A] OPERADOR NACIONAL DO SISTEMA ELÉTRICO: *SINMAPS - Sistema de Informações Geográficas Cadastrais do SIN*. URL https://www.ons.org.br/paginas/sobre-o-sin/mapas. - abgerufen am 2025-07-17

[OPER25B] OPERADOR NACIONAL DO SISTEMA ELÉTRICO: *PMO Agosto de 2025*. URL https://www.ccee.org.br/documents/80415/30265764/NW202508.zip/2f21ed48-380a-55b2-1af4-d809984f2f4a. - abgerufen am 2025-08-21

[PJM25A] PJM: *PJM Long-Term Load Forecast Report*, 2025

[PJM25B] PJM: *Long-Term Load Forecast Supplement*, 2025

[PRSS13] PRIETO, FAUSTINO ; SARABIA, JOSÉ MARÍA ; SÁEZ, ANTONIO JOSÉ: Modelling major failures in power grids in the whole range (2013)

[PSR25A] PSR: *Time Series Lab - Advanced Renewable Modeling*. URL https://www.psr-inc.com/software/tsl.html

[PSR25B] PSR: *SDDP - Energy Systems Operation Planning Download*. URL https://www.psr-inc.com/software/sddp.html

[RCJB21] RALSTON FONSECA, FRANCISCO ; CRAIG, MICHAEL ; JARAMILLO, PAULINA ; BERGÉS, MARIO ; SEVERNINI, ¶ EDSON ; LOEW, AVIVA ; ZHAI, HAIBO ; CHENG, YIFAN ; U. A.: *Effects of climate change on capacity expansion decisions of an electricity generation fleet in the Southeast U.S*, 2021

[SANT20] DOS SANTOS SANTOS, LEONARDO: Forced Outage Analysis of Brazilian Thermal Power Plants using the Kruskal-Wallis Test. In: *The Asian Institute of Research Engineering and Technology Quarterly Reviews* Bd. 3 (2020), Nr. 2, S. 98–126

[SDCB22] SILVA DA COSTA, WALINGSON DA ; DALLACORT, RIVANILDO ; CAMILLO DE CARVALHO, MARCOS ANTÔNIO ; BISPO DOS SANTOS, SILMARA: SISTEMA WEB PARA PRÉ-PROCESSAMENTO E ANÁLISE DE DADOS METEOROLÓGICOS Web System for pre-processing and analysis of Weather data. In: *Brazilian Journal of Climatology* (2022)

[SDZC23] SUN, HONGFEI ; DUAN, DONGLIANG ; ZHANG, HONGMING ; CHOI, SEONG ; LUO, JIE ROCKEY ; YANG, LIUQING: *Regional Medium-Term Hourly Electricity Demand Forecasting Based on LSTM: Preprint*, 2023

[SMFD25] SHENSTONE-HARRIS, SARAH ; MATTIODA, CHELSEA ; FUZAYLOV, ARIELLA ; DEJEANLOUIS, WOODDYNNE ; FAGAN, BOB: *Drivers of PJM's Capacity Market Price Surge and its Impacts on Electricity Consumers in the District of Columbia*, 2025 — ISBN 617.661.3248

[STPJ23] STAFFELL, IAIN ; PFENNINGER, STEFAN ; JOHNSON, NATHAN: A global model of hourly space heating and cooling demand at multiple spatial scales. In: *Nature Energy* Bd. 8, Nature Research (2023), Nr. 12, S. 1328–1344

[TIBS23] TIBSHIRANI, RYAN: Autoregressive Integrated Moving Average Models.

[WORL25] WORLD METEOROLOGICAL ORGANIZATION: *State of the Climate in Latin America and the Caribbean 2024*, 2025